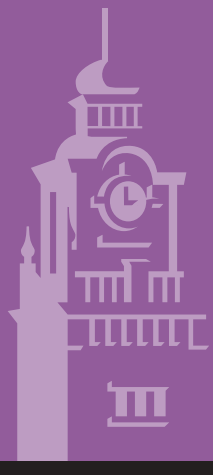

PART IV

참고자료

1. 연구원, 직원

1) 역대 연구원

연번	이름	근무기간	소속팀	학위(입학당시;진학;최종)
1	정재민	'82.03 ~ 현재	화학	학사;석사;박사
2	홍미경	'89.03 ~ 현재	화학	학사
3	한미경	'89.07 ~ '91	제3검사실	학사
4	황만용	'92.09 ~ '93	제3검사실	학사
5	김영주	'94.01 ~ 현재	화학	학사
6	이재성	'94.07 ~ 현재	물리	학사;석사;박사
7	황은경	'94.12 ~ '95.05	제3검사실	학사
8	박용우	'94.12 ~ '96	영상분석실	학사
9	이용진	'94.12 ~ '06.04	생물-종양	석사;박사
10	김중길	'95.01 ~ ?	제3검사실	학사
11	김채균	'95.12 ~ '97.10	생물-종양	박사
12	양묘근	'96.01 ~ '97.06	물리	학사
13	김경민	'96.01 ~ '99.11	물리	학사;석사;박사
14	안지영	'96.02 ~ '01.03	물리	학사
15	장영수	'96.02 ~ '08.06	화학	석사;박사
16	홍성현	'96.04 ~ '99.07	화학	학사;석사
17	이 진	'97.01 ~ '99.05	물리	학사
18	이은경	'97.03 ~ '97.10	화학	석사
19	봉정균	'97.03 ~ '97.10	물리	학사
20	김보광	'98.01 ~ '00.02	생물-종양	학사;석사
21	백미영	'98.01 ~ '00.02	물리	학사;석사
22	이윤상	'98.01 ~ 현재	화학	석사;박사
23	장명진	'98.09 ~ '02	물리	석사
24	정소현	'99.01 ~ '02	물리	학사;석사
25	최용운	'99.02 ~ '01.02	생물-종양	학사;석사
26	서강준	'99.12 ~ '01.02	물리	학사;석사
27	강은주	'99.12 ~ '05.02	인지신경과학	연구교수
28	홍성민	'00.01 ~ '02	화학	학사;석사
29	김영애	'00.01 ~ '01.03	물리	학사
30	강혜진	'00.04 ~ 현재	인지신경과학	학사;석사;박사
31	염정열	'00.07 ~ '01.06	물리	학사;
32	조성일	'00.08 ~ '01.02	물리	학사
33	김준식	'00.08 ~ '01.02	물리	학사
34	김희정	'00.09 ~ '12.12	인지신경과학	학사;석사;박사
35	조현주	'00.11 ~ '00.11	물리	학사
36	문인섭	'00.11 ~ '03.02	PET센터	학사
37	신재훈	'00.11 ~ '03.02	생물-종양	학사;석사
38	김진수	'00.12 ~ '07.09	물리	학사;석사;박사

39	김형우	'01.02 ~ '08.12	화학	석사;박사
40	최경묵	'01.03 ~ '01.09	인지신경과학	학사
41	조상수	'01.03 ~ '06.02	인지신경과학	석사;박사
42	신희원	'01.07 ~ '03	물리	학사
43	이병일	'01.09 ~ '06	물리	석사;박사
44	강주현	'01.10 ~ '02.11	생물-종양	박사연구교수
45	윤현미	'01.12 ~ '02.09	물리	학사
46	오현정	'01.12 ~ '03.02	생물-종양	학사;석사
47	윤영현	'02.01 ~ '03.03	화학	석사;박사
48	김광일	'02.02 ~ '09.02	생물-종양	학사;석사;박사
49	김숙아	'02.03 ~ '03.03	인지신경과학	학사
50	김윤희	'02.04 ~ '06.04	생물-뇌과학	학사;석사
51	소민경	'02.11 ~ '08.12	생물-종양	학사;석사;박사
52	이현정	'03.02 ~ '03.03	인지신경과학	학사
53	서선영	'03.02 ~ '03	화학	학사;석사
54	김현승	'03.02 ~ '04.02	인지신경과학	학사;석사
55	배여울	'03.02 ~ '04.08	인지신경과학	학사
56	류정화	'03.02 ~ '03.08	화학	학사
57	전용현	'03.03 ~ '08.08	생물-종양	학사;석사;박사
58	황도원	'03.03 ~ '19.08	생물-뇌과학	학사;석사;박사
59	김성봉	'03.05 ~ '03.07	인지신경과학	석사
60	정우석	'03.05 ~ '06.08	생물-종양	학사
61	황수영	'03.08 ~ '04.08	인지신경과학	학사
62	조혜주	'03.09 ~ '03.12	인지신경과학	학사
63	윤미선	'03.09 ~ '04.02	인지신경과학	석사;박사
64	김정희	'03.09 ~ '04.08	인지신경과학	석사
65	손지연	'03.12 ~ 현재	전임상분자영상-분당	학사;석사
66	이윤상	'04.03 ~ '05.02	인지신경과학	학사
67	정인순	'04.04 ~ '15.01	신경화학-분당	석사
68	김정태	'04.05 ~ '04.08	인지신경과학	석사
69	Ganesha Rai	'04.07 ~ '05.12	화학	박사
70	김영남	'04.07 ~ '07.02	생물-종양	석사;박사
71	김중현	'04.07 ~ '12.08	물리	학사;석사;박사과정
72	윤현석	'04.07 ~ '15.12	물리	학사;석박통합과정
73	이태선	'04.09 ~ '04.12	인지신경과학	학사
74	김수진	'04.09 ~ '09.08	물리	학사;석사;박사
75	이학정	'04.09 ~ '14.04	화학	학사;석사;박사과정
76	조상수	'04.10 ~ 현재	인지신경과학-분당	박사
77	류창형	'04.10 ~ '05.03	인지신경과학-분당	학사;석사
78	김승후	'04.11 ~ '11.01	생물-종양	학사;석사;박사
79	염찬주	'04.11 ~ '11.02	생물-종양	학사;박사
80	김수미	'04.01 ~ '10.08	물리	학사;석사;박사
81	이은주	'05.02 ~ '06.02	인지신경과학-분당	석사
82	황지희	'05.02 ~ '06.02	인지신경과학-분당	학사;석사

83	박창수	'05.02 ~ '06.02	인지신경과학-분당	석사
84	박소연	'05.02 ~ 현재	신경화학-분당	석사
85	정혜경	'05.02 ~ '08.09	생물-종양	석사;박사
86	이지영	'05.03 ~ '07.01	생물-뇌과학	학사;석사
87	김현주	'05.03 ~ '09.02	생물-종양	학사;석사;박사
88	라민균	'05.03 ~ '05.08	물리	학사
89	오정수	'05.03 ~ '06.12	물리	박사
90	윤은진	'05.04 ~ '14.02	인지신경과학-분당	학사;석사;박사
91	박효진	'05.04 ~ '13.04	인지신경과학	학사;석박통합과정
92	한상희	'05.08 ~ '06.09	물리	학사
93	최기준	'05.11 ~ '06	물리	학사
94	김지선	'05.12 ~ '11.02	화학-분당	석사
95	김순학	'06.01 ~ '09.03	생물-뇌과학	연구교수
96	홍수경	'06.03 ~ '08.09	신경화학-분당	석사;박사
97	박민재	'06.03 ~ '10.05	물리	석사;박사
98	Prashant	'06.06 ~ '07.08	화학	박사
99	방성애	'06.07 ~ '16.02	인지신경과학-분당	석사;박사
100	Dinesh Shetty	'06.08 ~ '11.05	화학	석사;박사
101	이병철	'06.09 ~ 현재	화학-분당	박사
102	박상근	'06.09 ~ '10.12.	물리	경기대 전자계산학과
103	박현수	'06.11 ~ 현재	영상분석-분당	석사;박사
104	권순일	'06.12 ~ '13.02	물리	학사;박사
105	김현희	'07.04 ~ '09.08	생물-종양	학사;석사
106	임윤경	'07.04 ~ '11	인지신경과학	학사;석사과정
107	이애리	'07.07 ~ '07.12	생물-뇌과학	학사
108	고해영	'07.07 ~ '09.11	생물-종양	학사;석사
109	김영하	'07.08 ~ '08.01	생물-뇌과학	학사
110	최재연	'07.11 ~ '11.07	화학	학사;석사과정
111	고미향	'07.12 ~ '09.03	생물-뇌과학	학사;석사
112	양보연	'08.01 ~ '14.02	화학	학사;박사
113	김영화	'08.01 ~ '13.12	생물-종양	학사;박사
114	전영신	'08.03 ~ '09.04	화학-분당	석사
115	유경현	'08.03 ~ '10.06	생물-종양	학사;석사
116	Lathika Hoigebazar	'08.03 ~ '11.02	화학	석사;박사
117	주창환	'08.04 ~ '09.12	화학	학사
118	윤혜원	'08.08 ~ '11.02	생물-종양	박사
119	김은경	'08.09 ~ '09.08	인지신경과학	학사;석사과정
120	김수진	'08.10 ~ 현재	영상분석-분당	박사
121	문병석	'09.01 ~ '19.02	화학-분당	박사
122	이찬미	'09.01 ~ '10.12	인지신경과학	학사;석사
123	진연아	'09.01 ~ '11.08	생물-뇌과학	학사;석사
124	이또오 미끼꼬	'09.01 ~ '12.03	물리	학사;석사;박사
125	함자랑	'09.01 ~ '15.09	인지신경과학	학사;석사;박사
126	김지후	'09.01 ~ '17.01	물리	학사;석사;박사

127	고근배	'09.01 ~ '17.04	물리	학사;박사
128	이지연	'09.01 ~ '19.01	화학	학사;석사;박사
129	조혜림	'09.03 ~ '09.05	물리	학사
130	이규임	'09.03 ~ '09.05	생물-뇌과학	학사
131	이혜경	'09.03 ~ 현재	인지신경과학	박사
132	이영경	'09.03 ~ '11.02	화학	학사;석사
133	이보은	'09.04 ~ '17.02	화학	석사;박사
134	한현정	'09.04 ~ '09.10	인지신경과학-분당	석사
135	장신정	'09.05 ~ '11.11	생물-종양	학사
136	오현정	'09.05 ~ '16.04	생물-뇌과학	학사;석사
137	송명근	'09.07 ~ 현재	생물-종양	석사;박사
138	손경일	'09.08 ~ '11.01	화학-분당	석사;박사과정
139	이 송	'09.09 ~ '13.03	생물-뇌과학	박사
140	장재호	'09.09 ~ '12.12	생물-뇌과학	학사;석사
141	나주리	'09.09 ~ '16.08	생물-종양	학사;석사;박사
142	임남희	'09.10 ~ '11.09	전임상분자영상-분당	학사
143	유은혜	'09.10 ~ '11.04	물리	학사
144	정재호	'09.11 ~ 현재	신경화학-분당	석사
145	김정환	'09.12 ~ 현재	화학-분당	학사
146	조은아	'10.02 ~ '17.03	화학	학사;석사;박사중퇴
147	유혜빈	'10.03 ~ '12.02	물리	
148	손정아	'10.09 ~ '13.08	물리	석사
149	Sudhakara Seelam	'10.08 ~ '17.01	화학	박사
150	방남영	'11.03 ~ '13.08	WCU	학사;석사
151	김은경	'11.03 ~ '17.03	인지	
152	정태문	'11.03 ~ '16.02	생물-종양	학사;석사;박사
153	문성현	'11.03 ~ '16.08	화학	학사;박사
154	김호영	'11.03 ~ '19.08	화학	학사;박사
155	장솔아	'11.09 ~ '13.08	종양	학사;석사
156	최재혁	'11.09 ~ '14.02	뇌과학	학사;석사
157	신성아	'12.03 ~ '19.02	물리	학사;석사;박사
158	안현준	'12.03 ~ '19.02	물리	학사;박사
159	함자랑	'12.03 ~ '15.02	인지	학사;박사
160	김경윤	'12.03 ~ '17.04	물리	학사;박사
161	이철희	'12.03 ~ '18.08	종양	학사;박사
162	이민선	'12.03 ~ '19.02	물리	학사;박사
163	손정환	'12.03 ~ '19.02	물리	학사;박사
164	Vinay K. Banka	'12.03 ~ '19.02	화학	학사;박사
165	허영민	'12.09 ~ 현재	인지	학사;석사;박사
166	김한수	'13.02 ~ '14.12.	뇌과학	석사연구원
167	원준연	'13.03 ~ '19.02	물리	학사;박사
168	박지용	'13.03 ~ 현재	화학	학사;석사;박사
169	김한영	'13.09 ~ '15.08		학사;석사
170	이영은	'13.09 ~ '16.02	종양	학사;석사

171	정석진	'14.03 ~ '19.02	종양	학사;박사
172	배성우	'14.03 ~ '16.01	종양	학사;석사
173	강승관	'14.03 ~ 현재	물리	학사;박사과정
174	박초롱	'14.03 ~ '19.12	종양	학사;석사;박사과정
175	M. K. Bakht	'14.09 ~ ?	종양-핵의학	석사;박사과정
176	김경민	'14.09 ~ '20.02	종양	학사;박사과정
177	김아란	'14.08 ~ '17.01	전임상분자영상-분당	학사
178	신재환	'15.12 ~ 현재	화학	박사
179	조정환	'15.03 ~ '17.08	종양	학사;석사
180	박해욱	'15.03 ~ 현재	물리	학사;박사과정
181	Arun Gupta	'15.03 ~ '18.08	임상	석사;박사
182	김도현	'15.07 ~ '18.10	뇌과학	석사연구원
183	Nadeem A. Lodhi	'15.09 ~ '19.08	화학	석사;박사
184	황동휘	'15.09 ~ 현재	물리	학사;박사과정
185	박도담	'15.01 ~ '17.06	전임상실험-분당	학사
186	정유진	'15.07 ~ '17.06	방사화학-분당	학사
187	배성환	'16.12 ~ '20.07	종양	석사연구원
188	G. B. Borjigon	'16.03 ~ '18.02	임상	학사;석사
189	이은지	'16.03 ~ 현재	뇌과학	학사;석사;박사과정
190	오세라	'16.03 ~ 현재	종양	학사;박사과정
191	오호림	'16.03 ~ 현재	종양	학사;박사과정
192	정다이	'16.09 ~ '19.02	뇌과학	학사;석사
193	이승은	'16.09 ~ 현재	물리	학사;박사과정
194	김영낭	'16.03 ~ '19.05	전임상실험-분당	학사
195	임관미	'16.05 ~ 현재	임상실험-분당	학사
196	박기선	'16.06 ~ 현재	전임상분자영상-분당	학사
197	유정민	'16.10 ~ '17.02	방사화학-분당	학사
198	권준호	'17.01 ~ '19.02	종양	석사연구원
199	장근녕	'17.03 ~ '19.03	뇌과학	학사;석사
200	박준영	'17.03 ~ '19.02	물리	학사;석사
201	장혜정	'17.03 ~ '19.02	종양	학사;석사
202	Qaid A. Shagera	'17.03 ~ '19.02	임상	학사;석사
203	오진혜	'17.03 ~ 현재	뇌과학	학사;석사과정
204	윤지원	'17.09 ~ '19.02	뇌과학	석사편입-석사
205	기영욱	'17.09 ~ '19.08	뇌과학	박사편입
206	정은진	'17.09 ~ '19.08	종양	학사;석사
207	이석용	'17.09 ~ 현재	화학	학사;석사과정
208	강형근	'17.01 ~ '17.12	전임상분자영상-분당	학사
209	육영청	'17.03 ~ '18.12	방사화학-분당	석사
210	김유경	'17.07 ~ '18.08	전임상실험-분당	학사
211	송인호	'17.11 ~ 현재	전임상실험-분당	박사
212	이영선	'18.03 ~ '19.02	뇌과학	학사;석사
213	권용경	'18.03 ~ '20.08	화학	학사;석사과정
214	이현구	'18.07 ~ '19.08	종양	학사연구원

215	김효영	'18.07 ~ '19.08	종양	학사연구원
216	서혜연	'18.09 ~ 현재	화학	학사;석사과정
217	이상현	'18.09 ~ '20.08	화학	학사;석사과정
218	김지현	'18.08 ~ 현재	방사화학-분당	석사
219	이수아	'19.03 ~ '20.02	물리	학사;석사과정
220	김 현	'19.09 ~ 현재	뇌과학	학사;석사과정
221	권석준	'19.09 ~ 현재	뇌과학	학사;석사과정
222	Azmal K. Sarker	'19.09 ~ 현재	임상	석사;박사과정
223	서민지	'19.09 ~ 현재	물리	학사;석사과정
224	이수정	'19.07 ~ 현재	전임상실험-분당	학사
225	황지희		인지신경과학-분당	학사;석사
226	박창수		인지신경과학-분당	석사

2) 역대 직원 해외연수

연수기간	이름	연수국	연수기관	지도교수	연수내용
'78.03~05	서일택	일본	Kyoto University Hospital	Kanji Torizuka	방사면역측정기술
'78.12~'79.03	조규진	일본	Tokyo Metropolitan Geriatric Hospital	Masahiro Iio	촬영기술
'78.12~'79.03	김현주	일본	Bioorganic Chemistry College of Pharmacy, Shizuoka	Noboru Yanai-hara	방사면역측정기술
'80.02~05	박현숙	미국	Michael Reese Hospital	Steven Pinsky	컴퓨터응용기술
'80.06~09	동희초	홍콩	University of Hong Kong Robert Black College	J. Prestoy	방사면역측정기술
'80.10~'81.01	안순자	대만	Veterans General Hospital	Shin-Hwa Yeh	방사성의약품합성기술
'82.04~06	진광호	일본	Gunma University	Teruo Nagai	감마카메라정도관리
'82.12~'83.03	정윤영	대만	Veterans General Hospital	Shin-Hwa Yeh	방사면역측정 법 정도관리
'83.06~08	유광열	일본	Kyoto University Hospital	Kanji Torizuka	컴퓨터응용기술
'85.02~07	조규진	미국	Michael Reese Hospital	Pinsky	촬영기술
'85.12~'86.03	전병길	일본	National Institute of Radiological Sciences	Toshiyaki Kumatory	방사성의약품정도관리
'87.01~04	이인원	일본	Osaka Cardio-vascular Center	Tsunehiko Nishimura	핵의학장비정도관리
'87.08~10	이재길	일본	Kyoto University Hospital	Kanji Kasagi	방사면역측정법 정도관리
'88.09~11	김문혜	일본	Kyoto University Hospital	Kanji Kasagi	핵의학 컴퓨터이용
'89.06~07	서일택	미국	George Washington University Medical Center	Chang H.Paik	방사수용체 검사 및 방사성의약품

'89.10	염미경	태국	IAEA/WHO/RCA program		IAEA/WHO/RCA Training Course
'90.02~04	조규진	호주	IAEA/WHO/RCA program Royal Prince Alfred Hospital	Brian Hitton	IAEA/WHO/RCA Training Course
'90.06~09	변대홍	일본	Kyoto University Hospital	Kanji Kasagi	SPECT 이용기술 습득
'92.03~04	김문혜	호주	IAEA/WHO/RCA program		감마카메라정도관리
'92.07~08	진광호	미국	University of Pennsylvania Hospital	Abass Alavi	SPECT 기술습득
'93.08~10	박은미	일본	Aging and Cencer, Tohoku University	Hiroshi Fukuda	방사수용체검사기술
'94.02~03	이인원	미국	Cleveland Metro Clinic	Batec	SPECT 도입에 따른 기술연수
'94.12	서일택	일본	Osaka City University	Hironobu Ochi.	중간관리자 교육
'94.12	김문혜	일본	Osaka Cardio-vascular Center	Tsunehiko Nishimura	PET 도입에 따른 연수
'95.09	정수욱	태국	IAEA/WHO/RCA program	IAEA	HBsAg 검사법
'95.09~10	김현주	일본	Kyoto University Hospital	Junji Konishi	RIA 정도관리
'96.10~11	노경운	영국	Hammersmith Hospital	Chapuman	RIA 정도관리
'98.06~07	임형태	미국	Royola Medical Center	Robert Henkin	영상검사기술
'99.10	조만익	일본	Daiichi Radioisotope Laboratory	Junzo Okuda	RIA 정도관리
'00.06~07	신성화	미국	Johns Hopkins Medical Institute	Zsolt Szabo	SPECT 기술연수
'02.05~06	김진의	미국	M.D. Anderson Cancer Center	Euishin E. Kim	심근SPECT 기술연수
'04.06~07	이홍재	미국	University of Pennsylvania	Abass Alavi	PET 선진기술
'05.09	장영수	미국	Winship Cancer Institute, Emory University	Jonathan W. Simons	방사성의약품 합성, 개발
'06.06	조규진	미국	M.D. Anderson Cancer Center	Euishin E. Kim	관리자 연수
'08.06	문일상	미국	M.D. Anderson Cancer Center	Euishin E. Kim	PET 영상 신기술
'12.08	신선영	싱가폴	Singapore General Hospital	Sidney Yu	체외검사 및 정도관리
'18.08	도용호	독일	Klinikum rechts der Isar	Wolfgang Weber	핵의학치료기술 습득

2. 진료통계

1) 서울대학교병원 본원

가. 진료량

영상검사 계열별 비율

단위 %

연도	갑상선	비뇨기계	소화기계	뇌신경계	순환기계	근골격계	PET	기타
1968	91.1	8.9						
1970	43.3	12.7	43.9	2.6	1.6			
1975	81.6	10.5	6.4	1.1	0.2			
1980	29.3	6.8	46.2	0.4	8.8	8.6		0.1
1985	21.8	5.9	43.2	0.4	10.7	17.3		0.8
1990	27.0	8.5	8.0	5.4	13.0	37.0		1.1
1995	25.7	6.9	3.0	6.6	15.4	39.3		3.0
2000	20.6	5.8	1.4	2.6	14.8	46.2		8.6
2005	18.5	3.3	1.2	3.6	20.2	41.3	9.3	2.5
2009	10.0	2.6	1.4	3.3	11.2	42.1	24.2	5.2
2010	8.9	2.6	2.1	3.5	10.7	40.9	26.8	4.5
2011	7.8	2.9	2.2	3.2	9.6	38.3	31.0	4.9
2012	7.4	2.7	2.2	2.9	9.0	41.7	29.8	4.3
2013	6.2	2.3	2.1	2.6	5.9	39.3	36.0	5.6
2014	5.7	2.6	1.8	2.2	5.6	37.6	39.0	5.4
2015	5.6	2.9	1.7	4.0	4.9	42.7	32.7	5.5
2016	4.4	3.3	1.6	3.7	9.5	42.8	30.9	3.9
2017	3.0	3.3	1.9	3.1	9.9	44.6	30.8	3.4
2018	3.4	3.1	2.0	3.0	10.3	45.8	28.9	3.5
2019	3.4	3.6	1.7	3.0	9.6	45.2	30.2	3.3

단반감기 동위원소 생산량

(단위: mCi)

	^{18}F	^{11}C	^{15}O	^{13}N	^{64}Cu	^{124}I	합계
1995	26,634						26,634
1996	26,095						26,095
1997	23,116		1,920	98			25,134
1998	39,045	831	3,120	473			43,469
1999	31,536	476	2,220				34,232
2000	53,234	1,138					54,372
2001	52,735	632					53,367
2002	73,637	535					74,172
2003	203,868	1,198	5,340				210,406
2004	154,456	1,264	1,520				157,240
2005	120,091	1,680					121,771
2006	119,867	3,551	630				124,048
2007	89,160	2,411					91,571
2008	183,576	12,423	320				196,319
2009	154,209	9,245	5,760				169,214
2010	176,566	7,413	320				184,299
2011	358,787	7,675					366,462
2012	665,094	27,064		100	60		692,318
2013	677,427	34,827	10,800	30,600	390	5	754,049
2014	740,644	36,626		29,850	20		807,140
2015	614,919	50,354		26.250			691,523
2016	631.162	45,405	160	29,100			705,827
2017	719,139	25598		12300			757,037
2018	748,249	38,480	240	15,450			802,419
2019	835,650	48,050	480	16.260			900,440
계							

^{18}F-FDG 생산량, 사용량, 판매량

(단위: mCi, 원)

	생산량	사용량	판매량	판매금액
1995	26,634	4,460		
1997	23,116	7,190		
1998	39,045	8,940	66	1,650,000
1999	31,536	10,200	264	6,300,000
2001	52,735	13,180	8,429	248,805,700
2003	203,370	23,030	16,042	441,155,000
2005	113,845	28,340	2,592	71,280,000
2007	86,648	52,490	2,540	58,674,000
2009	152,593	58,165	0	
2010	176,566	81,170		
2011	358,787	91,920	520	12,012,000
2012	665,094	100,813		
2013	677,427	118,650		
2014	740,644	135,300	160	3,696,000
2015	614,919	101,160		
2016	631.162	98,580	280	12,320,000
2017	719,139	105,720	160	6,160,000
2018	739,949	95,710	570	25,080,000
2019	826,900	92,680	580	25,520,000

검체검사 계열별 건수

연도	갑상선	호르몬	간염	암표지자	알레르기 외	생물학적검사	합 계
1970	74					34	108
1975	2,192	589			39	18	2,838
1976	4,226	844		550	20	23	5,663
1977	5,874	2,168	227	860	153	30	9,312
1980	18,901	4,507	22,254	7,336	3,410	68	56,476
1985	34,579	14,405	33,855	10,936	6,034	37	102,729
1990	73,523	32,002	54,199	30,510	18,938	134	182,859
1995	100,547	31,057	47,022	55,345	21,605	73	255,649
2000	123,320	34,518	41,365	84,268	19,374	27	302,872
2005	253,065	58,412	60,704	230,167	32,894	134	635,376
2009	333,466	107,584	62,474	320,809	44,349	432	869,114
2010	326,005	120,847	51,234	308,277	67,055	469	873,887
2011	317,247	112,077	52,087	293,270	90,159	497	864,337
2012	352,409	112,994	49,094	302,442	96,880	335	914,154
2013	346,358	113,101	46,969	306,078	107,393	413	920,312
2014	319,921	106,636	30,304	288,735	103,224	266	849,086
2015	269,112	105,947	31,532	197,847	96,835	311	701,584
2016	263,228	112,754	34,310	193,312	110,055	329	713,988
2017	253,731	108,342	29,564	191,809	100,257	342	684,045
2018	251,811	118,516	32,292	195,654	99,812	398	698,483
2019	257,420	111,623	33,619	191,838	104,152	164	698,816

검체검사 건수 변화 (1970~2019)

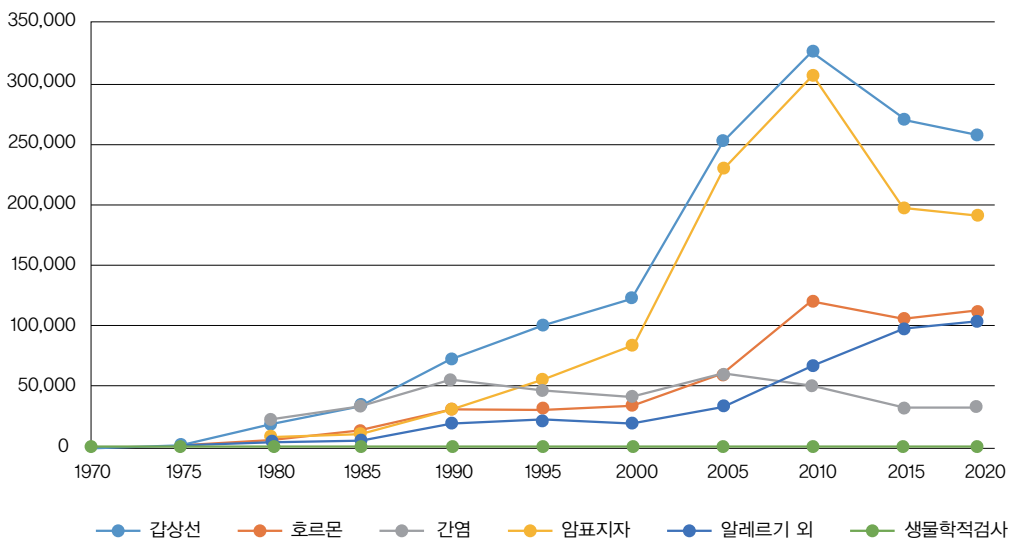

나. 장비

(1) 영상검사 장비

설치년도	장비명	제조사	모델명
1961	Scintiscanner		
	Rate meter system 2 channel		
1965	Spectrophotometer	BECKMAN	DU-2400
1969	Curimeter	ALOKA	F 38-11
	Gamma Camera	Nuclear Chicago	PHO GAMMA III
1977	Color Scanner		
1978	Gamma Camera System		Gamma 11 System GM-11PE DISITAL
	Spectro scaler	PICKER	111A
	Gamma Camera Scintillation	Nuclear Chicago	PHO GAMMA III
1979	Radiochromatogram scanner		7201
	Gamma Camera System	Ohio Nuclear	SIGMA 420
	Gamma Camera System	Ohio Nuclear	SIGMA 410
	Gamma Camera System	PICKER	DYNA 4/15
	Color Scanner		500/D 63020-G
1982	Gamma Camera (Detector for scintilation)		MEDX-S37
1985	Multi format imager		6825
1986	Fluorospectrophotometer		Farrand 3
	Gamma Camera System	SIEMENS	LEM
	Gamma Camera System		ZLC 75 ROTA
	Data processing computer system		MAX DELTA
1988	Dichromatic bone densitometer		
1989	Gamma Camera system	SIEMENS	ZLC 750 Orbiter
1994	Gamma Camera Whole Body Scan	SIEMENS	Body Scan
	Gamma Camera (SPECT)	PICKER	PRISM 2000
1995	Hot Cell	CAPINTEC	
	Cyclotron (PET Radioisotope)	EBCO	TR-13
	PET(Positron emission tomography)	SIEMENS	EXACT 47
	Beta flow detector system	GILSON	
	UV/VIS Spectrophotometer	HP	HP 8452 A
	Personal contamination monitor	BERTHOLD	LB 1043BX0
	Gamma Camera (SPECT)	PICKER	PRISM 3000
1996	Gamma Camera	ADAC	Solus
	Gas Chromatography	HP	5890II PRUS
	High Performance Liquid Chromatography		
	FDG Chemistry for PET		

1997	High speed image processing comp		
	High speed image processing comp		
	SUN Workstation Comp	SIEMENS	Ultra60
2001	Double Hot Cell	HEXCO	SYSTEM
2002	Gamma Camera	SIEMENS	E.CAM
	Vertex Gamma Camera	ADAC	ultra high tier
	Automatic F-18 FDG Labelling Sys.	IBA	W/Taget
2003	Gamma Camera	ADAC	FORTE
	Dose Calibrator	CAPINTEC	CRC-15R
	Fusion PET scanner	PHILIPS	Gemini
2005	Gamma Camera	ADAC	Sky Light
	FDG Module	EBCO	
2006	Gamma Camera	SIEMENS	E.CAM
	Gamma Camera	SIEMENS	E.CAM
	Gamma Camera	SIEMENS	E.CAM
2007	HPLC System	GILSON	321
	Gamma Camera	SIEMENS	E.CAM
	PET-CT Scanner	SIEMENS	Biograph 40
2008	Cardiac Gamma Camera	PHILIPS	CardioMD
	Gamma Camera(3-head)	TRIONIX	TRIAD XLT-9
2010	Thyroid Uptake System		Captus 3000
	Defibrillator		M-Series
	Clean Bench[RI 분배용 제작]		180LFC
	Clean Bench[Generator 저장용 제작]		150LFC
2011	Cyclotron	GE	PETtrace 10
	PET-CT Scanner	SIEMENS	MCT40
	SPECT-CT Scanner	GE	Discovery NM/CT 670
2012	PET-CT Scanner	SIEMENS	MCT64
	SPECT-CT Scanner	GE	Discovery NM/CT 670
2013	PET-MRI Scanner	SIEMENS	mMR
	HPLC System	Gilson	381H4A014
2015	Radiopharmaceutical Synthes Module	GE	Tracelab FXCpro
	HPLC Systems	Gilson	381H4A014
2017	Gas Chromatography		Clarus 680 GC
	Automated Synthesis for Radiopharmaceuticals	GE	Fastlab 2
2018	Gamma Camera (SPECT)	Spectrum Dynamics	D-SPECT
2019	Dual Head Gamma Camera	GE	NM 830
2020	Dual Head Gamma Camera	Siemens	Symbia Evo Excel

(2) 검체검사 장비

설치년도	장비명	제조사	모델명
1970	Spectro Scaler, Gamma Counter	PICKER	
1979	Liquid scintillation Counter	PACKARD	B-3255
	Centrifuge(Refiegerated)	DUPONT	Rc-5B
1984	Centrifuge, Refrigerated	DAMON	DPR-6000
1986	Ultracentrifuge		OTB-75B(52960)
	Gamma Counter	PACKARD	Multi-PRiAS 5304
	Gamma Counter four Detector	PACKARD	PRIAS
1989	Liquid Scintillation Counter	PACKARD	TRI-CARB 2200CA
	Gamma Counter (auto multidetector)	PACKARD	COBRA 5010
1995	Table top Refrigerated Centrifuge	HANIL	UNION 32R
	Centrifuge(Lage Capacity Refiegerated)	HANIL	UNION 5KR
	Beed Washer	ABBOTT	PROQUANTUM
1996	Gamma Counter (auto multidetector)	PACKARD	COBRA QUINTOM
	Autosampler	ML AT PLUS 2	ML AT PLUS 2
1997	Dynamic Incubator	ABBOTT	COMMANDER
2000	Automatic RIA System	STRATEC	RIA-MAT 280
2004	Gamma Counter		Wallac 1470
2005	Tube & Bead Washer	HOIL	Multi-Washer 50
2006	Autosampler	HAMILTON	Microlab AT Plus 2
2007	Ultra Refrigerated Centrifuge	KUBOTA	5930
	Autosampler	TECAN	Freedom EVO
	Shaking Water Bath		CYROMAX 929
2012	Gamma Counter		Gamma-10
	Refrigerated Centrifuge	KUBOTA	5930
	Auto washer		Multi-Washer 50
2013	Automation Radioimmunoassay Analyzer		GammaPro
2015	Auto sampler		DS8150
2016	Gamma Counter		DREAM GAMMA-10
	Auto washer		TW300
	Auto washer		Multi-Washer 50
2017	Refrigerated Centrifuge	KUBOTA	5930
	Refrigerated Centrifuge	KUBOTA	5930
	Refrigerated Centrifuge	KUBOTA	59360
2018	Auto Sampler		MASSIA DS 8150
	RI Hood		BH5 HEAVY
	Refrigerated Centrifuge		5930
2019	Automation Radioimmunoassay Analyzer		Dream Gamma 10
	TLC Scanner		AR-2000

다. 시설

(1) (구)방사성동위원소진료실

별관 연구동 건물(현 어린이병원) 1층에 위치하였다.

(2) 체내검사실

1979년 1월, 본원 1층 1파트로 이사 후 작은 시설변경이 있었으며 개보수를 위해 잠시 본원 지하 1층으로 옮겨 진료하였고 2000년 7월 현재 장소로 이전하였다. 면적은 207평이다. 2017년 11월에는 단계적 리모델링 공사를 거쳐 판독실, 영상분석실, 탈의실 등을 재배치하였다.

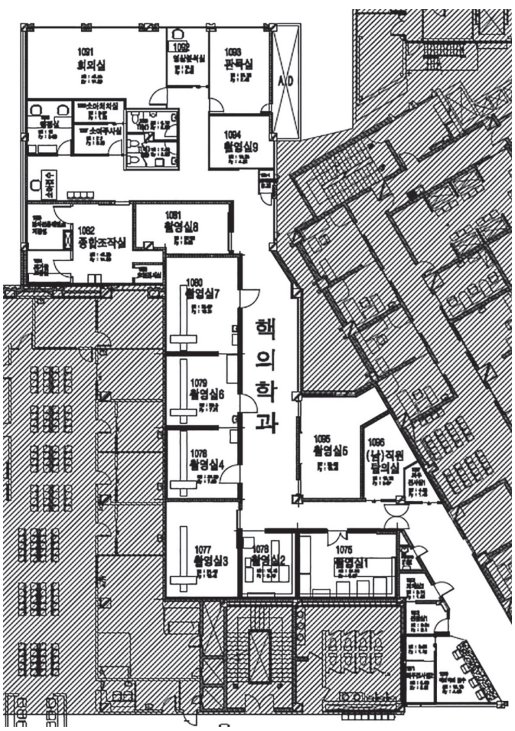

본관 1층 체내검사실 평면도 (2020)

(3) 체외검사실

1979년 1월, 설계당시 면적으로는 이전이 불가능하여 병실이었던 본원 3층 4파트로 이사하였고 핵의학동을 신축하여 1985년 12월, 본원 2층 8파트에 자리 잡았다. 개보수를 위해 2000년 8월 본원 지하 1층으로 옮겨 진료하였다가 과장실, 교수실을 포함하여 2001년 5월 다시 이전하였고 면적은 210평이었다. 부족한 교수실 2실은 13층에 위치하였다. 2017년 10월 교수실, 행정실, 체외검사실이 병원 본관 2층에서 의생명연구원 6층으로 이전하며 체외검사실이 기존 196평에서 206평으로 소폭 확장되어 보다 쾌적한 환경에서 핵의학 검체검사를 수행하고 있다.

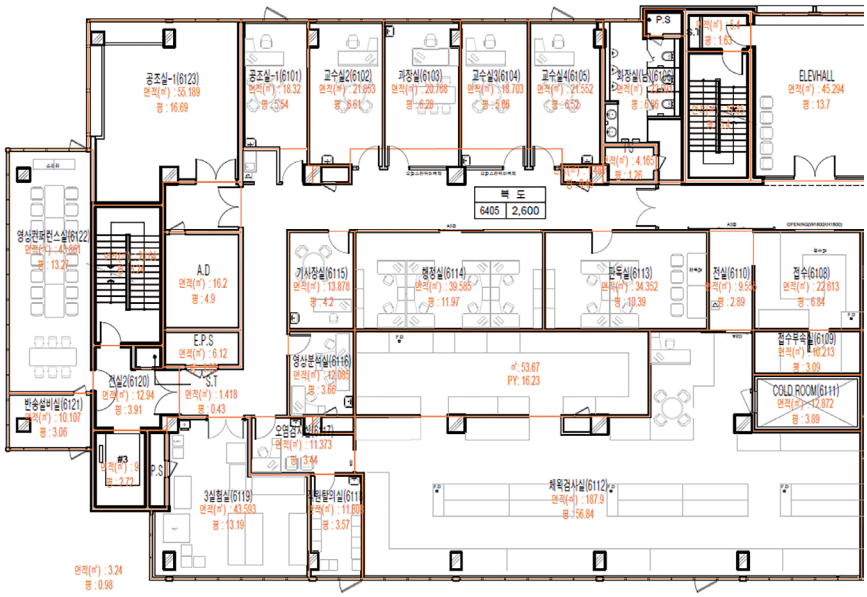

의생명연구원 6층 핵의학과 평면도 (2020)

(4) 소아핵의학검사실

1985년 소아병원 개원 시 지하 1층에 위치하였고 어린이병원 전체 개보수 계획에 의해 개보수 후 2009년 7월 4층으로 옮겼다. 면적은 47평이었다. 2017년 어린이병원의 공간부족 해소를 추진하는 병원에 협력하여 소아핵의학검사실은 본관 1층 핵의학과에 통합하였다.

(5) 종양핵의학검사실 (구 PET 센터)

1994년 6월 본원-소아병원 연결복도 지하 1층에 위치하였으며 2007년 9월 신규장비 설치로 인해 대기실을 분리, 복도 건너편으로 이전하였다. 면적은 180평이었다. 2011년 암병원 개원으로 시설, 장비 등을 새로운 환경에 걸맞게 개편하였으며, 암병원 내에 영상의학과와 함께 개설한 종양영상센터 종양핵의학검사실로 변경하였으며, 새로운 영상장비와 사이클로트론을 도입하였다.

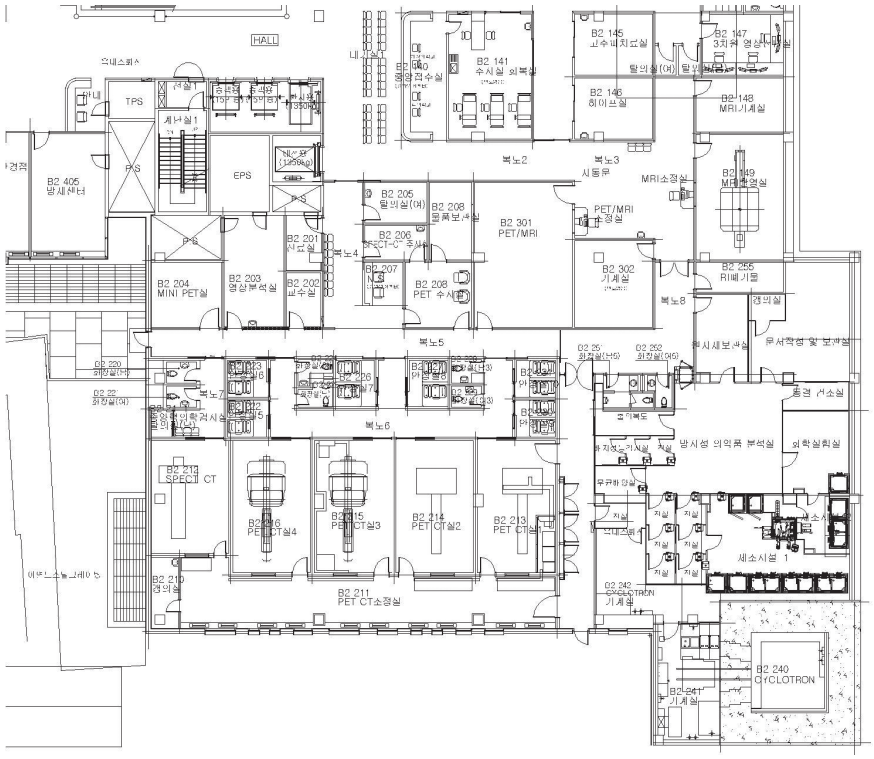

암병원 지하2층 종양핵의학검사실 평면도 (2020)

2) 분당서울대학교병원

가. 진료량

분당병원 전체 영상검사건수

	2003	2004	2005	2006	2007	2008	2009	2010	2011	2012	2013	2014	2015	2016	2017	2018	2019
순환기계	1,165	2,631	2,487	2,487	1,910	1,875	1,591	1,585	1,266	1,356	1,335	1,308	1,249	1,014	986	1,103	1,206
뇌신경계	265	927	1,135	1,135	783	696	684	651	931	945	1,387	1,300	1,296	1,365	1,318	1,224	868
소화기계	103	384	501	501	531	585	412	396	482	638	537	463	512	586	545	488	513
비뇨기계	153	237	164	164	203	180	326	463	600	976	851	905	1,145	1,448	1,627	1,845	1,972
근골격계	1,360	2,470	3,257	3,257	3,647	3,555	3,701	3,606	3,749	4,209	4,809	5,073	5,625	5,637	6,364	7,284	8,134
갑상선	704	1,463	1,626	1,374	1,246	1,745	1,780	1,760	1,458	1,424	1,197	1,091	814	1,038	1,050	983	1,040
PET	295	1,138	1,495	1,495	2,669	2,670	3,578	4,118	4,695	5,568	5,892	6,799	5,368	5,942	6,716	6,367	6,937
치료	2	86	252	321	437	945	1,083	1,021	917	896	789	750	424	348	355	423	418
기타	327	965	1,201	1,201	813	938	836	894	1,029	1,342	1,520	1,724	1,649	1,844	2,102	2,009	2,499
Total	4,374	10,301	12,118	11,935	12,239	13,189	13,991	14,494	15,127	17,354	18,317	19,413	18,082	19,222	21,063	21,726	23,587

영상검사 건수 변화 (분당병원)

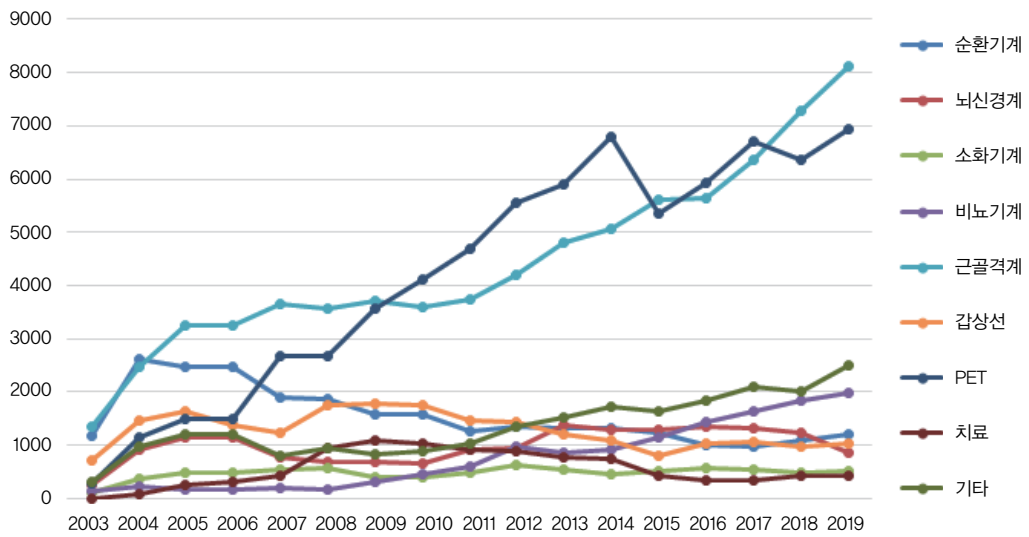

영상검사 계열별 비율

	2003	2004	2005	2006	2007	2008	2009	2010	2011	2012	2013	2014	2015	2016	2017	2018	2019
순환기계	27%	26%	21%	21%	16%	14%	11%	11%	8%	8%	7%	7%	7%	5%	5%	5%	5%
뇌신경계	6%	9%	9%	10%	6%	5%	5%	4%	6%	5%	8%	7%	7%	7%	6%	6%	4%
소화기계	2%	4%	4%	4%	4%	4%	3%	3%	3%	4%	3%	2%	3%	3%	3%	2%	2%
비뇨기계	3%	2%	1%	1%	2%	1%	2%	3%	4%	6%	5%	5%	6%	8%	8%	8%	8%
근골격계	31%	24%	27%	27%	30%	27%	26%	25%	25%	24%	26%	26%	31%	29%	30%	34%	34%
갑상선	16%	14%	13%	12%	10%	13%	13%	12%	10%	8%	7%	6%	5%	5%	5%	5%	4%
PET	7%	11%	12%	13%	22%	20%	26%	28%	31%	32%	32%	35%	30%	31%	32%	29%	29%
치료	0%	1%	2%	3%	4%	7%	8%	7%	6%	5%	4%	4%	2%	2%	2%	2%	2%
기타	7%	9%	10%	10%	7%	7%	6%	6%	7%	8%	8%	9%	9%	10%	10%	9%	11%

영상검사 계열별 비율 (분당병원)

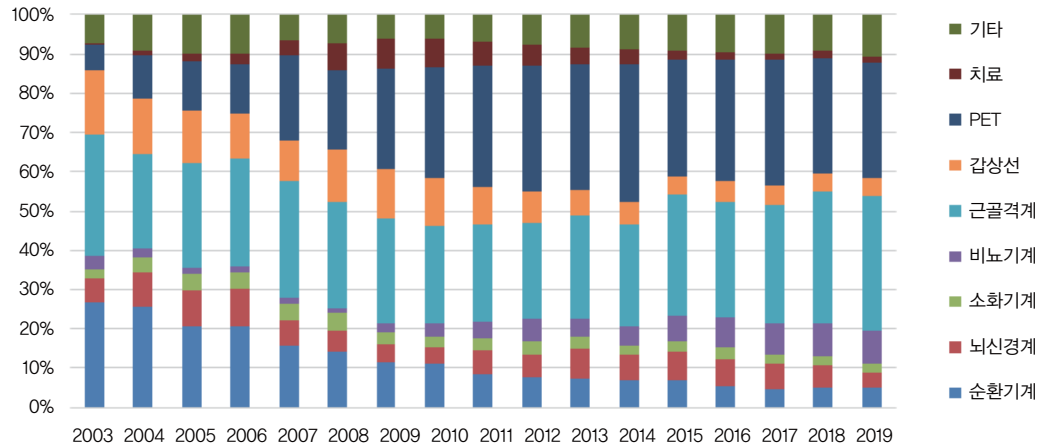

분당병원 검체검사 건수

	2003	2004	2005	2006	2007	2008	2009	2010	2011
Hormone	19,731	58,949	90,849	113,341	122,444	137,024	148,435	167,107	176,903
종양	7,260	20,442	31,779	54,026	61,887	69,249	72,912	83,706	96,476
빈혈	3,164	7,670	9,635	7,768	10,036	14,059	16,167	17,202	17,922
호르몬 자극검사	218	951	934	1,979	2,452	3,204	7,077	11,969	8,759
Biologic Study	0	1	0	0	19	41	46	0	0
기타	3,606	5,831	5,287	4,919	5,498	6,535	6,165	4,600	4,686
Total	33,979	93,844	138,484	182,033	202,336	230,112	250,802	284,584	304,746

	2012	2013	2014	2015	2016	2017	2018	2019
Hormone	191,862	204,297	219,221	234,514	262,693	278,569	289,706	299,633
종양	98,978	93,111	99,168	106,570	116,345	122,351	132,821	136,868
빈혈	17,669	20,268	22,927	22,867	25,925	24,384	23,662	25,794
호르몬 자극검사	7,155	8,748	8,635	11,100	14,933	17,360	16,563	15,396
Biologic Study	21	10	9	4	11	0	0	0
기타	4,889	5,288	5,071	6,041	7,959	11,563	16,259	13,544
Total	320,574	331,722	355,031	381,096	427,866	454,227	479,011	491,235

검체검사 건수 변화 (분당병원)

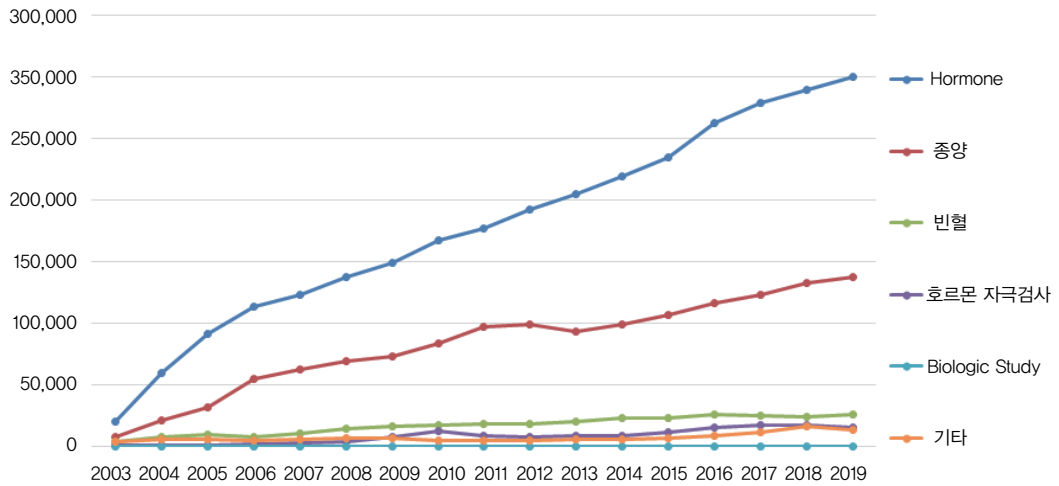

검체검사 계열별 변화 (분당병원)

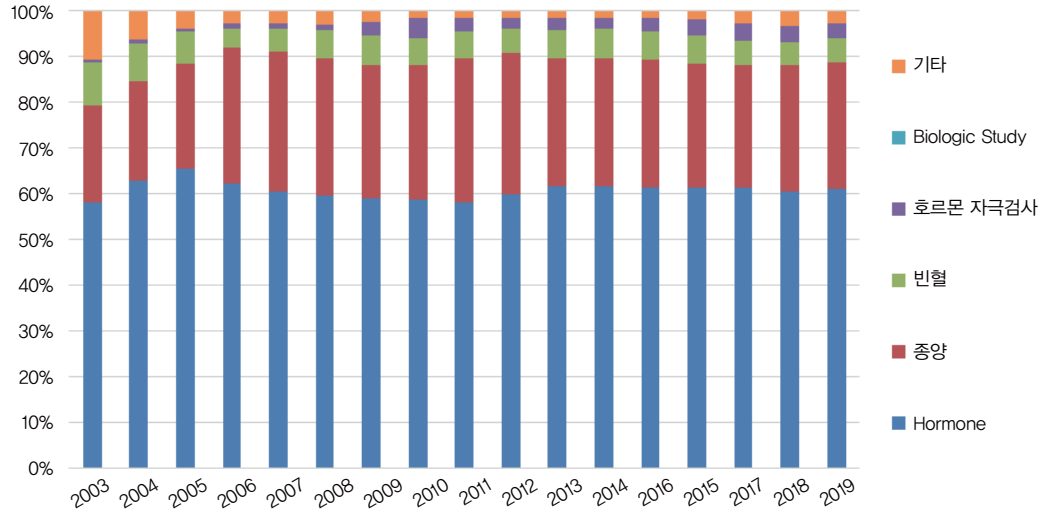

^{18}F-FDG 생산량, 사용량, 판매량

(단위: mCi, 원)

	생산량	사용량	판매량	판매금액
2008	115,106	15,750	70	1,617,000
2009	318,941	35,750	1,440	33,264,000
2010	275,544	40,910	3,150	72,765,000
2011	296,585	46,860	1,540	35,574,000
2012	364,162	55,550	620	14,322,000
2013	335,294	58,750		
2014	431,037	67,860		
2015	399,865	53,600		
2016	326,633	59,530		
2017	327,807	33,190		
2018	321,339	63,470		
2019	305,343	69,250		

동위원소 구입량

단위: mCi

	^{99m}Tc	^{131}I	^{201}Tl	^{18}F	^{125}I	^{123}I	기타	계
2003	24,000	22	3,412	1,820	6.9	89	16	29.366
2004	54,250	2,213	7,095	5,780	16.7	891	28.3	70.274
2005	111,700	7,205	6,796	12,460	22.3	810	26,8	139,025
2006	132,900	9,443	4,978	18,955	38.2	1,441	41.3	167,797
2007	129,700	11,984	14	26,390	32.4	573	15.9	168,709
2008	136,810	45,783	5,384	11,350	52.4	10	43.3	199,433
2009	130,250	52,610	7,634	830	123.2	735	25.5	45,904
2010	120,766	50,377	5,860	400	115.4	1,230	470.9	179,223
2011	128,250	44,925	5,989	3,380	85	388	18	183,035
2012	131,250	43,828	4,354	2,770	77.6	585	33.6	182,898
2013	129,350	33,948	4,468	6,210	50.8	5,627	601	180,255
2014	126,000	33,745	4,147	12,850	87.6	5,287	13.2	182,131
2015	193,028	25,370	4,179	3,059	423	4,798	12.8	230,870
2016	360,584	24,598	4,024	5,126	265	5,327	12	399,937
2017	379,947	25,260	3,527	12,840	254	4,182	23.2	426,084
2018	410,806	28,313	4,291	8,453	146	2,236	867.7	455,113
2019	455,067	31,290	3,850	9,574	252	361	656	501,041

나. 장비

(1) 영상검사 장비

설치년도	장비명	제조사	모델명
2003	Sinlge Head Gamma Camera	Philips	Argus
	Dual Head Gamma Camera	Philips	Vertex60
	Dual Head Gamma Camera	Philips	Forte
	PET	Philips	Allegro
	Thyroid Probe	세영엔디씨	koroid
2007	Triple Head Gamma Camera	Trionix	Triad XLT9
	Cyclotron	삼영유니텍	KIRAMS-13
2008	SPECT/CT	Bioscan	Nano SPECT/CT
2009	PET/CT	Ge Healthcare	Discovery VCT
	Module	GE	Tracelab FXCpro
	Module	GE	Tracelab FXFN
2011	PET/CT	Mediso	Nano PET/CT
2014	SPECT/CT	Ge Healthcare	Discovery NMCT 670
	Module	Ge Healthcare	Tracelab FXNpro

2015	PET/CT	Siemens	mCT FLOW
	Module	Synthra	MeI plus
	Module	Siemens	Explora One
2016	SPECT/CT	Ge Healthcare	Discovery NMCT 670 PRO
	HPLC	Agilent	G1311C
2017	Automated Synthesis for Radiopharmaceuticals	Ge Healthcare	Fastlab 2
2018	Ion Chromatograph System	Metrohm	Eco IC
2019	TLC Image Scanner	Brightspec	bSCAN
	Gas Chromatography	Perkin elmer	Clarus 690
	SPECT	Ge Healthcare	Discovery NM 630
	SPECT/CT	Ge Healthcare	Discovery NMCT 870 CZT

(2) 검체검사 장비

설치년도	장비명	제조사	모델명
2003	Centrifuge Table	한일과학	UNION 32R PLUS
	Centrifuge Refrigerated	한일과학	UNION 5KR
	Water Bath	비젼과학	KMC-1205WP
	Auto Sampler	Hamilton	Microlab AT Plus 2
	Gamma counter	Packard	COBRA5010
2004	Eppendorf Centrifuge	Eppendorf	Centrifuge 5810R
2006	Washer BEAD & TUBE	호일 바이오메드	MULTI - Washer 50
2010	Water Purification System	하나사이언스	PURE CHEM II
	Washer BEAD & TUBE	호일 바이오메드	MULTI - Washer 50
2011	Gamma counter	신진 메딕스	GAMMA 10
	Auto Sampler	신진 메딕스	DS8150
2012	Washer TUBE AUTO	신진 메딕스	DREAM TW300
2014	Gamma counter	신진 메딕스	GAMMA 10
2017	Auto RIA System	호일 바이오메드	Gamma PRO
2019	Auto RIA System	호일 바이오메드	Gamma PRO

다. 시설

분당병원은 1996년 3월 기공식을 하여 2002년 12월 준공식을 하였고 핵의학과는 본관 지하 1층에 위치하였으며 면적은 280평이다. 2007년 7월 사이클로트론센터를 본관 지하3층 120평 규모에 설치하기 시작하여 2008년 5월 준공식을 가졌고, 2011년 경기전임상분자영상센터 설립 관련하여 140평 규모로 증축하였다. 2016년 10월 검체검사실을 50평 규모로 이전 확장하였고, 11월에는 SPECT-CT실을 추가 하면서 50평 규모로 확장하였다. 2019년 단계적 리모델

링 공사를 거쳐 체내검사실 조정실, 안정실, 탈의실 등을 재배치하였으며, 2020년 현재 핵의학과의 총 면적은 380평 규모이다.

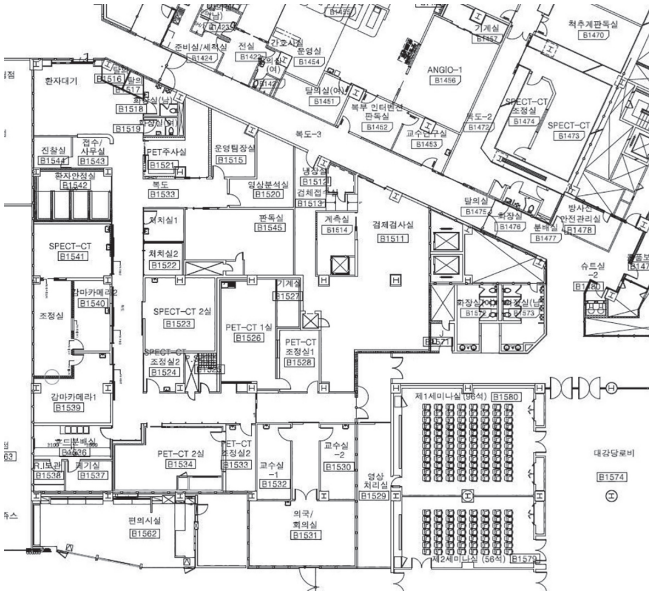

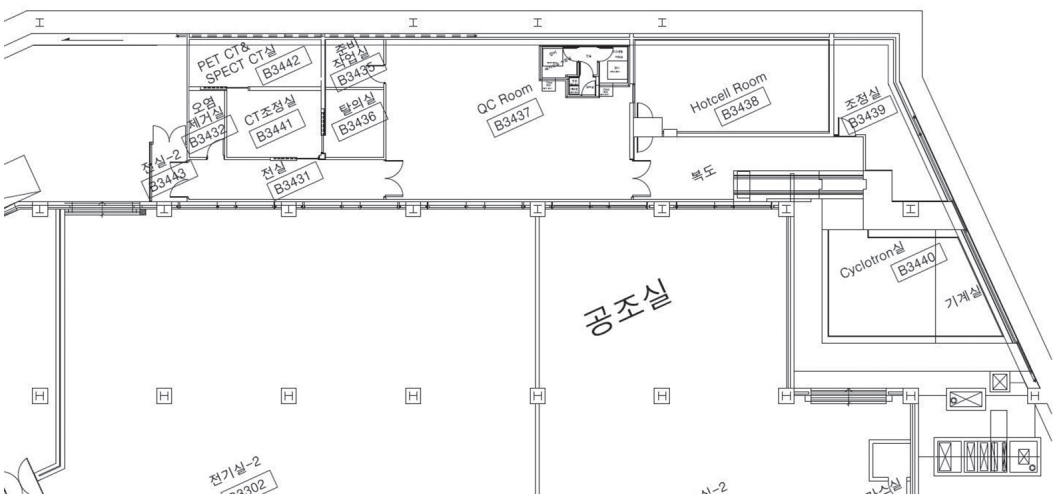

3) 서울특별시 보라매병원

가. 진료량

영상검사건수

구분	2013년	2014년	2015년	2016년	2017년	2018년	2019년
근골격계	3,966	3,778	4,831	5,439	4,833	4,979	4,806
비뇨기계	218	397	532	522	593	601	268
순환기계	1,328	2,633	2,588	2,740	2,623	2,254	2,997
소화기계	99	119	97	53	49	96	96
갑상선	808	632	539	489	363	565	413
뇌신경	8	187	170	207	228	137	171
종양	124	125	115	129	158	146	205
PET	3,819	3,665	2,027	2,377	2,137	2,362	2,676
치료	358	273	122	92	86	92	79
합계	10,370	11,536	10,899	11,956	10,984	11,140	11,711

영상검사 건수 변화 (보라매병원)

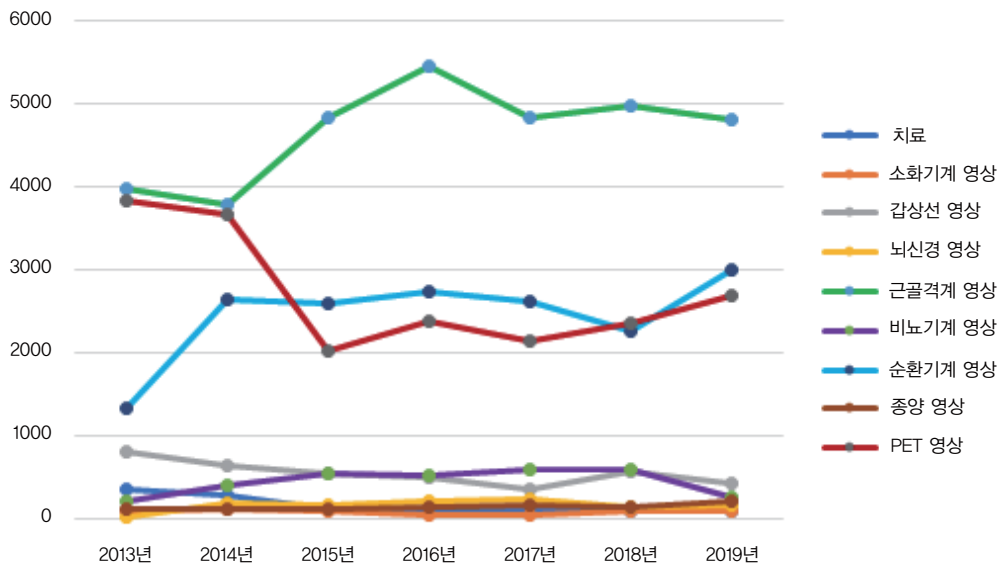

영상검사 계열별 비율

구분	2013년	2014년	2015년	2016년	2017년	2018년	2019년
근골격계	38.2	32.7	44.3	45.5	44.0	44.7	47.0
비뇨기계	2.1	3.4	4.9	4.4	5.4	5.4	2.6
순환기계	12.8	22.8	23.7	22.9	23.9	20.2	17.6
소화기계	1.0	1.0	0.9	0.4	0.4	0.9	0.9
갑상선	7.8	5.5	4.9	4.1	3.3	5.1	3.0
뇌신경	0.1	1.6	1.6	1.7	2.1	1.2	0.9
종양	1.2	1.1	1.1	1.1	1.4	1.3	1.6
PET	36.8	31.8	18.6	19.9	19.5	21.2	26.3
치료	3.5	2.4	1.1	0.8	0.8	0.8	0.8

영상검사 계열별 변화 (보라매병원)

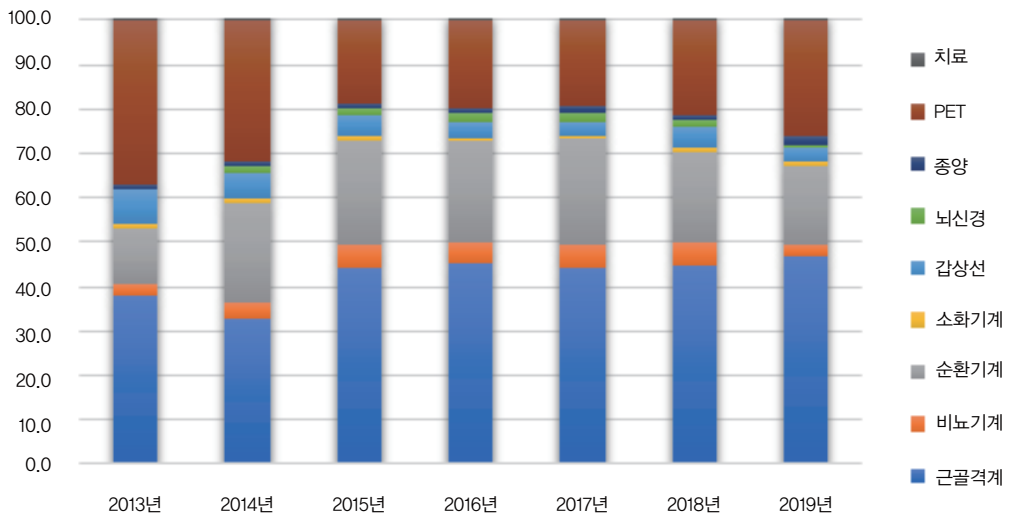

보라매병원 검체검사건수

	2013년	2014년	2015년	2016년	2017년	2018년	2019년
간염,종양,빈혈 및 기타	94,378	89,465	99,629	113,442	108,462	117,257	125,629
호르몬 자극검사	4,585	4,822	4,232	4,786	4,791	5,459	5,321
Biologic Study	208	231	125	96	83	86	0
Hormone	118,260	118,343	108,647	119,442	126,134	136,441	138,179
합계	217,431	222,136	212,633	237,766	239,470	259,243	269,129

검체검사 건수 변화

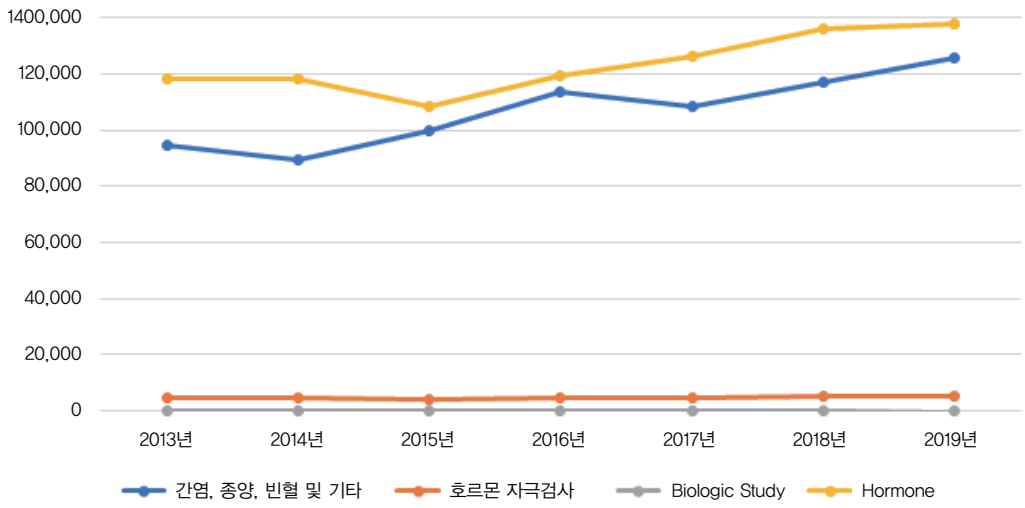

핵의학 체외검사 계열별 변화

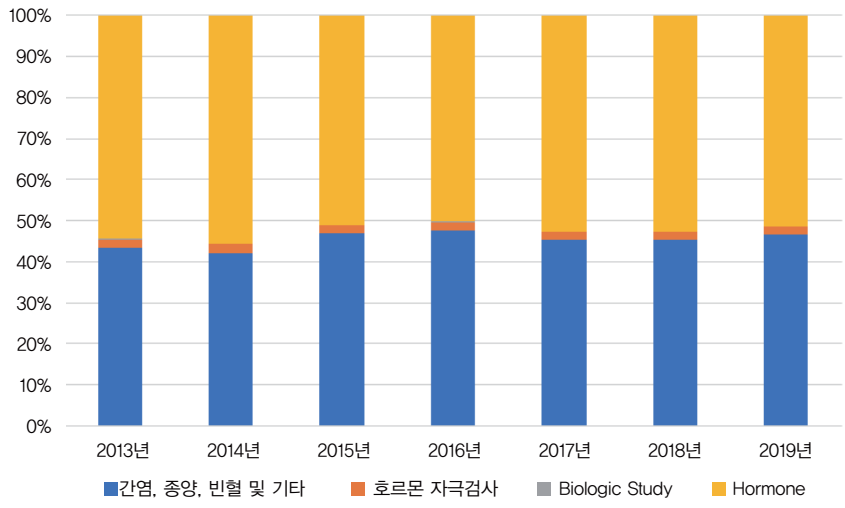

나. 장비

(1) 영상검사 장비

설치년도	장비명	제조사	모델명
2009	PET/CT Scanner	PHILIPS	Gemini TF64
	Gamma Camera (SPECT/CT)	GE	Hawkeye4
	Gamma Camera(3-head)	TRIONIX	TRIAD XLT9
	Gamma Camera	GE	INFINIA
	Gamma Camera	GE	INFINIA HE

(2) 검체검사 장비

설치년도	장비명	제조사	모델명
1997	Dynamic Incubator	ABBOTT	COMMANDER
1999	Gamma Counter	PACKARD	COBRA QUANTOM
2008	Autosampler	TECAN	Freedom EVO
	Tube & Bead Washer	HOIL	Multi-Washer 50
	Automatic RIA System	STRATEC	RIA-MAT 280

다. 시설

보라매병원은 1955년 서울특별시립영등포병원으로 출범하였고 1987년 본원에서 위, 수탁운영계약을 하게 되었으며 핵의학 검체검사실은 1991년 10월 본관 1층에 면적 40평 규모로 시작하였다. 새 병원이 신축됨에 따라 검체검사실은 2008년 5월 신관 3층 40평 규모로 이전하였고 이후 검체검사실을 포함한 주위면적 110평을 우선 개보수하여 2009년 5월부터 영상장비를 설치하고 8월에 진료를 시작하였다. 2013년 1월에는 희망관 4층에 약 10평 규모의 옥소치료병실 2실을 개설하여 운영하고 있다.

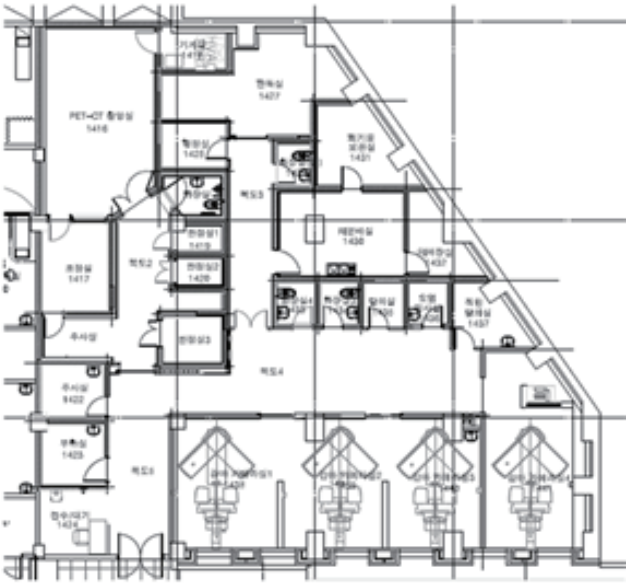

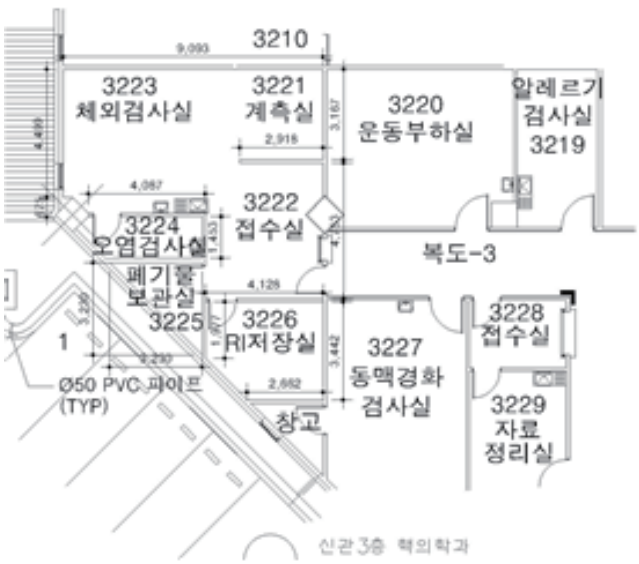
3210
3223
체외검사실
3221
계측실
3220
운동부하실
알레르기
검사실
3219
3222
접수실
3224
오염검사실
복도-3
폐기물
보관실
3225
3226
RI저장실
3227
동맥경화
검사실
3228
접수실
3229
자료
정리실
Ø50 PVC 파이프
(TYP)
창고
신관 3층 핵의학과

3. 주요 논문(2010년 이후)

2010년

1. Hong KS, Kang DW, Bae HJ, et al. Effect of cilnidipine vs losartan on cerebral blood flow in hypertensive patients with a history of ischemic stroke: a randomized controlled trial. Acta Neurol Scand. 2010;121:51–7.
2. Choo IH, Lee DY, Oh JS, et al. Posterior cingulate cortex atrophy and regional cingulum disruption in mild cognitive impairment and Alzheimer's disease. Neurobiol Aging. 2010;31:772–9.
3. Kim JS, Lee JS, Park MH, et al. Feasibility of template-guided attenuation correction in cat brain PET imaging. Mol Imaging Biol. 2010 Jun;12:250–8.
4. Seo H, Kim CH, Park JH, et al. Development of double-scattering-type Compton camera with double-sided silicon strip detectors and NaI(Tl) scintillation detector. Nucl Instr Meth A. 2010;615:333–9.
5. Kim JW, Yoon H, Kong SH, et al. Analysis of esophageal reflux after proximal gastrectomy measured by ireless ambulatory 24–hr esophageal pH monitoring and TC–99m diisopropyliminodiacetic acid (DISIDA) scan. J Surg Oncol. 2010;101:626–33.
6. Phi JH, Paeng JC, Lee HS, et al. Evaluation of focal cortical dysplasia and mixed neuronal and glial tumors in pediatric epilepsy patients using 18F-FDG and 11C-methionine pet. J Nucl Med. 2010;51:728–34
7. Phi JH, Cho B-K, Kim S-K, et al. Germinomas in the basal ganglia: magnetic resonance imaging classification and the prognosis. J Neuro-oncology. 2010;99:227–36.
8. Ito M, Lee JS, Park M-J, et al. Design and simulation of a novel method for determining depth-of-interaction in a PET scintillation crystal array using a single-ended readout by a multi-anode PMT. Phys Med Biol. 2010; 55:3827–41.
9. Ito M, Lee JS, Kwon SI, et al. A four-layer DOI detector with a relative offset for use in an animal PET system. IEEE Transactions on Nuclear Science. 2010;57:976–81.
10. Hwang DW, Ko HY, Lee JH, et al. A nucleolin-targeted multimodal nanoparticle imaging probe for tracking cancer cells using an aptamer. J Nucl Med. 2010;51:98–105.
11. Hwang DW, Song IC, Lee DS, et al. Smart magnetic fluorescent nanoparticle imaging probes to monitor microRNAs. Small. 2010;6:81–8.
12. Yang BY, Jeong JM, Kim YJ, et al. Formulation of 68Ga BAPEN kit for myocardial positron emission tomography imaging and biodistribution study. Nucl Med Biol. 2010;37):149–55.
13. Choi Y-S, Lee JY, Suh JS, et al. The systemic delivery of siRNAs by a cell penetrating peptide, low molecular weight protamine. Biomaterials. 2010;31:1429–43.
14. Lee YJ, Chung J-K, Kang JH, et al. Wild-type p53 enhances the cytotoxic effect of radionuclide gene therapy using sodium iodide symporter in a murine anaplastic thyroid cancer model. Eur J Nucl Med Mol Imaging. 2010;37:235–41.
15. Jeon YH, Kim Y-H, Choi K, et al. In Vivo Imaging of Sentinel Nodes Using Fluorescent Silica Nanoparticles in Living Mice. Mol Imaging Biol. 2010;12:155–62
16. Jeon YH, Choi Y, Kim CW, et al. Human sodium/iodide symporter-mediated radioiodine gene therapy enhances the killing activities of CTLs in a mouse tumor model. Mol Cancer Ther. 2010;9:126–33

17. Park YJ, Kim YA, Lee YJ, et al. Papillary microcarcimoma in comparison with larger papillary thyroid carcinoma in BRAF(V600E) mutation, clinicopathological features and immunohistochemical findings. Head Neck. 2010;32:38−45.
18. Choi Y, Jeon YH, Paik JH, et al. In vivo scintigraphic imaging of antitumor effects by combined radioiodine therapy and human sodium iodide symporter gene immunotherapy. Mol Imaging. 2010;9:141−52
19. Lee HY, Lee HJ, Kim YT, et al. Value of combined interpretation of computed tomography response and positron emission tomography response for prediction of prognosis after neoadjuvant chemotherapy in non-small cell lung cancer. J Thorac Oncol. 2010;5:497−503.
20. Kim S-K, Cho B-K, Phi JH, et al. Pediatric Moyamoya Disease: An Analysis of 410 Consecutive Cases. Ann Neurol. 2010;68:92−101
21. Shetty D, Jeong JM, Ju CH, et al. Synthesis of novel 68Ga-labeled amino acid derivatives for positron emission tomography of cancer cells. Nucl Med Biol. 2010;37:893−902.
22. Shetty D, Jeong JM, Ju CH, et al. Synthesis and evaluation of macrocyclic amino acid derivatives for tumor imaging by gallium−68 positron emission tomography. Bioorg Med Chem. 2010;18:7338−47.
23. Lim I, Kang KW, Myung JK, et al. Extravasation of hydroxymethylene diphosphonate-induced subcutaneous inflammation, histologically demonstrated in BALB/c mice. J Nucl Med. 2010;51:1573−5.
24. Kim SM, Lee JS, Lee CS, et al. Fully three-dimensional OSEM-based image reconstruction for Compton imaging using optimized ordering schemes. Phys Med Biol. 2010;55:5007−27.
25. Park M-H, Lee H-J, Kim JS, et al. Cross-modal and compensatory plasticity in adult deafened cats: a longitudinal PET study. Brain Res. 2010;1354:85−90.
26. Hoigebazar L, Jeong JM, Choi SY, et al. Synthesis and characterization of nitroimidazole derivatives for 68Ga-labeling and testing in tumor xenografted mice. J Med Chem. 2010;53:6378−85.
27. Shetty D, Choi SY, Jeong JM, et al. Formation and Characterization of Gallium(III) Complexes with Monoamide Derivatives of 1,4,7−Triazacyclononane−1,4,7−triacetic Acid: A Study of the Dependency of Structure on Reaction pH. Eur J Inorg Chem. 2010;5432−5438.
28. Kim HW, Lee Y-S, Shetty D, et al. Facile Chlorination of Benzyl Alcohols Using 1,8−Diazabicyclo[5.4.0]undec−7−ene (DBU) and Sulfonyl Chlorides. Bull Korean Chem Soc. 2010;31:3434−6.
29. Jhoo JH, Lee DY, Choo IH, et al. Discrimination of normal aging, MCI and AD with multimodal imaging measures on the medial temporal lobe. Psychiatry Res. 2010;30:183:237−43.
30. Chung HH, Kang KW, Cho JY, et al. Role of magnetic resonance imaging and positron emission tomography /computed tomography in preoperative lymph node detection of uterine cervical cancer. Am J Obstet Gynecol. 2010;203:156−65.
31. Chung HH, Nam B-H, Kim JW, et al. Preoperative [(18)F]FDG PET/CT maximum standardized uptake value predicts recurrence of uterine cervical cancer. Eur J Nucl Med Mol Imaging. 2010;37:1467−73.
32. Youn H, Jeong JM, Chung J-K. A new PET probe, (18)F-tetrafluoroborate, for the sodium/iodide symporter: possible impacts on nuclear medicine. Eur J Nucl Med Mol Imaging. 2010;37:2105−7.
33. Lee HW, Suh K-S, Kim J, et al. Pulmonary artery embolotherapy in a patient with type I hepatopulmonary syndrome after liver transplantation. Korean J Radiol. 2010l;11:485−9.

34. Kim YH, Oh SW, Lim YJ, et al. Differentiating radiation necrosis from tumor recurrence in high-grade gliomas: assessing the efficacy of 18F-FDG PET, 11C-methionine PET and perfusion MRI. Clin Neurol Neurosurg. 2010;112:758-65.

35. Ju CH, Jeong JM, Lee Y-S, et al. Development of a (177)Lu-Labeled RGD Derivative for Targeting Angiogenesis. Cancer Biother Radiopharm. 2010;25:687-91.

36. Seo H, Kim CH, Park JH, et al. Multitracing capability of double-scattering Compton imager with NaI(Tl) scintillator absorber. IEEE Trans Nucl Sci. 2010;57:1420-25.

37. Lee HY, Chung J-K, Lee JJ, et al. Radioiodine Treatment of Differentiated Thyroid Carcinoma: The Experience at Seoul National University Hospital. Current Medical Imaging 2010;6:2-7.

38. Lee HY, Kang KW, Kim T-Y, et al. Angiogenesis Imaging Using 68Ga-RGD PET: Preliminary Report from Seoul National University Hospital. Current Medical Imaging. 2010;6:56-59.

39. Lee BC, Lee HJ, Park JH, et al. Intensification of the KOTRON-13 Cyclotron by Optimizing the Ion Source. Journal of the Korean Physical Society 2010;57:1376-80.

40. Roh C, Lee H-Y, Kim S-E, et al. Quantum-dots-based detection of hepatitis C virus (HCV) NS3 using RNA aptamer on chip. J Chem Technol Biot. 2010;85:1130 - 4.

41. Roh C, Lee H-Y, Kim S-E, et al. A highly sensitive and selective viral protein detection method based on RNA oligonucleotide nanoparticle. Int J Nanomedicine. 2010;5:323-9.

42. Moon BS, Park JH, Lee HJ, et al. Highly efficient production of [(18)F]fallypride using small amounts of base concentration. Appl Radiat Isot. 2010;68:2279-2284.

43. Jhoo JH, Yoon JY, Kim YK, et al. Availability of brain serotonin transporters in patients with restless legs syndrome. Neurology. 2010;74(6):513-8.

44. Kim J-M, Kim JS, Kim KW, et al. Study of the prevalence of Parkinson's disease using dopamine transporter imaging. Neurol Res. 2010;32:845-51.

45. Kim J-M, Lee J-Y, Kim HJ, et al. The wide clinical spectrum and nigrostriatal dopaminergic damage in spinocerebellar ataxia type 6. J Neurol Neurosurg Psychiatry. 2010;81:529-32.

46. Kim J-M, Kim JS, Jeong S-H, et al. Dopaminergic neuronal integrity in parkinsonism associated with liver cirrhosis. Neurotoxicology. 2010;31:351-5.

47. Hwang JH, Kim SH, Park CS, et al. Acute high-frequency rTMS of the left dorsolateral prefrontal cortex and attentional control in healthy young men. Brain Res. 2010;1329:152-8.

48. Park HS, Kim SH, Bang SA, et al. Altered regional cerebral glucose metabolism in Internet game overusers: A 18F-fluorodeoxyglucosepositronemissiontomographystudy. CNS Spectr. 2010;15:159-166

49. Kim YK, Yoon I-Y, Kim J-M, et al. The implication of nigrostriatal dopaminergic degeneration in the pathogenesis of REM sleep behavior disorder. Eur J Neurol. 2010r;17:487-92.

50. Hong KS, Kang DW, Bae HJ, et al. Effect of cilnidipine vs losartan on cerebral blood flow in hypertensive patients with a history of ischemic stroke: a randomized controlled trial. Acta Neurol Scand. 2010;121:51-7

51. Park YJ, Lee EJ, Lee YJ, et al. Subclinical hypothyroidism (SCH) is not associated with metabolic derangement, cognitive impairment, depression or poor quality of life (QoL) in elderly subjects. Arch Gerontol Geriat. 2010;50:e68-73.

52. Chung SY, Lee K-Y, Chun EJ, et al. Comparison of Stress Perfusion MRI and SPECT for Detection of Myocardial Ischemia in Patients with Angiographically Proven Three-Vessel Coronary Artery Disease. Am J Roentgenol. 2010;195:356–62.

53. Leuschner F, Panizzi P, Isabel C-C, et al. Matthias Nahrendorf Angiotensin-converting enzyme inhibition prevents the release of monocytes from their splenic reservoir in mice with myocardial infarction. Circ Res. 2010;107:1364–73.

54. Ju CH, Jeong JM, Lee Y-S, et al. Development of a 177Lu-labeled RGD derivative for targeting angiogenesis. Cancer Biother Radio. 2010;25:687–91.

55. Moon BS, Park JH, Lee HJ, et al. Highly efficient production of [18F]fallyprideusings mall amounts of base concentration. Appl Radiat Isot. 2010;68:2279–2284.

56. Lee BC, Lee HJ, Park JH, et al. Intensification of the KOTRON–13 Cyclotron by Optimizing the Ion Source. J Korean Phy Soc. 2010;57:1376–80.

2011년

57. Moon SH, Lee H-Y, Eo JS, et al. Use of granulocyte colony-stimulating factor for fluorine–18–fluorodeoxyglucose labeling in human leukocytes. Nucl Med Commun. 2011;32:186–91

58. Chung HH, Kim JW, Han KH, et al. Prognostic value of metabolic tumor volume measured by FDG-PET/CT in patients with cervical cancer. Gynecol Oncol. 2011;120:270–4.

59. Chung HH, Kim JW, Kang KW, et al. Post-treatment [(18)F]FDG maximum standardized uptake value as a prognostic marker of recurrence in endometrial carcinoma. Eur J Nucl Med Mol Imaging. 2011;38:74–80.

60. Choi JY, Jeong JM, Yoo BC, et al. Development of (68)Ga-labeled mannosylated human serum albumin (MSA) as a lymph node imaging agent for positron emission tomography. Nucl Med Biol. 2011;38:371–9.

61. Hoigebazar L, Jeong JM, Hong MK, et al. Synthesis of 68Ga-labeled DOTA-nitroimidazole derivatives and their feasibilities as hypoxia imaging PET tracers. Bioorg Med Chem. 2011;19:2176–81.

62. Park JS, Yim J-J, Kang WJ, et al. Detection of primary sites in unknown primary tumors using FDG-PET or FDG-PET/CT. BMC Res Notes. 2011;4:56.

63. Choi Y, Jeon YH, Jang J-Y, et al. Treatment With mANT2 shRNA Enhances Antitumor Therapeutic Effects Induced by MUC1 DNA Vaccination. Mol Ther. 2011;19:979–89.

64. Chun IK, Eo JS, Paeng JC, et al. Pulmonary Artery Sarcoma Detected on F–18 FDG PET/CT as Origin of Multiple Spinal Metastases. Clin Nucl Med. 2011 Aug;36(8):e87–9.

65. Kwon SI, Lee JS, Yoon HS, et al. Development of small-animal PET prototype using silicon photomultiplier (SiPM): initial results of phantom and animal imaging studies. J Nucl Med. 2011;52:572–9.

66. Kim Y-H, Jeon J, Hong SW, et al. Tumor Targeting and Imaging Using Cyclic RGD-PEGylated Gold Nanoparticle Probes with Directly Conjugated Iodine–125. 2011;7:2052–60.

67. Shetty D, Choi SY, Jeong JM, et al. Stable aluminium fluoride chelates with triazacyclononane derivatives proved by X-ray crystallography and (18)F-labeling study. Chem Commun (Camb). 2011;47:9732–4.

68. Oh SW, Moon S-H, Park DJ, et al. Combined therapy with (131)I and retinoic acid in Korean patients with radioiodine-refractory papillary thyroid cancer. Eur J Nucl Med Mol Imaging. 2011;38:1798−805.
69. Kim HY, Kim S, Youn HW, et al. The cell penetrating ability of the proapoptotic peptide, KLAKLAKKLAKLAK fused to the N-terminal protein transduction domain of translationally controlled tumor protein, MIIYRDLISH. Biomaterials. 2011;32:5262−8.
70. Keam B, Im S-A, Koh Y, et al. Early metabolic response using FDG PET/CT and molecular phenotypes of breast cancer treated with neoadjuvant chemotherapy. BMC Cancer. 2011;11:452.
71. Park JS, Moon WK, Lyou CY, et al. The assessment of breast cancer response to neoadjuvant chemotherapy: comparison of magnetic resonance imaging and 18F-fluorodeoxyglucose positron emission tomography. Acta Radiol. 2011;52:21−8.
72. Lee KE, Koo DH, Im HJ, et al. Surgical completeness of bilateral axillo-breast approach robotic thyroidectomy: Comparison with conventional open thyroidectomy after propensity score matching. Surgery. 2011;150:1266−74.
73. Hwang DW, Son S, Jang J, et al. A brain-targeted rabies virus glycoprotein-disulfide linked PEI nanocarrier for delivery of neurogenic microRNA. Biomaterials. 2011;32:4968−75.
74. Lee BC, Kim JS, Kim BS, et al. Aromatic radiofluorination and biological evaluation of 2−aryl−6−[18F]fluorobenzothiazoles as a potential positron emission tomography imaging probe for β-amyloid plaques. Bioorg Med Chem. 2011;19:2980−90.
75. Kim E, Howes O, Kim B-Y, et al. The use of healthy volunteers instead of patients to inform drug dosing studies: a [11C]raclopride PET study. Psychopharmacology (Berl). 2011;217:515−23.
76. Kim E, Howes O, Yu K-W, et al. Calculating occupancy when one does not have baseline: a comparison of different options. J Cereb Blood Flow Metab. 2011;31:1760−7.
77. Choi SH, Kim YT, Kim SK, et al. Positron emission tomography-computed tomography for postoperative surveillance in non-small cell lung cancer. Ann Thorac Surg. 2011;92:1826−32.
78. Liu J, Youn H, Yang J,.G-protein alpha-s and −12 subunits are involved in androgen-stimulated PI3K activation and adrogen receptor transactivation in prostate cancer cells. Prostate. 2011;71:1276−86.
79. Lim J-Y, Choi M-S, Youn H, et al. The influence of pre-transplant conditioning on graft-versus-leukemia effect in mice. Exp Hematol. 2011;39:1018−29.
80. Choi M-S, Lim J-Y, Cho B-S, et al. The role of regulatory T cells during the attenuation of graft-versus-leukemia activity following donor leukocyte infusion in mice. Leuk Res. 2011;35:1549−56.
81. Yang BY, Jeong JM, Lee Y-S, et al. Facile calculation of specific rate constants and activation energies of 18F-fluorination reaction using combined processes of coat-captureeelution and microfluidics. Tetrahedron. 2011;67:2427−33.
82. Kim HK, Kim SE, Park JJ, et al. Sentinel node identification using technetium−99m neomannosyl human serum albumin in esophageal cancer. Ann Thorac Surg. 2011;91:1517−22.
83. Kim D-E, Park K-J, Schellingerhout D, et al. A new image-based stroke registry containing quantitative magnetic resonance imaging data. Cerebrovasc Dis. 2011;32:567−76.
84. Kim HJ, Yun JY, Kim J-M, et al. Extranigral extension of structural midbrain lesions overshadows parkinsonism. J Neural Transm. 2011;118:1209−13.

85. Moon BS, Kil HS, Park JH, et al. Facile aromatic radiofluorination of [18F]flumazenil from diaryliodonium salts with evaluation of their stability and selectivity. Org. Biomol. Chem., 2011,9:8346 – 55.
86. Roh C, Kim SE, Jo SK etl al. Label free inhibitor screening of hepatitis C virus (HCV) NS5B viral protein using RNA oligonucleotide. Sensors. 2011;11:6685–96.
87. Yun JY, Lee W-W, Kim HJ, et al. Relative contribution of SCA2, SCA3 and SCA17 in Korean patients with parkinsonism and ataxia. Parkinsonism Relat Disord. 2011;17:338–42.
88. Kim SH, Baik S-H, Park CS, et al. Reduced striatal dopamine D2 receptors in people with Internet addiction. NeuroReport. 2011;22:407–11.
89. Park DJ, Kim H-H, Park HS, et al. Simultaneous Indocyanine Green and 99mTc-Antimony Sulfur Colloid-Guided Laparoscopic Sentinel Basin Dissection for Gastric Cancer. An Sur Oncol. 2011;18:160–5.
90. Florian L, Partha D, Rostic G, et al. Therapeutic siRNA silencing in inflammatory monocytes in mice. Nat Biotechnol. 2011;29:1005–10.
91. Florian L, Peter P, Isabel C, et al. Angiotensin-converting enzyme inhibition prevents the release of monocytes from their splenic reservoir in mice with myocardial infarction. Circ Res. 2010;107:1364–73.
92. Lee BC, Kim JS, Kim BS, et al. Aromatic radiofluorination and biological evaluation of 2–aryl–6– [18F]fluorobenzothiazoles as a potential positron emission tomography imaging probe for β-amyloid plaques. Bioorg Med Chem. 2011;19:2980–90.
93. Moon BS, Kil HS, Park JH, et al. Facile aromatic radiofluorination of [18F]flumazenil from diaryliodonium salts with evaluation of their stability and selectivity. Org Biomol Chem. 2011;9:8346–55.

2012년

94. Quan B, Choi K, Kim YH, et al. Near infrared dye indocyanine green doped silica nanoparticles for biological imaging. Talanta. 2012;99:387–93.
95. Noh YW, Kong SH, Choi DY, et al. Near-Infrared Emitting Polymer Nanogels for Efficient Sentinel Lymph Node Mapping. ACS Nano. 2012;6:7820–31.
96. Chung HH, Kim JW, Kang KW, et al. Predictive role of post-treatment [(18)F]FDG PET/CT in patients with uterine cervical cancer. Eur J Radiol. 2012;81:e817–22.
97. Kim JG, Kang MJ, Yoon YK, et al. Heterodimerization of glycosylated insulin-like growth factor–1 receptors and insulin receptors in cancer cells sensitive to anti-IGF1R antibody. PLoS One. 2012;7:e33322.
98. Chung HH, Kwon HW, Kang KW, et al. Preoperative [F]FDG PET/CT predicts recurrence in patients with epithelial ovarian cancer. J Gynecol Oncol. 2012;23:28–34.
99. Eguchi M, Kim YH, Kang KW, et al. Ischemia-Reperfusion Injury Leads to Distinct Temporal Cardiac Remodeling in Normal versus Diabetic Mice. PLoS One. 2012;7:e30450.
100. Ahn S, Kim SM, Son J, et al. Gap compensation during PET image reconstruction by constrained, total variation minimization. Med Phys. 2012;39:589–602.
101. Yoon HS, Ko GB, Kwon SI, et al. Initial Results of Simultaneous PET/MRI Experiments with an MR-compatible Silicon Photomultiplier PET Scanner. J Nucl Med. 2012;53:608–14.

102. Kim E, Howes O, Kim B-H, et al. Predicting brain occupancy from plasma levels using PET: superiority of combining pharmacokinetics with pharmacodynamics while modeling the relationship. J Cereb Blood Flow Metab. 2012:759–68.

103. Shin KH, Kim KP, Lim KS, et al. A positron emission tomography microdosing study with sertraline in healthy volunteers. Int J Clin Pharmacol Ther. 2012;50:224–32.

104. Eo JS, Chun IK, Paeng JS, et al. Imaging sensitivity of dedicated positron emission mammography in relation to tumor size. Breast. 2012;21:66–71.

105. Shetty D, Jeong JM, Kim YJ, et al. Development of a bifunctional chelating agent containing isothiocyanate residue for one step F–18 labeling of peptides and application for RGD labeling. Bioorg Med Chem. 2012;20:5941–7.

106. Lee YK, Jeong JM, Hoigebazar L, et al. Nanoparticles modified by encapsulation of ligands with a long alkyl chain to affect multispecific and multimodal imaging. J Nucl Med. 2012;53:1462–70.

107. Kim KI, Park JH, Lee YJ, et al. In vivo bioluminescent imaging of α-fetoprotein-producing hepatocellular carcinoma in the diethylnitrosamine-treated mouse using recombinant adenoviral vector. J Gene Med. 2012;14:513–20.

108. Hoigebazar L, Jeong JM, Lee JY, et al. Syntheses of 2–nitroimidazole derivatives conjugated with 1,4,7–triazacyclononane-N,N′–diacetic acid labeled with F–18 using an aluminum complex method for hypoxia imaging. J Med Chem. 2012;55:3155–62.

109. Im HJ, Koo DH, Paeng JC, et al. Evaluation of surgical completeness in endoscopic thyroidectomy compared with open thyroidectomy with regard to remnant ablation. Clin Nucl Med. 2012;37:148–51.

110. Lee CM, Kwon SI, Ko GB, et al. A novel compensation method for the anode gain non-uniformity of multi-anode photomultiplier tubes. Phys Med Biol. 2012;57:191–207.

111. Kim JS, Kim Y-H, Kim JH, et al. evelopment and in vivo imaging of a PET/MRI nanoprobe with enhanced NIR fluorescence by dye encapsulation. Nanomedicine (Lond). 2012;7:219–29.

112. Kim JH, Lee JS, Kang KW, et al. Whole-body distribution and radiation dosimetry of (68)Ga-NOTA-RGD, a positron emission tomography agent for angiogenesis imaging. Cancer Biother Radiopharm. 2012;27:65–71.

113. Hwang DW, Lee DS, Kim S. Gene expression profiles for genotoxic effects of silica-free and silica-coated cobalt ferrite nanoparticles. J Nucl Med. 2012;53:106–12.

114. Song YS, Oh SW, Kim YK, et al. Hemodynamic improvement of anterior cerebral artery territory perfusion induced by bifrontal encephalo(periosteal) synangiosis in pediatric patients with moyamoya disease: a study with brain perfusion SPECT. Ann Nucl Med. 2012;26:47–57.

115. Jun B-H, Hwang DW, Jung HS, et al. Ultrasensitive, Biocompatible, Quantum-Dot-Embedded Silica Nanoparticles for Bioimaging. Advanced Funtional Materials. 2012;22:1844–8.

116. Kim HK, Kim S, Sung HK, et al. Comparison between Preoperative Versus Intraoperative Injection of Technetium–99 m Neomannosyl Human Serum Albumin for Sentinel Lymph Node Identification in Early Stage Lung Cancer. Ann Surg Oncol. 2012;19:1343–9.

117. Lee JJ, Shetty D, Lee YS, et al. Evaluation of (111)In-labeled macrocyclic chelator-amino acid derivatives for cancer imaging. Nucl Med Biol. 2012;39:325–33.

118. Hoigebazar L, Jeong JM. Hypoxia imaging agents labeled with positron emitters. Recent Results Cancer Res. 2012;194:285–99.
119. Shetty D, Jeong JM, Shim H. Stroma targeting nuclear imaging and radiopharmaceuticals. Int J Mol Imaging. 2012:817682.
120. Kim JH, Lee JS, Song IC, et al. Comparison of segmentation-based attenuation correction methods for PET/MRI: evaluation of bone and liver standardized uptake value with oncologic PET/CT data. J Nucl Med. 2012;53:1878–82.
121. Hong SJ, Kang HG, Ko GB, et al. SiPM-PET with a short optical fiber bundle for simultaneous PET-MR imaging. Phys Med Biol. 2012;57:3869–83.
122. Kim JW, Lee JS, Kim SJ, et al. Compartmental modeling and simplified quantification of [11C] sertraline distribution in human brain. Arch Pharm Res. 2012;35:1591–7.
123. Kang JY, Lee JS, Kang H, et al. Regional cerebral blood flow abnormalities associated with apathy and depression in Alzheimer disease. Alzheimer Dis Assoc Disord. 2012;26:217–24.
124. Lee CM, Hong SJ, Yoon HS, et al. Spatial and energy resolutions of a hexagonal animal pet scanner based on LGSO crystal and flat-panel PMT. Nucl Eng Tech. 2012;44:53–60.
125. Lee DS. In Vivo Neuronal Cell Differentiation Imaging From Transplanted Stem Cells. Current Medical Imaging Reviews. 2012;8:278–83.
126. Yoon HS, Ko GB, Kwon SI, et al. Initial results of simultaneous PET/MRI experiments with an MRI-compatible silicon photomultiplier PET scanner. J Nucl Med. 2012;53:608–14.
127. Park SH, Moon WK, Cho N, et al. Comparison of diffusion-weighted MR imaging and FDG PET/CT to predict pathological complete response to neoadjuvant chemotherapy in patients with breast cancer. Eur Radiol. 2012;22:18–25.
128. Jung SH, Kim YK, Kim SE, et al. Prediction of Motor Function Recovery after Subcortical Stroke: Case Series of Activation PET and TMS Studies. Ann Rehabil Med. 2012;36:501–11.
129. Kim KW, Jhoo JH, Lee SB, et al. Increased striatal dopamine transporter density in moderately severe old restless legs syndrome patients. Eur J Neurol. 2012;19:1213–8.
130. Kim YK, Hong S-L, Yoon EJ, et al. Central presentation of postviral olfactory loss evaluated by positron emission tomography scan: a pilot study. Am J Rhinol Allergy. 2012;26:204–8.
131. Pae C-U, Jhoo JH, Yoon I-Y, et al. Availability of brain serotonin transporters (5–HTT) is associated with low positive mood in healthy elderly subjects. Int J Clin Pharmacol Ther. 2012;50:533–9.
132. Kim SH, Han HJ, Ahn HM, et al. Effects of five daily high-frequency rTMS on Stroop task performance in aging individuals. Neurosci Res. 2012;74:256–60.
133. Roh C, Kim SE, Jo S-K. A Simple and Rapid Detection of Viral Protein Using RNA Oligonucleotide in a Biosensor, J Anal Chem. 2012;67:925 – 9.
134. Cho SS, Yoon EJ, Lee J-M, et al. Repetitive transcranial magnetic stimulation of the left dorsolateral prefrontal cortex improves probabilistic category learning. Brain Topogr. 2012;25:443–449.
135. Choi HY, Kim YK, Lee JJ, et al. Bronchial anthracofibrosis: a potential false-positive finding on F–18 FDG PET. Ann Nucl Med. 2012;26:681–3.
136. Lee JJ, Shetty D, Lee Y-S, et al. Evaluation of (111)In-labeled macrocyclic chelator-amino acid derivatives for cancer imaging. Nucl Med Biol. 2012;39:325–33.

137. Baik S-H, Yoon HS, Kim SE. Extraversion and striatal dopaminergic receptor availability in young adults: an [18F]fallypridePETstudy. NeuroReport. 2012;23:251−254.

138. Kim SH, Cornwell B, Kim SE. Individual differences in emotion regulation and hemispheric metabolic asymmetry. Biol Psychol. 2012;89:382−6.

139. Cho SS, Yoon EJ, Bang SA, et al. Metabolic changes of cerebrum by repetitive transcranial magnetic stimulation over lateral cerebellum: A study with FDG PET. Cerebellum. 2012;11:739−748

140. Lee M-S, Ahn S-H, Lee J-H, et al. What is the best reconstruction method after distal gastrectomy for gastric cancer? Surgical Endosc. 2012;26:1539−47.

141. Florian L, Philipp J, Takuya U, et al. Rapid monocyte kinetics in acute myocardial infarction are sustained by extramedullary monocytopoiesis. J Exp Med. 2012;209:123−37.

142. Lee WW, Marinelli B, Anja M, et al. PET/MRI of inflammation in myocardial infarction. J Am Coll Cardiol. 2012;59:153−63.

143. Cheng H, Marta B, Cathy T, et al. Stem cell membrane engineering for cell rolling using peptide conjugation and tuning of cell-selectin interaction kinetics. Biomaterials. 2012;33:5004−12.

144. Lee YK, Jeong JM, Hoigebazar L, et al. Nanoparticles modified by encapsulation of ligands with a long alkyl chain to affect multispecific and multimodal imaging. J Nucl Med. 2012;53:1462−70.

145. Kim JH, Lee JS, Kang KW, et al. Whole-Body distribution and radiation dosimetry of (68)Ga-NOTA-RGD, a positron emission tomography agent for angiogenesis imaging. Cancer Biother Radiopharm. 2012;27:65−71.

146. Ju Gw, Yoon I-Y, Lee SD, et al. Modest changes in cerebral glucose metabolism in patients with sleep apnea syndrome after continuous positive airway pressure treatment. Respiration. 2012;84:212−8.

2013년

147. Kim SM, Seo H, Park JH, et al. Resolution recovery reconstruction for a Compton camera. Phys Med Biol. 2013;58:2823−40.

148. Kim JH, Chung HH, Jeong MS, et al. One-step detection of circulating tumor cells in ovarian cancer using enhanced fluorescent silica nanoparticles. Int J Nanomedicine. 2013;8:2247−57.

149. Kim JH, Kim YH, Kim YJ, et al. Quantitative positron emission tomography imaging of angiogenesis in rats with forelimb ischemia using (68)Ga-NOTA-c(RGDyK). Angiogenesis. 2013;16:837−46.

150. Kim E, Howes OD, Turkheimer FE, et al. The relationship between antipsychotic D2 occupancy and change in frontal metabolism and working memory : A dual [(11)C]raclopride and [(18)F]FDG imaging study with aripiprazole. Psychopharmacology (Berl). 2013;227:221−9.

151. Kim TM, Paeng JC, Chun IK, et al. Total lesion glycolysis in positron emission tomography is a better predictor of outcome than the International Prognostic Index for patients with diffuse large B cell lymphoma. Cancer. 2013;119:1195−202.

152. Paeng JC, Lee YS, Lee JS, et al. Feasibility and kinetic characteristics of (68)Ga-NOTA-RGD PET for in vivo atherosclerosis imaging. Ann Nucl Med. 2013;27:847−54.

153. Cho BY, Choi HS, Park YJ, et al. Changes in the clinicopathological characteristics and outcomes of thyroid cancer in Korea over the past four decades. Thyroid. 2013;23:797−804.

154. Choi H, Phi JH, Paeng JC, et al. Imaging of integrin α(V)β(3) expression using (68)Ga-RGD positron emission tomography in pediatric cerebral infarct. Mol Imaging. 2013;12:213−7.

155. Choi H, Paeng JC, Kim DW, et al. Metabolic and metastatic characteristics of ALK-rearranged lung adenocarcinoma on FDG PET/CT. Lung Cancer. 2013;79:242–7.
156. Lee ES, Paeng JC, Park CM, et al. Metabolic characteristics of Castleman disease on 18F-FDG PET in relation to clinical implication. Clin Nucl Med. 2013;38:339–42.
157. Eo JS, Paeng JC, Lee S, et al. Angiogenesis imaging in myocardial infarction using 68Ga-NOTA-RGD PET: characterization and application to therapeutic efficacy monitoring in rats. Coron Artery Dis. 2013;24:303–11.
158. Seo EH, Lee DY, Lee JM, et al. Whole-brain functional networks in cognitively normal, mild cognitive impairment, and Alzheimer's disease. PLoS One. 2013;8:e53922.
159. Youn H, Chung JK. Reporter gene imaging. AJR Am J Roentgenol. 2013;201:W206–14.
160. Yoon HJ, Paeng JC, Kwak C, et al. Prognostic implication of extrarenal metabolic tumor burden in advanced renal cell carcinoma treated with targeted therapy after nephrectomy. Ann Nucl Med. 2013;27:748–55.
161. Ito M, Lee MS, Lee JS. Continuous depth-of-interaction measurement in a single-layer pixelated crystal array using a single-ended readout. Phys Med Biol. 2013;58:1269–82.
162. Ko GB, Yoon HS, Kwon SI, et al. Development of a front-end analog circuit for multi-channel SiPM readout and performance verification for various PET detector designs. Nucl Instr Meth A. 2013;703:38–44.
163. Han HJ, Kim HB, Cha J, et al. Primo Vessel as a Novel Cancer Cell Migration Path from Testis with Nanoparticle-Labeled and GFP Expressing Cancer Cells. J Acupunct Meridian Stud. 2013;6:298–305.
164. Im HJ, Hwang dW, Lee HK, et al. In vivo visualization and monitoring of viable neural stem cells using noninvasive bioluminescence imaging in the 6–hydroxydopamine-induced mouse model of Parkinson disease. Mol Imaging. 2013;12:224–34.
165. So Y, Lee YJ, Lee WW, et al. Determination of the optimal time for radioiodine therapy in anaplastic thyroid carcinoma using the adenovirus-mediated transfer of sodium iodide symporter gene. Oncol Rep. 2013;29:1666–70.
166. Moon JH, Kim YI, Lim JA, et al. Thyroglobulin in washout fluid from lymph node fine-needle aspiration biopsy in papillary thyroid cancer: large-scale validation of the cutoff value to determine malignancy and evaluation of discrepant results. J Clin Endocrinol Metab. 2013;98:1061–8.
167. Oh HJ, Hwang dW, Youn H, et al. In vivo bioluminescence reporter gene imaging for the activation of neuronal differentiation induced by the neuronal activator neurogenin 1 (Ngn1) in neuronal precursor cells. Eur J Nucl Med Mol Imaging. 2013;40:1607–17.
168. Koo HR, Moon WK, Chun IK, et al. Background ^{18}F-FDG uptake in positron emission mammography (PEM): correlation with mammographic density and background parenchymal enhancement in breast MRI. Eur J Radiol. 2013;82:1738–42.
169. Chung HH, Lee I, Kim HS, et al. Prognostic value of preoperative metabolic tumor volume measured by ^{18}F-FDG PET/CT and MRI in patients with endometrial cancer. Gynecol Oncol. 2013;130:446–51.
170. Hoigebazar L, Jeong JM. Hypoxia imaging agents labeled with positron emitters. Recent Results Cancer Res. 2013;194:285–99.

171. Ito M, Lee JP, Lee JS. Timing performance study of new fast PMTs with LYSO for time-of-flight PET. IEEE Transactions on Nuclear Science. 2013;60:30−37.

172. Kim JS, Kim JM, Kim YK, et al. Striatal dopaminergic functioning in patients with sporadic and hereditary spastic paraplegias with parkinsonism. J Korean Med Sci. 2013;28:1661−6.

173. Im H-J, Kim YK, Kim Y-i, et al. Usefulness of Combined Metabolic－Volumetric Indices of 18F-FDGPET/CT for the Early Prediction of Neoadjuvant Chemo therapy Outcomes in Breast Cancer. Nucl Med Mol Imaging. 2013;47:36－43.

174. Yoon EJ, Kim YK, Shin HI, et al. Cortical and white matter alterations in patients with neuropathic pain after spinal cord injury. Brain Res. 2013;1540:64−73.

175. Moon BS, Jang SJ, Kim SJ, et al. Synthesis and evaluation of a 18F-labeled 4−ipomeanol as an imaging agent for CYP4B1 gene prodrug activation therapy. Cancer Biother Radiopharm. 2013;28:588−97.

176. Kim N-H, Vincent A, Irani S, et al. Long-term clinical course with voltage-gated potassium channel antibody in Morvan's syndrome. J Neurol. 2013;260:2407−8.

177. Moon JH, Kim YI, Lim JA, et al. Thyroglobulin in washout fluid from lymph node fine-needle aspiration biopsy in papillary thyroid cancer: large-scale validation of the cutoff value to determine malignancy and evaluation of discrepant results. J Clin Endocrinol Metab. 2013;98:1061−8.

178. Lee Sj, Lee WW, Yoon H-J, et al. Regional PET/CT after water gastric inflation for evaluating loco-regional disease of gastric cancer. Eur J Radiol. 2013;82:935−942.

179. Lee SJ, Lee WW, Kim SE. Bone positron emission tomography with or without CT is more accurate than bone scan for detection of bone metastasis. Korean J Radiol. 2013;14:510−9.

180. Ahn HM, Kim SE, Kim SH. The effects of high-frequency rTMS over the left dorsolateral prefrontal cortex on reward responsiveness. Brain Stimul. 2013;6:310−4.

181. Lee BC, Moon BS, Kim JS, et al. Synthesis and biological evaluation of RGD peptides with the 99mTc/188Re chelated iminodiacetate core: Highly enhanced uptake and excretion kinetics of theranostics against tumor angiogenesis. RSC Adv. 2013;3:782－792.

182. Lim H-S, Kim SJ, Noh Y-H, et al. Exploration of Optimal Dosing Regimens of Haloperidol, a D2 Antagonist, via Modeling and Simulation Analysis in a D2 Receptor Occupancy Study. Pharm Res. 2013;30:683−693.

183. Lee ES, Paeng JC, Park CM, et al. Metabolic Characteristics of Castleman Disease on 18F-FDG PET in Relation to Clinical Implication. Clin Nucl Med. 2013;38:339−42.

184. So Y, Lee YJ, Lee WW, et al. Determination of the optimal time for radioiodine therapy in anaplastic thyroid carcinoma using the adenovirus-mediated transfer of sodium iodide symporter gene. Oncol Rep. 2013;29:1666−1670.

185. Lee BC, Moon BS, Kim JS, et al. Synthesis and biological evaluation of RGD peptides with the 99mTc/188Re chelated iminodiacetate core: Highly enhanced uptake and excretion kinetics of theranostics against tumor angiogenesis. RSC Adv. 2013;3:782−792.

186. Moon BS, Jang SJ, Kim SJ, et al. Synthesis and evaluation of a 18F-labeled4−ipomeanolasanimagingagent for CYP4B1geneprodrugactivationtherapy. Cancer Biother Radiopharm. 2013;28:588−97.

187. Kang HM, Jeong SY, Park YG, et al. Near-Infrared SERS Nanoprobes with Plasmonic Au/Ag Hollow-Shell Assemblies for In Vivo Multiplex Detection. Adv Funct Mater. 2013;23:3719−27.

188. Jeong H-H, Erdene N, Park J-H, Real-time label-free immunoassay of interferon-gamma and prostate-specific antigen using a Fiber-Optic Localized Surface Plasmon Resonanace sensor. Biosens Bioelectron. 2013;39:346-51.

189. Jeong H-H, Son Y-J, Kang S-K, et al. Fiber-optic Refractive Index Sensors Based on the Cone-based round structure. IEEE Sens J. 2013;13:351-358.

190. Cho W-S, Lee H-Y, Kang H-S, et al. Symptomatic cerebral hyperperfusion of SPECT after indirect revascularization surgery for moyamoya disease. Clin Nucl Med. 2013;38:44-6.

2014년

191. Lee I, Budiawan H, Moon JY, et al. The Value of SPECT/CT in Localizing Pain Site and Prediction of Treatment Response in Patients with Chronic Low Back Pain. J Korean Med Sci. 2014;29:1711-6.

192. Jung KO, Kim YH, Kim YH, et al. Relationship between Apoptosis Imaging and Radioiodine Therapy in Tumor Cells with Different Sodium Iodide Symporter Gene Expression. Mol Imaging. 2014;13:1-9.

193. Carr R, Fanti S, Paez D, et al. Prospective International Cohort Study Demonstrates Inability of Interim PET to Predict Treatment Failure in Diffuse Large B-Cell Lymphoma. J Nucl Med. 2014;55:1936-44.

194. Chung JK, Kim MJ, Youn H. Lesionalized Therapy beyond Personalized Therapy in Cancer Management. J Korean Med Sci. 2014;29:1331-2.

195. Chung JK, Cheon GJ. Radioiodine therapy in differentiated thyroid cancer: the first targeted therapy in oncology. Endocrinol Metab (Seoul). 2014;29:233-9.

196. Lee S, Youn H, Chung T, et al. In vivo bioluminescence imaging of transplanted mesenchymal stem cells as a potential source for pancreatic regeneration. Mol Imaging. 2014;13:1-12.

197. Choi J, Jeong JM, Yoo BC, et al. Ga-68-labeled neolactosylated human serum albumin (LSA) for PET imaging of hepatic asialoglycoprotein receptor. Nucl Med Biol. 2014;pii: S0969-8051(14)00484-3.

198. Cerci JJ, Györke T, Fanti S, et al. Combined PET and biopsy evidence of marrow involvement improves prognostic prediction in diffuse large B-cell lymphoma. J Nucl Med. 2014;55:1591-7.

199. Choi H, Lim JA, Ahn HY, et al. Secular trends in the prognostic factors for papillary thyroid cancer. Eur J Endocrinol. 2014;171:667-75.

200. Cho Y, Lee DH, Lee YB, et al. Does 18F-FDG positron emission tomography-computed tomography have a role in initial staging of hepatocellular carcinoma? PLoS One. 2014;25;9:e105679.

201. Choi H, Cheon GJ, Kim HJ, et al. Segmentation-based MR attenuation correction including bones also affects quantitation in brain studies: an initial result of 18F-FP-CIT PET/MR for patients with parkinsonism. J Nucl Med. 2014;55:1617-22.

202. Kim YI, Phi JH, Paeng JC, et al. In vivo evaluation of angiogenic activity and its correlation with efficacy of indirect revascularization surgery in pediatric moyamoya disease. J Nucl Med. 2014;55:1467-72.

203. Pak K, Cheon GJ, Kang KW, et al. The effectiveness of recombinant human thyroid-stimulating hormone versus thyroid hormone withdrawal prior to radioiodine remnant ablation in thyroid cancer: a meta-analysis of randomized controlled trials. J Korean Med Sci. 2014;29:811-7.

204. Choi H, Kim YK, Kang H, et al. Abnormal metabolic connectivity in the pilocarpine-induced epilepsy rat model: a multiscale network analysis based on persistent homology. Neuroimage. 2014;99:226-36.

205. Pak K, Cheon GJ, Nam HY, et al. Prognostic Value of Metabolic Tumor Volume and Total Lesion Glycolysis in Head and Neck Cancer: A Systematic Review and Meta-Analysis. J Nucl Med. 2014;55:884-890.

206. Choi H, Paeng JC, Cheon GJ, et al. Correlation of 11C-methionine PET and diffusion-weighted MRI: is there a complementary diagnostic role for gliomas? Nucl Med Commun. 2014;35:720-6.

207. Choi H, Kim YK, Oh SW, et al. In vivo imaging of mGluR5 changes during epileptogenesis using [11C]ABP688 PET in pilocarpine-induced epilepsy rat model. PLoS One. 2014;9:e92765.

208. Yoon HJ, Kang KW, Chun IK, et al. Correlation of breast cancer subtypes, based on estrogen receptor, progesterone receptor, and HER2, with functional imaging parameters from ^{68}Ga-RGD PET/CT and 18F-FDG PET/CT. Eur J Nucl Med Mol Imaging. 2014;41:1534-43.

209. Im HJ, Lee IK, Paeng JC, et al. Functional evaluation of parathyroid adenoma using 99mTc-MIBI parathyroid SPECT/CT: correlation with functional markers and disease severity. Nucl Med Commun. 2014;35:649-54.

210. Kim YI, Cheon GJ, Paeng JC, et al. Total lesion glycolysis as the best 18F-FDG PET/CT parameter in differentiating intermediate-high risk adrenal incidentaloma. Nucl Med Commun. 2014;35:606-12.

211. Pak K, Cheon GJ, Lee KE, et al. Incidental thyroid cancer detected by (18)F-FDG PET: does it have different clinicopathological features? Nucl Med Commun. 2014;35:453-8.

212. Lee JY, Jeong JM, Kim YJ, et al. Preparation of Ga-68-NOTA as a renal PET agent and feasibility tests in mice. Nucl Med Biol. 2014;41:210-5.

213. Im HJ, Yoon HJ, Lee ES, et al. Prognostic implication of retrocrural lymph node involvement revealed by (18)F-FDG PET/CT in patients with uterine cervical cancer. Nucl Med Commun. 2014;35:268-75.

214. Seo HJ, Chung JK, Go H, et al. A hepatoid adenocarcinoma of the stomach evaluated with (18)F-FDG PET/CT: intense (18)F-FDG uptake contrary to the previous report. Clin Nucl Med. 2014;39:442-5.

215. Pak K, Cheon GJ, Lee KE, et al. Incidental thyroid cancer detected by (18)F-FDG PET: does it have different clinicopathological features? Nucl Med Commun. 2014;35:453-8.

216. Choi H, Lim JA, Ahn HY, et al. Secular trends in the prognostic factors for papillary thyroid cancer. Eur J Endocrinol. 2014;171:667-75.

217. Koo HR, Park JS, Kang KW, et al. 18F-FDG uptake in breast cancer correlates with immunohistochemically defined subtypes. Eur Radiol. 2014;24:610-8.

218. Kim CE, Kim YK, Chung G, et al. Identifying neuropathic pain using (18)F-FDG micro-PET: a multivariate pattern analysis. Neuroimage. 2014;86:311-6.

219. Lee WW, So Y, Kim KB, et al. Impaired coronary flow reserve is the most important marker of viable myocardium in the myocardial segment-based analysis of dual-isotope gated myocardial perfusion single-photon emission computed tomography. Korean J Radiol. 2014r;15:277-85.

220. Jin SH, Jeong W, Lee DS, et al. Preserved high-centrality hubs but efficient network reorganization during eyes-open state compared with eyes-closed resting state: an MEG study. J Neurophysiol. 2014;111:1455-65.

221. Eo JS, Paeng JC, Lee DS. Nuclear imaging for functional evaluation and theragnosis in liver malignancy and transplantation. World J Gastroenterol. 2014 May 14;20:5375-88.

222. Park H, Lee DS, Kang E, et al. Blocking of irrelevant memories by posterior alpha activity boosts memory encoding. Hum Brain Mapp. 2014;35:3972-87.

223. Moon JH, Kim JH, Im HJ, et al. Proposed Motor Scoring System in a Porcine Model of Parkinson's Disease induced by Chronic Subcutaneous Injection of MPTP. Exp Neurobiol. 2014;23:258-65.

224. Kim E, Kang H, Lee H, et al. Morphological brain network assessed using graph theory and network filtration in deaf adults. Hear Res. 2014;315:88-98.

225. Kim CE, Kim YK, Chung G, et al. Large-scale plastic changes of the brain network in an animal model of neuropathic pain. Neuroimage. 2014;98:203-15.

226. Lee JS, Kim JH. Recent advances in hybrid molecular imaging systems. Semin Musculoskelet Radiol. 2014;18:103-22.

227. Lee JY, Seo SH, Kim YK, et al. Extrastriatal dopaminergic changes in Parkinson's disease patients with impulse control disorders. J Neurol Neurosurg Psychiatry. 2014;85:23-30.

228. Yoon HS, Lee JS. Bipolar analog signal multiplexing for position-sensitive PET block detectors. Phys Med Biol. 2014;59:7835-46.

229. Kwon SI, Lee JS. Signal encoding method for a time-of-flight PET detector using a silicon photomultiplier array. Nucl Instr Meth A. 2014;761:39-45.

230. Oh Y, Lee YS, Quan YH, et al. Thoracoscopic color and fluorescence imaging system for sentinel lymph node mapping in porcine lung using indocyanine green-neomannosyl human serum albumin: intraoperative image-guided sentinel nodes navigation. Ann Surg Oncol. 2014;21:1182-8.

231. Kim YK, Park EA, Park SJ, et al. Non-ischemic perfusion defects due to delayed arrival of contrast material on stress perfusion cardiac magnetic resonance imaging after coronary artery bypass graft surgery. Korean J Radiol. 2014;15:188-94.

232. Park TG, Yu YD, Park BJ, et al. Implication of lymph node metastasis detected on 18F-FDG PET/CT for surgical planning in patients with peripheral intrahepatic cholangiocarcinoma. Clin Nucl Med. 2014;39:1-7.

233. Yoon SH, Goo JM, Lee SM, et al. Positron emission tomography/magnetic resonance imaging evaluation of lung cancer: current status and future prospects. J Thorac Imaging. 2014;29:4-16.

234. Oh ES, Kim JM, Kim YE, et al. The Prevalence of Essential Tremor in Elderly Koreans. J Korean Med Sci. 2014;29:1694-8.

235. Kim YE, Kim JM, Jeong HY, et al. Parkinsonism in early Creutzfeldt-Jacob disease: possible pre- and post-synaptic mechanism. J Neurol Sci. 2014;343:228-9.

236. Lee SJ, Lee HY, Lee WW, et al. The effect of recombinant human thyroid stimulating hormone on sustaining liver and renal function in thyroid cancer patients during radioactive iodine therapy. Nucl Med Commun. 2014;35:727-32.

237. Kim YI, Ha SG, So Y, et al. Improved measurement of the glomerular filtration rate from Tc-99m DTPA scintigraphy in patients following nephrectomy. Eur Radiol. 2014;24:413-22.

238. Yoon EJ, Kim YK, Kim HR, et al. Transcranial Direct Current Stimulation to Lessen Neuropathic Pain After Spinal Cord Injury: A Mechanistic PET Study. Neurorehabil Neural Repair. 2014;28:250−9.

239. Lee ES, Lee HY, et al. Extraskeletal intraspinal mesenchymal chondrosarcoma;18F-FDG PET/CT finding. Clin Nucl Med. 2014;39:e64−6.

240. Lee YK, Chung JH, Kim SE, et al. Adenosquamous carcinoma of the lung: CT, FDG PET, and clinicopathologic findings. Clin Nucl Med. 2014;39:107−12.

241. Park HS, Jung IS, Lim NH, et al. Proof of mechanism study of a novel serotonin transporter blocker, DA−8031, using [11C]DASB positron emission tomography and invivo microdialysis. Urology. 2014;84:245.e1−7.

242. Park HJ, Moon JH, Yom CK, et al. Thyroid "atypia of undetermined significance" with nuclear atypia has high rates of malignancy and BRAF mutation. Cancer Cytopathol. 2014;122:512−20.

243. Kim JI, Lee HJ, Kim YJ, et al. Multiparametric Monitoring of Early Response to Antiangiogenic Therapy: A Sequential Perfusion CT and PET/CT Study in a Rabbit VX2 Tumor Model. Sci World J. 2014;2014:701954.

244. Suh MS, Park HJ, Choi HS, et al. Case Report of PET/CT Imaging of a Patient with Neuroblastoma Using 18F-FPBG.Pediatrics. 2014;134:e1731−e1734.

245. Lee WW, So Y, Kim KB, et al. Impaired Coronary Flow Reserve Is the Most Important Marker of Viable Myocardium in the Myocardial Segment-Based Analysis of Dual-Isotope Gated Myocardial Perfusion Single-Photon Emission Computed Tomography. Korean J Radiol. 2014;15:277−285.

246. Kim JY, Son MH, Choi KH, et al. Synthesis and In vivo Evaluation of 5−Methoxy−2−(phenylethynyl)quinoline (MPEQ) and [11C]MPEQTargetingMetabotropicGlutamateReceptor5(mCluR5). Bull. Korean Chem Soc. 2014;35:2304−2310.

247. Moon BS, Park JH, Lee HJ, et al. Routine production of [18F]flumazenil from iodonium to sylateusingasamplepretreatment method: a 2.5−year production report. Mol Imaging Biol. 2014;16:619−25.

248. Moon BS, Kim BS, Park CS, et al. [18F]Fluoromethyl-PBR28 as a potential radiotracer for TSPO: preclinical comparison with [11C]PBR28 in a rat model of neuroinflammation. Bioconjug Chem. 2014;25:442−50.

249. Lee HE, Lee HK, Chang HJ, et al. Virus templated gold nanocube chain for SERS nanoprobe. Small. 2014;10:3007−11

250. Yang JK, Kang HM, Lee HM, et al. Single-step and rapid growth of silver nanoshells as SERS-active nanostructures for label-free detection of pesticides. ACS Appl Mater Interfaces. 2014;6:12541−9

251. Kang HM, Yang JK, Noh MS, et al. One-step synthesis of silver nanoshells with bumps for highly sensitive near-IR SERS nanoprobes. 2014;2:4415−21

252 Chang HJ, Kang HM, Yang JK, et al. Ag shell-Au satellite hetero-nanostructure for ultra-sensitive, reproducible, and homogeneous NIR SERS activity. ACS Appl Mater Interfaces. 2014;6:11859−63

253. Kim YI, Kim SK, Paeng JC, et al. Comparison of F−18−FDG PET/CT findings between pancreatic solid pseudopapillary tumor and pancreatic ductal adenocarcinoma. Eur J Radiol. 2014;83:231−5.

2015년

254. Chung T, Youn H, Yeom CJ, et al. Glycosylation of Sodium/Iodide Symporter (NIS) Regulates Its Membrane Translocation and Radioiodine Uptake. PLoS One. 2015;10:e0142984.

255. Seo HJ, Pagsisihan JR, Paeng JC, et al. Hemodynamic Significance of Internal Carotid or Middle Cerebral Artery Stenosis Detected on Magnetic Resonance Angiography. Yonsei Med J. 2015;56:1686–93.

256. Keam B, Lee SJ, Kim TM, et al. Total Lesion Glycolysis in Positron Emission Tomography Can Predict Gefitinib Outcomes in Non-Small-Cell Lung Cancer with Activating EGFR Mutation. J Thorac Oncol. 2015;10:1189–94.

257. Song YS, Paeng JC, Kim HC, et al. PET/CT-Based Dosimetry in 90Y-Microsphere Selective Internal Radiation Therapy: Single Cohort Comparison With Pretreatment Planning on (99m)Tc-MAA Imaging and Correlation With Treatment Efficacy. Medicine (Baltimore). 2015;94:e945.

258. Lee SJ, Seo HJ, Kang KW, et al. Clinical Performance of Whole-Body 18F-FDG PET/Dixon-VIBE, T1–Weighted, and T2–Weighted MRI Protocol in Colorectal Cancer. Clin Nucl Med. 2015;40:e392–8.

259. Koo HR, Park JS, Kang KW, et al. Correlation between (18)F-FDG uptake on PET/CT and prognostic factors in triple-negative breast cancer. Eur Radiol. 2015;25:3314–21.

260. Jeong S, Kim YI, Kang H, et al. Fluorescence-Raman dual modal endoscopic system for multiplexed molecular diagnostics. Sci Rep. 2015;5:9455.

261. Kim YI, Cheon GJ, Paeng JC, et al. Usefulness of MRI-assisted metabolic volumetric parameters provided by simultaneous (18)F-fluorocholine PET/MRI for primary prostate cancer characterization. Eur J Nucl Med Mol Imaging. 2015;42:1247–56.

262. Ha S, Hong SH, Paeng JC, et al. Comparison of SPECT/CT and MRI in Diagnosing Symptomatic Lesions in Ankle and Foot Pain Patients: Diagnostic Performance and Relation to Lesion Type. PLoS One. 2015;10:e0117583.

263. Kim YH, Youn H, Na J, et al. Codon-optimized human sodium iodide symporter (opt-hNIS) as a sensitive reporter and efficient therapeutic gene. Theranostics. 2015;5:86–96.

264. Pak K, Cheon GJ, Kang KW, et al. Prognostic value of SUVmean in oropharyngeal and hypopharyngeal cancers: comparison with SUVmax and other volumetric parameters of 18F-FDG PET. Clin Nucl Med. 2015;40:9–13.

265. Kim YI, Im HJ, Paeng JC, et al. Serum thyroglobulin level after radioiodine therapy (Day 3) to predict successful ablation of thyroid remnant in postoperative thyroid cancer. Ann Nucl Med. 2015;29:184–9.

266. Choi H, Bang JI, Cheon GJ, et al. 18F-fluorodeoxyglucose and ^{11}C-methionine positron emission tomography in relation to methyl-guanine methyltransferase promoter methylation in high-grade gliomas. Nucl Med Commun. 2015;36:211–8.

267. Im HJ, Pak K, Cheon GJ, et al. Prognostic value of volumetric parameters of (18)F-FDG PET in non-small-cell lung cancer: a meta-analysis. Eur J Nucl Med Mol Imaging. 2015;42:241–51.

268. Pak K, Suh S, Hong H, et al. Chung JK. Diagnostic values of thyroglobulin measurement in fine-needle aspiration of lymph nodes in patients with thyroid cancer. Endocrine. 2015;49:70–7.

269. Khang AR, Cho SW, Choi HS, et al. The risk of second primary malignancy is increased in differentiated thyroid cancer patients with a cumulative (131) I dose over 37 GBq. Clin Endocrinol (Oxf). 2015;83:117–23.

270. Pak K, Park S, Cheon GJ, et al. Update on nodal staging in non-small cell lung cancer with integrated positron emission tomography/computed tomography: a meta-analysis. Ann Nucl Med. 2015;29:409–19.

271. Kong SH, Noh YW, Suh YS, et al. Evaluation of the novel near-infrared fluorescence tracers pullulan polymer nanogel and indocyanine green/γ-glutamic acid complex for sentinel lymph node navigation surgery in large animal models. Gastric Cancer. 2015;18:55–64.

272. Sim JA, Shin JS, Park SM, et al. Association between Information Provision and Decisional Conflict in Cancer Patients. Ann Oncol. 2015;26:1974–80.

273. Park S, Choi H, Cheon GJ, et al. 18F-FDG PET/CT in anti-LGI1 encephalitis: initial and follow-up findings. Clin Nucl Med. 2015;40:156–8.

274. Ko GB, Lee JS, Yoon HS, et al. Lymph node imaging using novel simultaneous PET/MRI and dual-modality imaging agent. EJNMMI Phys. 2015;2:A53.

275. Park HR, Lee JM, Moon HE, et al. A Short Review on the Current Understanding of Autism Spectrum Disorders. Exp Neurobiol. 2016;25:1–13.

276. An HJ, Seo S, Kang H, et al. MRI-Based Attenuation Correction for PET/MRI Using Multiphase Level-Set Method. J Nucl Med. 2016;57:587–93.

277. Yoo HJ, Lee JS, Lee JM. Integrated whole body MR/PET: where are we? Korean J Radiol. 2015;16:32–49.

278. Ko GB, Lee JS. Performance characterization of high quantum efficiency metal package photomultiplier tubes for time-of-flight and high-resolution PET applications. Med Phys. 2015;42:510–20.

279. Eo JS, Kim HK, Kim S, et al. Gallium–68 neomannosylated human serum albumin-based PET/CT lympho scintigraphy for sentinel lymph node mapping in non-small cell lung cancer. Ann Surg Oncol. 2015;22:636–41.

280. Cho SW, Bae JH, Noh GW, et al. The Presence of Thyroid-Stimulation Blocking Antibody Prevents High Bone Turnover in Untreated Premenopausal Patients with Graves' Disease. PLoS One. 2015;10:e0144599.

281. Ahn HY, Min HS, Yeo Y, et al. Radioactive Iodine Therapy Did Not Significantly Increase the Incidence and Recurrence of Subsequent Breast Cancer. J Clin Endocrinol Metab. 2015;100:3486–93.

282. Ha S, Oh SW, Kim YK, et al. Clinical Outcome of Remnant Thyroid Ablation with Low Dose Radioiodine in Korean Patients with Low to Intermediate-risk Thyroid Cancer. J Korean Med Sci. 2015;30:876–81.

283. Youn H, Chung JK. Modified mRNA as an alternative to plasmid DNA (pDNA) for transcript replacement and vaccination therapy. Expert Opin Biol Ther. 2015;15:1337–48.

284. Lee YA, Jung HW, Kim HY, et al. Pediatric patients with multifocal papillary thyroid cancer have higher recurrence rates than adult patients: a retrospective analysis of a large pediatric thyroid cancer cohort over 33 years. J Clin Endocrinol Metab. 2015;100:1619–29.

285. Lee D, Na J, Ryu J, et al. Interaction of tetraspan(in) TM4SF5 with CD44 promotes self-renewal and circulating capacities of hepatocarcinoma cells. Hepatology. 2015;61:1978–97.

286. Kwon SJ, Lee SK, Na J, et al. Targeting BRG1 Chromatin Remodeler via Its Bromodomain for Enhanced Tumor Cell Radiosensitivity In Vitro and In Vivo. Mol Cancer Ther. 2015;14:597–607.

287. Yoon SH, Goo JM, Lee SM, et al. PET/MR Imaging for Chest Diseases: Review of Initial Studies on Pulmonary Nodules and Lung Cancers. Magn Reson Imaging Clin N Am. 2015;23:245-59.
288. Ahn SY, Lee JM, Joo I, et al. Prediction of microvascular invasion of hepatocellular carcinoma using gadoxetic acid-enhanced MR and (18)F-FDG PET/CT. Abdom Imaging. 2015;40:843-51.
289. Suh YJ, Choi JY, Kim SJ, et al. Comparison of 4D CT, Ultrasonography, and 99mTc Sestamibi SPECT/CT in Localizing Single-Gland Primary Hyperparathyroidism. Otolaryngol Head Neck Surg. 2015;152:438-43.
290. Lee SP, Lee ES, Choi H, et al. 11C-Pittsburgh B PET imaging in cardiac amyloidosis. JACC Cardiovasc Imaging. 2015;8:50-9.
291. Kang KM, Sohn CH, Kim BS, et al. Correlation of Asymmetry Indices Measured by Arterial Spin-Labeling MR Imaging and SPECT in Patients with Crossed Cerebellar Diaschisis. AJNR Am J Neuroradiol. 2015;36:1662-8.
292. Lee JS, Kang JH, Boo HJ, et al. STAT3-mediated IGF-2 secretion in the tumour microenvironment elicits innate resistance to anti-IGF-1R antibody. Nat Commun. 2015;6:8499.
293. Yoo KI, Jeon JY, Ryu SJ, et al. Subdominant H60 antigen-specific CD8 T-cell response precedes dominant H4 antigen-specific response during the initial phase of allogenic skin graft rejection. Exp Mol Med. 2015;47:e140.
294. Kim S, Jung J, Lee I, et al. Thyroid disruption by triphenyl phosphate, an organophosphate flame retardant, in zebrafish (Danio rerio) embryos/larvae, and in GH3 and FRTL-5 cell lines. Aquat Toxicol. 2015;160:188-96.
295. Lim Y, Han SW, Yoon JH, et al. Clinical Implication of Anti-Angiogenic Effect of Regorafenib in Metastatic Colorectal Cancer. PLoS One. 2015;10:e0145004.
296. Hwang HY, Paeng JC, Oh HC, et al. Comparison of perfusion and thickening between vein and right internal thoracic artery composite grafts from a randomized trial substudy. J Thorac Cardiovasc Surg. 2015;150:1187-94.
297. Lee SJ, Paeng JC. Nuclear Molecular Imaging for Vulnerable Atherosclerotic Plaques. Korean J Radiol. 2015;16:955-66.
298. Lee KH, Park CM, Lee SM, et al. Pulmonary Nodule Detection in Patients with a Primary Malignancy Using Hybrid PET/MRI: Is There Value in Adding Contrast-Enhanced MR Imaging? PLoS One. 2015;10:e0129660.
299. Stacy MR, Paeng JC, Sinusas AJ. The role of molecular imaging in the evaluation of myocardial and peripheral angiogenesis. Ann Nucl Med. 2015;29:217-23.
300. Choi H, Choi Y, Kim KW, et al. Maturation of metabolic connectivity of the adolescent rat brain. Elife. 2015;27;4. pii: e11571.
301. Kim H, Hahm J, Lee H, et al. Brain Networks Engaged in Audiovisual Integration During Speech Perception Revealed by Persistent Homology-Based Network Filtration. Brain Connect. 2015;5:245-58.
302. Song YS, Lee WW, Lee JS, et al. Prediction of Central Nervous System Relapse of Diffuse Large B-Cell Lymphoma Using Pretherapeutic [18F]2-Fluoro-2-Deoxyglucose (FDG) Positron Emission Tomography/Computed Tomography. Medicine (Baltimore). 2015;94:e1978.

303. Park HS, Kim E, Moon BS, et al. In Vivo Tissue Pharmacokinetics of Carbon−11−Labeled Clozapine in Healthy Volunteers: A Positron Emission Tomography Study. CPT: Pharmacometrics & Systems Pharmacology 2015;4:305 – 311

304. Yun JY, Kim JM, Kim HJ, et al. Parkinsonism in corticobasal syndrome may not be primarily due to presynaptic dopaminergic deficiency. Neurology Asia. 2015;20:23−27.

305. Cho SS, Yoon EJ, Kim SE. Asymmetry of dopamine D2/3 receptor availability in dorsal putamen and body mass index in non-obese healthy males. Exp Neurobiol. 2015;24:90−94.

306. Kim J, Chey JY, Kim SE, et al. The effect of education on regional brain metabolism and its functional connectivity in an aged population utilizing positron emission tomography. Neurosci Res. 2015;94:50−61.

307. Suh MS, Lee HY, Jung KW, et al. Diagnostic Accuracy of Meckel Scan with Initial Hemoglobin Level to Detect Symptomatic Meckel Diverticulum. Eur J Pediatr Surg. 2015;25:449−53.

308. Han JH, Lim JS, Lee MS, et al. Sodium [18F]Fluoride PET/CT in Myocardial Infarction. Mol Imaging Biol. 2015;17:214−21.

309. Youn SW, Kang SY, Kim SA, et al. Subclinical systemic and vascular inflammation detected by 18F-fluorodeoxyglucose positron emission tomography/computed tomography in patients with mild psoriasis. J Dermatol. 2015;42:559−66.

310. Kwon HG, Choi JY, Moon JH, et al. Effect of Hashimoto thyroiditis on low-dose radioactive-iodine remnant ablation. Head Neck. 2015;20

311. So Y, Yi JG, Song IY, et al. Detection of skeletal muscle metastasis: torso FDG PET-CT versus ontrast-enhanced chest or abdomen CT. Acta Radiol. 2015;56:860−6.

312. Lee HJ, Lee KS, Lee WW. 18F-NaF PET/CT Findings in Fibrous Dysplasia. Clin Nucl Med. 2015;40:912−4.

313. Ahn KS, Han HS, Cho JY, et al. Long-term follow-up of non-operated patients with symptomatic gallbladder stones: a retrospective study evaluating the role of Hepatobiliary scanning. BMC Gastroenterol. 2015:15;15:136−40..

314. Woo HN, Lee WI, Kim JH,et al. Combined antitumor gene therapy with herpes simplex virus-thymidine kinase and short hairpin RNA specific for mammalian target of rapamycin. Int J Oncol. 2015;47:2233−9.

315. Moon BS, Lee HJ, Lee WK, et al. Development of additive [11C]CO2 target system in the KOTRON−13 cyclotron and its application for [11C]radiopharmaceutical production. Nucl Instrum Meth B. 2015;356−357:1−7.

316. Yoo JS, Lee JH, Jung JH, et al. SPECT/CT Imaging of High-Risk Atherosclerotic Plaques using Integrin-Binding RGD Dimer Peptides. Sci. Rep. 2015;5:11752.

317. Lee HY, Chang CB, Kang SB. Value of SPECT-CT Imaging for Middle-Aged Patients with Chronic Anterior Knee Pain. BMC Musculoskelet Disord. 2015;16:169.

318. Chang H, Kang H, Jeong S, et al. A fast and reliable readout method for quantitative analysis of surface-enhanced Raman scattering nanoprobes on chip surface. Rev Sci Instrum. 2015;86:055004.

319. Jang HL, Lee K, Kang CS, et al. Biofunctionalized ceramic with self-assembled networks of nanochannels. ACS Nano. 2015;9:4447−57

320. Yang HC, Kim HR, Jheon S, et al. Recurrence Risk-Scoring Model for Stage I Adenocarcinoma of the Lung. Ann Surg Oncol. 2015;22:4089–97.

321. Chung KH, Kim W, Kim BG, et al. Hepatitis B Surface Antigen Quantification across Different Phases of Chronic Hepatitis B Virus Infection Using an Immunoradiometric Assay. Gut Liver. 2015;9:657–64.

322. Hwang I, Park YJ, Kim YR, et al. Alteration of gut microbiota by vancomycin and bacitracin improves insulin resistance via glucagon-like peptide 1 in diet-induced obesity. FASEB J. 2015;29:2397–411.

323. Kim YI, Suh M, Kim YK, et al. The usefulness of bone SPECT/CT imaging with volume of interest analysis in early axial spondyloarthritis. BMC Musculoskelet Disord. 2015;16:9.

324. Song YS, Paeng JC, Kim HC, et al. PET/CT-Based Dosimetry in 90Y-Microsphere Selective Internal Radiation Therapy: Single Cohort Comparison With Pretreatment Planning on (99m)Tc-MAA Imaging and Correlation With Treatment Efficacy. Medicine. 2015;94:e945.

2016년

325. Kwon HW, Kim JP, Lee HJ, et al. Radiation Dose from Whole-Body F–18 Fluorodeoxyglucose Positron Emission Tomography/Computed Tomography: Nationwide Survey in Korea. J Korean Med Sci. 2016;311:S69–74.

326. Song YS, Won JK, Kim MJ, et al. Graves' Patient with Thymic Expression of Thyrotropin Receptors and Dynamic Changes in Thymic Hyperplasia Proportional to Graves' Disease Activity. Yonsei Med J. 2016;57:795–798.

327. Han HJ, Kwon N, Choi MA, et al. Peptidyl Prolyl Isomerase PIN1 Directly Binds to and Stabilizes Hypoxia-Inducible Factor–1α. PLoS One. 2016;19;11:e0147038.

328. Sarker A, Im HJ, Cheon GJ, et al. Prognostic Implications of the SUVmax of Primary Tumors and Metastatic Lymph Node Measured by 18F-FDG PET in Patients With Uterine Cervical Cancer: A Meta-analysis. Clin Nucl Med. 2016;41:34–40.

329. Chung T, Na J, Kim YI, et al. Dihydropyrimidine Dehydrogenase Is a Prognostic Marker for Mesenchymal Stem Cell-Mediated Cytosine Deaminase Gene and 5–Fluorocytosine Prodrug Therapy for the Treatment of Recurrent Gliomas. Theranostics. 2016;6:1477–90.

330. Sarker AK, Im HJ, Paeng JC, et al. Plasmablastic lymphoma exclusively involving bones mimicking osteosarcoma in an immunocompetent patient: A case report. Medicine (Baltimore). 2016;95:e4241.

331. Park S, Cheon GJ, Paeng JC, et al. Phase analysis of gated myocardial perfusion single-photon emission computed tomography after coronary artery bypass graft surgery: reflection of late reverse remodeling in patients with patent grafts after coronary artery bypass graft surgery. Nucl Med Commun. 2016;37:1139–47.

332. Jung KO, Youn H, Kim SH, et al. A new fluorescence/PET probe for targeting intracellular human telomerase reverse transcriptase (hTERT) using Tat peptide-conjugated IgM. Biochem Biophys Res Commun. 2016;477:483–9.

333. Lee H, Paeng JC, Hong SH, et al. Appropriate margin thresholds for isocontour metabolic volumetry of fluorine–18 fluorodeoxyglucose PET in sarcoma: a hybrid PET/MRI study. Nucl Med Commun. 2016;37:1088–94.

334. Kim YI, Yoon HJ, Paeng JC, et al. Prognostic Value of 68Ga-NOTA-RGD PET/CT for Predicting Disease-Free Survival for Patients With Breast Cancer Undergoing Neoadjuvant Chemotherapy and Surgery: A Comparison Study With Dynamic Contrast Enhanced MRI. Clin Nucl Med. 2016;41:614–20.

335. Im HJ, Oo S, Jung W, et al. Prognostic Value of Metabolic and Volumetric Parameters of Preoperative FDG-PET/CT in Patients With Resectable Pancreatic Cancer. Medicine (Baltimore). 2016;95:e3686.

336. Kim WH, Kim CG, Kim MH, et al. Preclinical evaluation of isostructural Tc–99m– and Re–188–folate-Gly-Gly-Cys-Glu for folate receptor-positive tumor targeting. Ann Nucl Med. 2016;30:369–79.

337. Kim YI, Paeng JC, Cheon GJ, et al. Prediction of Posttransplantation Recurrence of Hepatocellular Carcinoma Using Metabolic and Volumetric Indices of 18F-FDG PET/CT. J Nucl Med. 2016;57:1045–51.

338. Choi H, Cheon GJ, Kim HJ, et al. Gray matter correlates of dopaminergic degeneration in Parkinson's disease: A hybrid PET/MR study using (18) F-FP-CIT. Hum Brain Mapp. 2016;37:1710–21.

339. Im HJ, Paeng JC, Cheon GJ, et al. Feasibility of simultaneous 18F-FDG PET/MRI for the quantitative volumetric and metabolic measurements of abdominal fat tissues using fat segmentation. Nucl Med Commun. 2016;37:616–22.

340. Im HJ, Hahm J, Kang H, et al. Disrupted brain metabolic connectivity in a 6–OHDA-induced mouse model of Parkinson's disease examined using persistent homology-based analysis. Sci Rep. 2016;21;6:33875.

341. Moon SH, Yang BY, Kim YJ, et al. Development of a complementary PET/MR dual-modal imaging probe for targeting prostate-specific membrane antigen (PSMA). Nanomedicine. 2016;12:871–9.

342. Kim EJ, Kim S, Seo HS, et al. Novel PET Imaging of Atherosclerosis with 68Ga-Labeled NOTA-Neomannosylated Human Serum Albumin. J Nucl Med. 2016;57:1792–7.

343. Eo JS, Jeong JM. Angiogenesis Imaging Using (68)Ga-RGD PET/CT: Therapeutic Implications. Semin Nucl Med. 2016;46:419–27.

344. Kim HK, Quan YH, Oh Y, et al. Macrophage-Targeted Indocyanine Green-Neomannosyl Human Serum Albumin for Intraoperative Sentinel Lymph Node Mapping in Porcine Esophagus. Ann Thorac Surg. 2016;102:1149–55.

345. Ko GB, Yoon HS, Kim KY, et al. Simultaneous Multiparametric PET/MRI with Silicon Photomultiplier PET and Ultra-High-Field MRI for Small-Animal Imaging. J Nucl Med. 2016;57:1309–15.

346. Park HR, Lee JM, Moon HE, et al. A Short Review on the Current Understanding of Autism Spectrum Disorders. Exp Neurobiol. 2016;25:1–13.

347. An HJ, Seo S, Kang H, et al. MRI-Based Attenuation Correction for PET/MRI Using Multiphase Level-Set Method. J Nucl Med. 2016;57:587–93.

348. Choi SA, Kwak PA, Kim SK, et al. In vivo bioluminescence imaging for leptomeningeal dissemination of medulloblastoma in mouse models. BMC Cancer. 2016;8;16:723.

349. Seo S, Kim SJ, Yoo HB, et al. Noninvasive bi-graphical analysis for the quantification of slowly reversible radioligand binding. Phys Med Biol. 2016;21;61:6770–90.

350. Choi Y, Hwang do W, Kim MY, et al. Transgenic Mouse Expressing Optical MicroRNA Reporter for Monitoring MicroRNA-124 Action during Development. Front Mol Neurosci. 2016;12;9:52.

351. Im HJ, England CG, Feng L, et al. Accelerated Blood Clearance Phenomenon Reduces the Passive Targeting of PEGylated Nanoparticles in Peripheral Arterial Disease. ACS Appl Mater Interfaces. 2016 ;20;8:17955-63.

352. Park H, Lee DS, Kang E, et al. Formation of visual memories controlled by gamma power phase-locked to alpha oscillations. Sci Rep. 2016;16;6:28092.

353. England CG, Im HJ, Feng L, et al. Re-assessing the enhanced permeability and retention effect in peripheral arterial disease using radiolabeled long circulating nanoparticles. Biomaterials. 2016;100:101-9.

354. Jang J, Lee S, Oh HJ, et al. Fluorescence imaging of in vivo miR-124a-induced neurogenesis of neuronal progenitor cells using neuron-specific reporters. EJNMMI Res. 2016;6:38.

355. Choi H, Lee DS. Illuminating the physiology of extracellular vesicles. Stem Cell Res Ther. 2016;16;7:55.

356. England CG, Kamkaew A, Im HJ, et al. ImmunoPET Imaging of Insulin-Like Growth Factor 1 Receptor in a Subcutaneous Mouse Model of Pancreatic Cancer. Mol Pharm. 2016;13:1958-66.

357. Kim MY, Hwang DW, Li F, et al. Detection of intra-brain cytoplasmic 1 (BC1) long noncoding RNA using graphene oxide-fluorescence beacon detector. Sci Rep. 2016;6:22552.

358. Hwang DW, Bahng N, Ito K, et al. In vivo targeting of c-Met using a non-standard macrocyclic peptide in gastric carcinoma. Cancer Lett. 2016;31 pii: S0304-3835(16)30661-9.

359. Kwon HW, Lee HY, Hwang YH, et al. Diagnostic performance of 18F-FDG-labeled white blood cell PET/CT for cyst infection in patients with autosomal dominant polycystic kidney disease: a prospective study. Nucl Med Commun. 2016;37:493-8.

360. Kang KW. History and Organizations for Radiological Protection. J Korean Med Sci. 2016;31:S4-5.

361. Lee DH, Lee JM, Hur BY, et al. Colorectal Cancer Liver Metastases: Diagnostic Performance and Prognostic Value of PET/MR Imaging. Radiology. 2016;280:782-92.

362. Jeong HJ, Lee BC, Ahn BC, et al. Development of Drugs and Technology for Radiation Theragnosis. Nuclear Engineering and Technology 2016;48:597-607.

363. Won JY, Ko GB, Lee JS. Delay grid multiplexing: simple time-based multiplexing and readout method for silicon photomultipliers. Phys Med Biol. 2016;7;61:7113-35.

364. Lee SH, Ha S, An HJ, et al. Association between partial-volume corrected SUVmax and Oncotype DX recurrence score in early-stage, ER-positive/HER2-negative invasive breast cancer. Eur J Nucl Med Mol Imaging. 2016;43:1574-84.

365. Won JY, Lee JS. Time-to-digital converter using a tuned-delay line evaluated in 28, 40, and 45 nm FPGAs. IEEE Trans Instrum Meas. 2016;65(7):1678-89.

366. Son J-W, Ko GB, Won JY, et al. Development and performance evaluation of a time-of-flight positron emission tomography detector based on a high-quantum-efficiency multi-anode photomultiplier tube. IEEE Trans Nucl Sci. 2016;63(1):44-51.

367. Ko GB, Kim KY, Yoon HS, et al. Evaluation of a silicon photomultiplier PET insert for simultaneous PET and MR imaging. Med Phys. 2016;43:72-83.

368. Won JY, Kwon SI, Yoon HS, et al. Dual-Phase Tapped-Delay-Line Time-to-Digital Converter With On-the-Fly Calibration Implemented in 40 nm FPGA. IEEE Trans Biomed Circuits Syst. 2016;10:231-42.

369. Lee SH, Seo HG, Oh BM, et al. Increased (18)F-FDG uptake in the trapezius muscle in patients with spinal accessory neuropathy. J Neurol Sci. 2016;15;362:127-30.

370. Park JH, Pahk K, Kim S, et al. Fluorine-18 fluorodeoxyglucose positron emission tomography imaging of T-lymphoblastic lymphoma patients. Oncol Lett. 2016;12:1620-1622.

371. Kim JH, Hong SJ, Park CY, et al. Intramyocardial Adipose-Derived Stem Cell Transplantation Increases Pericardial Fat with Recovery of Myocardial Function after Acute Myocardial Infarction. PLoS One. 2016;11:e0158067.

372. Song C, Hong BJ, Bok S, et al. Real-time Tumor Oxygenation Changes After Single High-dose Radiation Therapy in Orthotopic and Subcutaneous Lung Cancer in Mice: Clinical Implication for Stereotactic Ablative Radiation Therapy Schedule Optimization. Int J Radiat Oncol Biol Phys. 2016;1;95:1022-31.

373. Lee SM, Goo JM, Park CM, et al. Preoperative staging of non-small cell lung cancer: prospective comparison of PET/MR and PET/CT. Eur Radiol. 2016;26:3850-7.

374. Lee JW, Heo EJ, Moon SH, et al. Prognostic value of total lesion glycolysis on preoperative 18F-FDG PET/CT in patients with uterine carcinosarcoma. Eur Radiol. 2016;26:4148-54.

375. Chung HH, Kang SY, Ha S, et al. Prognostic value of preoperative intratumoral FDG uptake heterogeneity in early stage uterine cervical cancer. J Gynecol Oncol. 2016;27:e15.

376. Kim R, Ock CY, Keam B, et al. Predictive and prognostic value of PET/CT imaging post-chemoradiotherapy and clinical decision-making consequences in locally advanced head & neck squamous cell carcinoma: a retrospective study. BMC Cancer. 2016;17;16:116.

377. Kang B, Lee JM, Song YS, et al. Added Value of Integrated Whole-Body PET/MRI for Evaluation of Colorectal Cancer: Comparison With Contrast-Enhanced MDCT. AJR Am J Roentgenol. 2016;206:W10-20.

378. Hong G, Suh KS, Suh SW, et al. Alpha-fetoprotein and (18)F-FDG positron emission tomography predict tumor recurrence better than Milan criteria in living donor liver transplantation. J Hepatol. 2016;64:852-9.

379. Yun TJ, Paeng JC, Sohn CH, et al. Monitoring Cerebrovascular Reactivity through the Use of Arterial Spin Labeling in Patients with Moyamoya Disease. Radiology. 2016;278:205-13.

380. Kim BS, Lee ST, Yun TJ, et al. Capability of arterial spin labeling MR imaging in localizing seizure focus in clinical seizure activity. Eur J Radiol. 2016;85:1295-303.

381. Paeng JC. Nuclear Cardiac Imaging: Principles and Applications. J Nucl Med. 2016;57:1323.

382. Tekin N, Omidvar N, Morris TP, et al. Protocol for qRT-PCR analysis from formalin fixed paraffin embedded tissue sections from diffuse large b-cell lymphoma: Validation of the six-gene predictor score. Oncotarget. 2016;13;7:83319-83329.

383. Son HY, Jeon YH, Chung JK, et al. In vivo monitoring of transfected DNA, gene expression kinetics, and cellular immune responses in mice immunized with a human NIS gene-expressing plasmid. Int J Immunopathol Pharmacol. 2016;29:612-25.

384. Palner M, Beinat C, Banister S, et al. Effects of common anesthetic agents on [18F]flumazenil binding to the GABA A receptor. EJNMMI Res. 2016;6:80.
385. Park SH, Park HS, Kim SE. Regional Cerebral Glucose Metabolism in Novelty Seeking and Antisocial Personality: A Positron Emission Tomography Study. Exp Neurobiol. 2016;25:185-190.
386. Lee MS, Park HS, Lee BC, et al. Identification of Angiogenesis Rich-Viable Myocardium using RGD Dimer based SPECT after Myocardial Infarction. Sci Rep. 2016;6:27520.
387. Bang SA, Song YS, Moon BS, et al. Neuropsychological, Metabolic, and GABAA Receptor Studies in Subjects with Repetitive Traumatic Brain Injury. J Neurotrauma. 2016;33:1005-14.
388. Kim JM, Jeong HJ, Bae YJ, et al. Loss of substantia nigra hyperintensity on 7 Tesla MRI of Parkinson's disease, multiple system atrophy, and progressive supranuclear palsy. Parkinsonism Relat Disord. 2016;26:47-54.
389. Bae YJ, Kim JM, Kim E, et al. Loss of Nigral Hyperintensity on 3 Tesla MRI of Parkinsonism: Comparison With (123) I-FP-CIT SPECT. Mov Disord. 2016;31:684-92.
390. Bang JI, Ha SG, Kang SB, et al. Prediction of neoadjuvant radiation chemotherapy response and survival using pretreatment [(18)F]FDG PET/CT scans in locally advanced rectal cancer. Eur J Nucl Med Mol Imaging. 2016;43:422-31.
391. Bang JI, Jung IS, Song YS, et al. PET imaging of dopamine transporters with [18F]FE-PE2I: Effects of anti-Parkinsonian drugs. Nucl Med Biol. 2016;43:158-64.
392. Bang JI, Ha SG, Kang SB, et al. F-18 Sodium Fluoride Positron Emission Tomography/Computed Tomography for Detection of Thyroid Cancer Bone Metastasis Compared with Bone Scintigraphy. Korean J Radiol. 2016;17:281-8.
393. Suh MS, Lee WW, Kim YK, et al. Maximum Standardized Uptake Value of (99m)Tc Hydroxymethylene Diphosphonate SPECT/CT for the Evaluation of Temporomandibular Joint Disorder. Radiology. 2016;280:890-6.
394. Lee HJ, Kim JH, Kang YK, et al. Quantitative Single-Photon Emission Computed Tomography/Computed Tomography for Technetium Pertechnetate Thyroid Uptake Measurement. Medicine. 2016;95:e4170.
395. Kwon HJ, Choi JY, Moon JH, et al. Effect of Hashimoto thyroiditis on low-dose radioactive-iodine remnant ablation. Head Neck. 2016;38:E730-5.
396. Moon JH, Choi JY, Jeong WJ, et al. Recombinant human thyrotropin-stimulated thyroglobulin level at the time of radioactive iodine ablation is an independent prognostic marker of differentiated thyroid carcinoma in the setting of prophylactic central neck dissection. Clin Endocrinol. 2016;85:459-65.
397. Kim SK, So Y, Chung HW, et al. Analysis of predictability of F-18 fluorodeoxyglucose-PET/CT in the recurrence of papillary thyroid carcinoma. Cancer Med. 2016;5:2756-62.
398. Choi JY, Iacobazzi R, Perrone M, et al. Synthesis and evaluation of tricarbonyl 99mTc-labeled 2-(4-chloro)phenyl-imidazo[1,2-a]pyridine analogs as novel SPECT imaging radiotracer for TSPO-rich cancer. Int J Mol Sci. 2016;17:1085.
399. Perrone M, Moon BS, Park HS, et al. A Novel PET Imaging Probe for the Detection and Monitoring of Translocator Protein 18kDa Expression in Pathological Disorders. Sci Rep. 2016;6:20422.

400. Lee JH, Jung JH, Lee BC, et al. Design and synthesis of phenoxypyridyl acetamide or aryl-oxodihydropurine derivatives for the development of novel PET imaging targeting the translocator protein 18 kDa (TSPO). Bull. Korean Chem. Soc. 2016;37:1874−7.

401. Jeong HJ, Lee BC, Ahn BC, et al. Development of drugs and technology for radiation theragnosis. Nucl Eng Technol. 2016;48:597−607.

402. Song IH, Lee TS, Park YS, et al. Immuno-PET Imaging and Radioimmunotherapy 64Cu−/177Lu-Labeled Anti-EGFR Antibody in Esophageal Squamous Cell Carcinoma Model. J Nucl Med. 2016;57:1105−11.

403. Lu Y, Jung JH, Lee HJ, et al. Synthesis and In Vivo Evaluation of a Kit-Type 99mTc-labeled N−(2−Aminoethyl)−3−(4−(2−hydroxy−3−(isopropylaminopropoxy)phenyl)propanamide as a Selective β1−Adrenoceptor-binding SPECT Radiotracer. Bull. Korean Chem. Soc. 2016;37:2029 − 2035.

404. Chang HJ, Kang HM, Ko EB, et al. PSA Detection with Femtomolar Sensitivity and a Broad Dynamic Range Using SERS Nanoprobes and an Area-Scanning Method. ACS Sens. 2016;1:645−9.

405. Lee SJ, Jung YS, Yoon MH, et al. Interruption of progerin-lamin A/C binding ameliorates Hutchinson-Gilford progeria syndrome phenotype. J Clin Invest. 2016;126:3879−93.

406. Kwon HW, Lee HY, Hwang YH, et al. Diagnostic performance of 18F-FDG-labeled white blood cell PET/CT for cyst infection in patients with autosomal dominant polycystic kidney disease: a prospective study. Nucl Med Commun. 2016;37:493−8.

407. Kim Y, Lee HY, Yoon HJ, et al. Utility of 18F-fluorodeoxy glucose and 18F-sodium fluoride positron emission tomography/computed tomography in the diagnosis of medication-related osteonecrosis of the jaw: A preclinical study in a rat model. J Craniomaxillofac Surg. 2016;44:357−63.

408. Yun TJ, Paeng JC, Sohn CH, et al. Monitoring Cerebrovascular Reactivity through the Use of Arterial Spin Labeling in Patients with Moyamoya Disease. Radiology. 2016;278:205−13.

2017년

409. Kim YI, Jeong S, Jung KO, et al. Simultaneous Detection of EGFR and VEGF in Colorectal Cancer using Fluorescence-Raman Endoscopy. Sci Rep. 2017;7:1035.

410. Kim YI, Paeng JC, Cheon GJ, et al. Discrepancy Between Tumor Antigen Distribution and Radiolabeled Antibody Binding in a Nude Mouse Xenograft Model of Human Melanoma. Cancer Biother Radiopharm. 2017;32:83−89.

411. Lee SJ, Paeng JC, Goo JM, et al. Comparative characteristics of quantitative indexes for 18F-FDG uptake and metabolic volume in sequentially obtained PET/MRI and PET/CT. Nucl Med Commun. 2017;38:333−9.

412. Lim YJ, Chang JH, Kim HJ, et al. Superior Treatment Response and In-field Tumor Control in Epidermal Growth Factor Receptor-mutant Genotype of Stage III Nonsquamous Non-Small cell Lung Cancer Undergoing Definitive Concurrent Chemoradiotherapy. Clin Lung Cancer. 2017;18:e169−e178.

413. Jung KO, Youn H, Lee CH, et al. Visualization of exosome-mediated miR−210 transfer from hypoxic tumor cells. Oncotarget. 2017;8:9899−9910.

414. Paek SH, Yi KH, Kim SJ, et al. Feasibility of sentinel lymph node dissection using Tc−99m phytate in papillary thyroid carcinoma. Ann Surg Treat Res. 2017;93:240−245.

415. Lee IJ, Park JY, Kim YI, et al. Image-Based Analysis of Tumor Localization After Intra-Arterial Delivery of Technetium−99m-Labeled SPIO Using SPECT/CT and MRI. Mol Imaging. 2017;16:1−9.

416. Kim YI, Kim YJ, Paeng JC, et al. Heterogeneity index evaluated by slope of linear regression on 18F-FDG PET/CT as a prognostic marker for predicting tumor recurrence in pancreatic ductal adenocarcinoma. Eur J Nucl Med Mol Imaging. 2017;44:1995–2003.
417. Kim YI, Kim YJ, Paeng JC, et al. Prediction of breast cancer recurrence using lymph node metabolic and volumetric parameters from 18F-FDG PET/CT in operable triple-negative breast cancer. Eur J Nucl Med Mol Imaging. 2017;44:1787–95.
418. Kim JW, Seo S, Kim HS, et al. Erratum to: Comparative evaluation of the algorithms for parametric mapping of the novel myocardial PET imaging agent 18F-FPTP. Ann Nucl Med. 2017;31:480.
419. Kim JW, Seo S, Kim HS, et al. Comparative evaluation of the algorithms for parametric mapping of the novel myocardial PET imaging agent 18F-FPTP. Ann Nucl Med. 2017;31:469–79.
420. Bakht MK, Oh SW, Hwang DW, et al. The Potential Roles of Radionanomedicine and Radioexosomics in Prostate Cancer Research and Treatment. Curr Pharm Des. 2017;23:2976–2990.
421. Kim MJ, Oh SW, Youn H, et al. Thyroid-Related Protein Expression in the Human Thymus. Int J Endocrinol. 2017;2017:8159892.
422. Sim JA, Chang YJ, Shin A, et al. Perceived needs for the information communication technology (ICT)–based personalized health management program, and its association with information provision, health-related quality of life (HRQOL), and decisional conflict in cancer patients. Psychooncology. 2017;26:1810–7.
423. Heo JY, Kang SH, Kim YH, et al. Toward redesigning the PEG surface of nanocarriers for tumor targeting: impact of inner functionalities on size, charge, multivalent binding, and biodistribution. Chem Sci. 2017;8:5186–95.
424. Oh HJ, Shin Y, Chung S, et al. Convective exosome-tracing microfluidics for analysis of cell-non-autonomous neurogenesis. Biomaterials. 2017;112:82–94.
425. Lee B, Kim YK, Lee JY, et al. Preclinical anaylses of [18F]cEFQ as a PET tracer for imaging metabotropic glutamate receptor type 1 (mGluR1). J Cereb Blood Flow Metab. 2017;37:2283–93.
426. Jeong S, Park JY, Cha MG, et al. Highly robust and optimized conjugation of antibodies to nanoparticles using quantitatively validated protocols. Nanoscale. 2017;9:2548–55.
427. Hwang DW, Kim HY, Li F, et al. In vivo visualization of endogenous miR–21 using hyaluronic acid-coated graphene oxide for targeted cancer therapy. Biomaterials. 2017;121:144–154.
428. Jeon SY, Seo S, Lee JS, et al. [11C]–(R)–PK11195 positron emission tomography in patients with complex regional pain syndrome: A pilot study. Medicine (Baltimore). 2017;96:e5735.
429. Choi H, Ha S, Im HJ, et al. Refining diagnosis of Parkinson's disease with deep learning-based interpretation of dopamine transporter imaging. Neuroimage Clin. 2017;16:586–94.
430. Hwang DW, Kwon HW, Jang J, et al. Neuron-Specific Fluorescence Reporter-Based Live Cell Tracing for Transdifferentiation of Mesenchymal Stem Cells into Neurons by Chemical Compound. Stem Cells Int. 2017;2017:8452830.
431. Jiang D, Im HJ, Sun H, et al. Radiolabeled pertuzumab for imaging of human epidermal growth factor receptor 2 expression in ovarian cancer. Eur J Nucl Med Mol Imaging. 2017;44:1296–1305.
432. Lee KH, Kang SK, Goo JM, et al. Relationship Between Ktrans and K1 with Simultaneous Versus Separate MR/PET in Rabbits with VX2 Tumors. Anticancer Res. 2017;37:1139–1148.

433. Lee SP, Im HJ, Kang S, et al. Noninvasive Imaging of Myocardial Inflammation in Myocarditis using 68Ga-tagged Mannosylated Human Serum Albumin Positron Emission Tomography. Theranostics. 2017;7:413−424.

434. Coenen HH, Gee AD, Adam M, et al. Consensus nomenclature rules for radiopharmaceutical chemistry − Setting the record straight. Nucl Med Biol. 2017;55:v-xi.

435. Kim HY, Park C, Lee JY, et al. One-pot radiosynthesis of O−[18F]fluoromethyl-D−tyrosine via intra-molecular nucleophilic 18F-fluorination with 1,2,3−triazolium triflate salt precursor. Appl Radiat Isot. 2017;132:105−9.

436. Chen Q, Zhang Y, Hou H, et al. Neural correlates of the popular music phenomenon: evidence from functional MRI and PET imaging. Eur J Nucl Med Mol Imaging. 2017;44:1033−41.

437. Carr R, Ozdag H, Tekin N, et al. The effect of biological heterogeneity on R-CHOP treatment outcome in diffuse large B-cell lymphoma across five international regions. Leuk Lymphoma. 2017;58:1178−83.

438. Park S, Ha S, Kwon HW, et al. Prospective Evaluation of Changes in Tumor Size and Tumor Metabolism in Patients with Advanced Gastric Cancer Undergoing Chemotherapy: Association and Clinical Implication. J Nucl Med. 2017;58:899−904.

439. Park JY, Lee JW, Lee HJ, et al. Prognostic significance of preoperative ^{18}F-FDG PET/CT in uterine leiomyosarcoma. J Gynecol Oncol. 2017;28:e28.

440. Hwang D, Jeon KH, Lee JM, et al. Diagnostic Performance of Resting and Hyperemic Invasive Physiological Indices to Define Myocardial Ischemia: Validation With 13N-Ammonia Positron Emission Tomography. JACC Cardiovasc Interv. 2017;10:751−760.

441. Lee KH, Kang SK, Goo JM, et al. Relationship Between Ktrans and K1 with Simultaneous Versus Separate MR/PET in Rabbits with VX2 Tumors. Anticancer Res. 2017;37:1139−48.

442. Kim TH, Kim J, Kang YK, et al. Identification of Metabolic Biomarkers Using Serial 18F-FDG PET/CT for Prediction of Recurrence in Advanced Epithelial Ovarian Cancer. Transl Oncol. 2017;10:297−303.

443. Kang SY, Cheon GJ, Lee M, et al. Prediction of Recurrence by Preoperative Intratumoral FDG Uptake Heterogeneity in Endometrioid Endometrial Cancer. Transl Oncol. 2017;10:178−183.

444. Kim OH, Kim H, Kang J, et al. Impaired phagocytosis of apoptotic cells causes accumulation of bone marrow-derived macrophages in aged mice. BMB Rep. 2017;50:43−48.

445. Lee JM, Hwang D, Park J, et al. Exploring Coronary Circulatory Response to Stenosis and Its Association With Invasive Physiologic Indexes Using Absolute Myocardial Blood Flow and Coronary Pressure. Circulation. 2017;136:1798−1808.

446. Chung HH, Lee M, Kim HS, et al. Prognostic implication of the metastatic lesion-to-ovarian cancer standardised uptake value ratio in advanced serous epithelial ovarian cancer. Eur Radiol. 2017;27:4510−4515.

447. Chung HH, Cheon GJ, Kim JW, et al. Prognostic importance of lymph node-to-primary tumor standardized uptake value ratio in invasive squamous cell carcinoma of uterine cervix. Eur J Nucl Med Mol Imaging. 2017;44:1862−1869.

448. Jo J, Kwon HW, Park S, et al. Prospective Evaluation of the Clinical Implications of the Tumor Metabolism and Chemotherapy-Related Changes in Advanced Biliary Tract Cancer. J Nucl Med. 2017;58:1255–1261.

449. Lee MS, Cho JY, Kim SY, et al. Diagnostic value of integrated PET/MRI for detection and localization of prostate cancer: Comparative study of multiparametric MRI and PET/CT. J Magn Reson Imaging. 2017;45:597–609.

450. Lee M, Lee H, Cheon GJ, et al. Prognostic value of preoperative intratumoral FDG uptake heterogeneity in patients with epithelial ovarian cancer. Eur Radiol. 2017;27:16–23.

451. Biswas S, Better N, Pascual TN, et al. Nuclear Cardiology Practices and Radiation Exposure in the Oceania Region: Results From the IAEA Nuclear Cardiology Protocols Study (INCAPS). Heart Lung Circ. 2017;26:25–34.

452. Pascual TN, Mercuri M, El-Haj N, et al. Nuclear Cardiology Practice in Asia: Analysis of Radiation Exposure and Best Practice for Myocardial Perfusion Imaging-Results From the IAEA Nuclear Cardiology Protocols Cross-Sectional Study (INCAPS). Circ J. 2017;81:501–510.

453. Vitola JV, Mut F, Alexánderson E, et al. Opportunities for improvement on current nuclear cardiology practices and radiation exposure in Latin America: Findings from the 65–country IAEA Nuclear Cardiology Protocols cross-sectional Study (INCAPS). J Nucl Cardiol. 2017;24:851–859.

454. Im HJ, Cheon GJ. Sex difference in cardiac metabolism in nonischemic heart failure: Insight for prognostic value of altered cardiac metabolism. J Nucl Cardiol. 2017;24:1236–1238.

455. Park SW, Kim JH, Park JH, et al. Temporal bone chondroblastoma: Imaging characteristics with pathologic correlation. Head Neck. 2017;39:2171–9.

456. Chong S, Park JD, Chae JH, et al. Extensive brain infarction involving deep structures during an acetazolamide-challenged single-photon emission computed tomography scan in a patient with moyamoya disease. Childs Nerv Syst. 2017;33:2029–33.

457. Choi JW, Yoo MY, Kim HC, et al. Prophylactic Temporary Occlusion of the Cystic Artery Using a Fibered Detachable Coil During 90Y Radioembolization. Cardiovasc Intervent Radiol. 2017;40:1624–30.

458. Lim Y, Bang JI, Han SW, et al. Total lesion glycolysis (TLG) as an imaging biomarker in metastatic colorectal cancer patients treated with regorafenib. Eur J Nucl Med Mol Imaging. 2017;44:757–64.

459. Cho SG, Park KS, Kim J, et al. Coronary flow reserve and relative flow reserve measured by N–13 ammonia PET for characterization of coronary artery disease. Ann Nucl Med. 2017;31:144–52.

460. Wang MJ, Yi S, Han JY, et al. Oligomeric forms of amyloid-β protein in plasma as a potential blood-based biomarker for Alzheimer's disease. Alzheimers Res Ther. 2017;9:98

461. Song YS, Park HS, Lee BC et al. Imaging of Integrin αvβ3 Expression in Lung Cancers and Brain Tumors Using Single-Photon Emission Computed Tomography with a Novel Radiotracer 99mTc-IDA-D–[c(RGDfK)]2. Cancer Biother Radiopharm. 2017;32:288–296.

462. Song YS, Kim JM, Kim KJ et al. Serum Ceruloplasmin and Striatal Dopamine Transporter Density in Parkinson Disease: Comparison With 123I-FP-CIT SPECT. Clin Nucl Med. 2017;42:675–679.

463. Yun CH, Lee HY, Lee SK et al. Amyloid Burden in Obstructive Sleep Apnea. J Alzheimers Dis. 2017;59:21–29.

464. Kim W, Park HS, Moon BS, Lee BC et al. PET measurement of "GABA shift" in the rat brain: a preclinical application of bolus plus constant infusion paradigm of [18F]flumazenil. Nucl Med Biol. 2017;45:30–34

465. Kim JH, Lee JO, Jin Ho Paik JG et al. Different predictive values of interim 18F-FDG PET/CT in germinal center like and non-germinal center like diffuse large B-cell lymphoma. Ann Nucl Med. 2017;31:1–11.

466. Lee WW, So Y, Kang SY et al. F–18 fluorodeoxyglucose positron emission tomography for differential diagnosis and prognosis prediction of vascular tumors. Oncol Lett. 2017;14:665–72.

467. Ji Hyun Kim, Hwan Hee Lee, Yu Suhn Kang, et al. Maximum Standardized Uptake Value of Quantitative Bone Single-Photon Emission Computed Tomography/Computed Tomography in Patients with Medial Compartment Osteoarthritis of the Knee. Clin Radiol. 2017;72:580–9.

468. Choi HY, Han JH, Lim SY, et al. Imaging of Myocardial Ischemia-reperfusion Injury using Sodium [18F]Fluoride Positron Emission Tomography/Computed Tomography in Rats and Humans. Mol Imaging. 2017;16:1536012117704767.

469. Lee BC, Moon BS, Park HS, et al. The position of fluorine in CP–118,954 affects AChE inhibition potency and PET imaging quantification for AChE expression in the rat brain. Eur J Pharm Sci. 2017;109:209–216.

470. Song IH, Noh Y, Kwon JH, et al. Immuno-PET imaging based radioimmunotherapy in head and neck squamous cell carcinoma model Oncotarget. 2017;8:92090–92105.

471. Kim JH, Moon BS, Lee BC, Cho YS, et al. A potential PET radiotracer for 5–HT2c receptor: Synthesis and in vivo evaluation of 4–(3–[18F]fluorophenethoxy pyrimidine. ACS Chem Neurosci. 2017;8:996–1003.

472. Ha SG, Park SH, Bang JI, et al. Metabolic Radiomics for Pretreatment 18F-FDG PET/CT to Characterize Locally Advanced Breast Cancer: Histopathologic Characteristics, Response to Neoadjuvant Chemotherapy, and Prognosis. Sci Rep. 2017;8:7:1556

473. Kang HG, Lee HY, Kim KM, et al. A feasibility study of an integrated NIR/gamma/visible imaging system for endoscopic sentinel lymph node mapping. Med Phys. 2017;44:227–39

474. Shin HB, Sheen HS, Lee HY, et al. Digital Imaging and Communications in Medicine (DICOM) information conversion procedure for SUV calculation of PET scanners with different DICOM header information. Phys Med. 2017;44:243–8

475. Kim JW, Seo SH, Kim HS, et al. Comparative evaluation of the algorithms for parametric mapping of the novel myocardial PET imaging agent 18F-FPTP. Ann Nucl Med. 2017;31:469–79.

476. Byun JM, Kim KH, Kim M, et al. Diagnosis of secondary peripheral neurolymphomatosis: a multi-center experience. Leuk Lymphoma. 2017;58:2624–32

477. Lee BH, Kim KD, Choi JY, et al. Efficacy of the multidisciplinary tumor board conference in gynecologic oncology A prospective study. Medicine. 2017;96:e8089

478 Uh MH, Kim JS, Park JH, et al. Fabrication of Localized Surface Plasmon Resonance Sensor Based on Optical Fiber and Micro Fluidic Channel. J Nanosci Nanotechnol. 2017;17:1083–91.

479. Lee JS, Kim HY, Jo CS, et al. Enzyme-Driven Hasselback-Like DNA-Based Inorganic Superstructures. Adv. Funct. Mater. 2017;27:1704213.

2018년

480. Bakht MK, Derecichei I, Li Y, et al. Neuroendocrine differentiation of prostate cancer leads to PSMA suppression. Endocr Relat Cancer. 2018;23:26:131–46.

481. Chung SJ, Youn H, Jeong EJ, et al. In vivo imaging of activated macrophages by 18F-FEDAC, a TSPO targeting PET ligand, in the use of biologic disease-modifying anti-rheumatic drugs (bDMARDs). Biochem Biophys Res Commun. 2018;17:506:216–22.

482. Kim YI, Paeng JC, Park YS, et al. Relation of EGFR Mutation Status to Metabolic Activity in Localized Lung Adenocarcinoma and Its Influence on the Use of FDG PET/CT Parameters in Prognosis. AJR Am J Roentgenol. 2018;210:1346–51.

483. Park S, Paeng JC, Kang CH, et al. Dual-time point 18F-FDG PET/CT for the staging of oesophageal cancer: the best diagnostic performance by retention index for N-staging in non-calcified lymph nodes. Eur J Nucl Med Mol Imaging. 2018;45:1317–28.

484. Chung SJ, Yoon HJ, Youn H, et al. 18F-FEDAC as a Targeting Agent for Activated Macrophages in DBA/1 Mice with Collagen-Induced Arthritis: Comparison with 18F-FDG. J Nucl Med. 2018;59:839–45.

485. Kim YI, Cheon GJ, Kang SY, et al. Prognostic value of simultaneous 18F-FDG PET/MRI using a combination of metabolo-volumetric parameters and apparent diffusion coefficient in treated head and neck cancer. EJNMMI Res. 2018;8:2.

486. Lee MS, Kim JH, Paeng JC, et al. Whole-Body Voxel-Based Personalized Dosimetry: The Multiple Voxel S-Value Approach for Heterogeneous Media with Nonuniform Activity Distributions. J Nucl Med. 2018;59:1133–9.

487. Lee HS, Lee S, Park S, et al. The association between somatic and psychological discomfort and health-related quality of life according to the elderly and non-elderly. Qual Life Res. 2018;27:673–81.

488. Oh HJ, Kim J, Park H, Chung S, et al. Graphene-oxide quenching-based molecular beacon imaging of exosome-mediated transfer of neurogenic miR–193a on microfluidic platform. Biosens Bioelectron. 2018;20:647–56.

489. Lee H, Chung MK, Kang H, et al. ABNORMAL HOLE DETECTION IN BRAIN CONNECTIVITY BY KERNEL DENSITY OF PERSISTENCE DIAGRAM AND HODGE LAPLACIAN. Proc IEEE Int Symp Biomed Imaging. 2018;2018:20–23.

490. Choi H, Kang H, Lee DS et al. Predicting Aging of Brain Metabolic Topography Using Variational Autoencoder. Front Aging Neurosci. 2018;12:212.

491. Moon SH, Hong MK, Kim YJ, et al. Development of a Ga–68 labeled PET tracer with short linker for prostate-specific membrane antigen (PSMA) targeting. Bioorg Med Chem. 2018;15;26:2501–2507.

492. Choe MK, Lim M, Kim JS, et al. Disrupted Resting State Network of Fibromyalgia in Theta frequency. Sci Rep. 2018;1:8:2064.

493. Park H, Lee S, Ko GB, et al. Achieving reliable coincidence resolving time measurement of PET detectors using multichannel waveform digitizer based on DRS4 chip. Phys Med Biol. 2018;10:63:24NT02.

494. Won JY, Lee JS. Highly Integrated FPGA-Only Signal Digitization Method Using Single-Ended Memory Interface Input Receivers for Time-of-Flight PET Detectors. IEEE Trans Biomed Circuits Syst. 2018;12:1401−9.

495. Park J, Hwang D, Kim KY, et al. Computed tomography super-resolution using deep convolutional neural network. Phys Med Biol. 2018;63:145011.

496. Shin S, Kim S, Seo S, et al. The relationship between dopamine receptor blockade and cognitive performance in schizophrenia: a [11C]−raclopride PET study with aripiprazole. Transl Psychiatry. 2018;8:87.

497. Lee S, Lee MS, Kim KY, et al. Systematic study on factors influencing the performance of inter-detector scatter recovery in small-animal PET. Med Phys. 2018;45:3551−62.

498. Lee MS, Kang SK, Lee JS. Novel inter-crystal scattering event identification method for PET detectors. Phys Med Biol. 2018;63:115015.

499. Lee S, Lee MS, Won JY, et al. Performance of a new accelerating-electrode-equipped fast-time-response PMT coupled with fast LGSO. Phys Med Biol. 2018;63:05NT03.

500. Lee JY, Kim HY, Lee YS, et al. Naphthol Blue Black and 99mTc-Labeled Mannosylated Human Serum Albumin(99mTc-MSA) Conjugate as a Multimodal Lymph Node Mapping Nanocarrier. Sci Rep. 2018;8:13636

501. Lee YS, Kim DY, Kim TJ, et al. Loss of toll-like receptor 3 aggravates hepatic inflammation but ameliorates steatosis in mice. Biochem Biophys Res Commun. 2018;497:957−62.

502. Kim HY, Park C, Lee JY, et al. One-pot radiosynthesis of O−[18F]fluoromethyl-D−tyrosine via intra-molecular nucleophilic 18F-fluorination with 1,2,3−triazolium triflate salt precursor. Appl Radiat Isot. 2018;132:105−9

503. Chung HH, Cheon GJ, Kim JW, et al. Prognostic value of lymph node-to-primary tumor standardized uptake value ratio in endometrioid endometrial carcinoma. Eur J Nucl Med Mol Imaging. 2018;45:47−55.

504. Lee JW, Park JY, Lee HJ, et al. Preoperative [18F]FDG PET/CT tumour heterogeneity index in patients with uterine leiomyosarcoma: a multicentre retrospective study. Eur J Nucl Med Mol Imaging. 2018;45:1309−16.

505. Lee YA, Cho SW, Sung HK, et al. Effects of Maternal Iodine Status during Pregnancy and Lactation on Maternal Thyroid Function and Offspring Growth and Development: A Prospective Study Protocol for the Ideal Breast Milk Cohort. Endocrinol Metab(Seoul). 2018;33:395−402.

506. Oh SW, Cheon GJ. Prostate-Specific Membrane Antigen PET Imaging in Prostate Cancer: Opportunities and Challenges. Korean J Radiol. 2018;19:819−31.

507. Chung HH, Kim JW, Park NH, et al. Prognostic importance of peritoneal lesion-to-primary tumour standardized uptake value ratio in advanced serous epithelial ovarian cancer. Eur Radiol. 2018;28:2107−114.

508. Cho N, Im SA, Cheon GJ, et al. Integrated 18F-FDG PET/MRI in breast cancer: early prediction of response to neoadjuvant chemotherapy. Eur J Nucl Med Mol Imaging. 2018;45:328−339.

509. Yoon SH, Goo JM, Lee CH, et al. Virtual reality-assisted localization and three-dimensional printing-enhanced multidisciplinary decision to treat radiologically occult superficial endobronchial lung cancer. Thorac Cancer. 2018;9:11:1525−7.

510. Park EH, Lee EY, Lee YJ, et al. Infliximab biosimilar CT-P13 therapy in patients with Takayasu arteritis with low dose of glucocorticoids: a prospective single-arm study. Rheumatol Int. 2018;38:2233–2242.

511. Moon SH, Choi WH, Yoo IR, et al. Prognostic Value of Baseline 18F-Fluorodeoxyglucose PET/CT in Patients with Multiple Myeloma: A Multicenter Cohort Study. Korean J Radiol. 2018;19:481–8.

512. Joo I, Kim HC, Kim GM, et al. Imaging Evaluation Following 90Y Radioembolization of Liver Tumors: What Radiologists Should Know. Korean J Radiol. 2018;19:209–22.

513. Yoo RE, Kim JH, Paeng JC, et al. Radiofrequency ablation for treatment of locally recurrent thyroid cancer presenting as a metastatic lymph node with dense macrocalcification: A case report and literature review. Medicine (Baltimore). 2018;97:9:e0003.

514. Ahn SY, Goo JM, Lee KH, et al. Monitoring tumor response to the vascular disrupting agent CKD–516 in a rabbit VX2 intramuscular tumor model using PET/MRI: Simultaneous evaluation of vascular and metabolic parameters. PLoS One. 2018;13:13:e0192706.

515. Park S, Ha S, Lee SH, Paeng JC, et al. ntratumoral heterogeneity characterized by pretreatment PET in non-small cell lung cancer patients predicts progression-free survival on EGFR tyrosine kinase inhibitor. PLoS One. 2018;31;13:e0189766.

516. Kim HC, Kim YJ, Paeng JC, et al. Yttrium–90 Radioembolization of the Right Inferior Phrenic Artery in 20 Patients with Hepatocellular Carcinoma. J Vasc Interv Radiol. 2018;29:556–63.

517. Choi H, Lee DS, Alzheimer's Disease Neuroimaging Initiative. Generation of Structural MR Images from Amyloid PET: Application to MR-Less Quantification. J Nucl Med. 2018;59:1111–7.

518. Choi H, Jin KH, Alzheimer's Disease Neuroimaging Initiative. Predicting cognitive decline with deep learning of brain metabolism and amyloid imaging. Behav Brain Res. 2018;15:344:103–9.

519. Na KJ, Choi H. Immune landscape of papillary thyroid cancer and immunotherapeutic implications. Endocr Relat Cancer. 2018;25:523–31.

520. Choi H, Na KJ. Integrative analysis of imaging and transcriptomic data of the immune landscape associated with tumor metabolism in lung adenocarcinoma: Clinical and prognostic implications. Theranostics. 2018;1956–65.

521. Choi H, Na KJ. A Risk Stratification Model for Lung Cancer Based on Gene Co expression Network and Deep Learning. Biomed Res Int. 2018;16:2914280.

522. Choi H, Na KJ. Pan-cancer analysis of tumor metabolic landscape associated with genomic alterations. Mol Cancer. 2018;17:150.

523. Kim KJ, Kim JM, Bae YJ, et al. 123I-FP-CIT SPECT and MRI Findings in a Patient With Parkinsonism After Fenpyroximate Intoxication. Clin Nucl Med. 2018;43:e178–e179.

524. Lee CD, Kim GR, Yoon JH et al. In vivo delineation of glioblastoma by targeting tumor-associated macrophages with near-infrared fluorescent silica coated iron oxide nanoparticles in orthotopic xenografts for surgical guidance. Sci Rep. 2018;8:11122.

525. Song YS, Kim JH, Lee BC, et al. Biodistribution and Internal Radiation Dosimetry of 99mTc-IDA-D–[c(RGDfK)]2(BIK–505), a Novel SPECT Radio tracer for the Imaging of Integrinαvβ3 Expression. Cancer Biother Radiopharm. 2018;33:396–402.

526. Kang YK, Song YS, Cho SK, et al. Prognostic stratification model for patients with stage I non-small cell lung cancer adenocarcinoma treated with surgical resection without adjuvant therapies using metabolic features measured on F-18 FDG PET and postoperative pathologic factors. Lung Cancer. 2018;119:1-6.

527. Kim JH, Song YS, Lee JS, et al. Risk stratification of diffuse large B-cell lymphoma with interim PET-CT based on different cutoff Deauville scores. Leuk Lymphoma. 2018;59:340-7.

528. Bae YJ, Kim JM, Kim KJ, et al. Loss of Substantia Nigra Hyperintensity at 3.0-T MR Imaging in Idiopathic REM Sleep Behavior Disorder: Comparison with 123I-FP-CIT SPECT. Radiology. 2018;287:285-293.

529. Suh MS, Park SH, Kim YK et al. 18F-NaFPET/CT for the evaluation of temporo mandibular joint disorder. Clin Radiol. 2018;73:414.e7-414.e13.

530. Park DJ, Park YS, Son SY, et al. Long-Term Oncologic Outcomes of Laparoscopic Sentinel Node Navigation Surgery in Early GastricCancer: A Single-Center, Single-Arm, Phase II Trial. Ann Surg Oncol. 2018;25:2357-65.

531. Moon BS, Jung JH, Park HS, et al. Preclinical comparison study between [18F]fluoromethyl-PBR28 and itsdeuteratedanaloginarat model of neuro inflammation. Bioorg Med Chem Lett. 2018;28:2925-9.

532. Woo SK, Moon BS, Kim BS, et al. Feasibility of myocardial PET imaging using a benzylguanidine analog: meta-(3-[18F]fluoropropyl) benzylguanidine([18F]mFPBG). Nucl Med Biol. 2018;61:63-70.

533. Lim SB, Song DN, Jeon SW, et al. Cobalt-Catalyzed C-F Bond Borylation of Aryl Fluorides. Org Lett. 2018;20:7249-52.

534. Kim GR, Paeng JC, Jung JH, et al. Assessment of TSPO in a Rat Experimental Autoimmune Myocarditis Model: A Comparison Study between [18F]Fluoromethyl-PBR28 and [18F]CB251.Int J Mol Sci. 2018;19:276.

535. Kwon YD, Kang SW, Park HJ, et al. Novel potential pyrazolopyrimidine based translocator protein ligands for the evaluation of neuroinflammation with PET. Eur J Med Chem. 2018;159:292-306.

536. Song HS, Cho SH, Lee HY, et al. The Effects of Progressive Resistance Exercise on Recovery Rate of Bone and Muscle in a Rodent Model of Hindlimb Suspension. Front Physiol. 2018;9:1085.

537. Cho JH, Oh AY, Park SY, et al. Loss of NF2 induces TGF-β receptor 1 mediated Non-canonical and oncogenic TGF-β signaling; Implication of Therapeutic effect of TβR1 inhibitor on NF2 syndrome. Mol Cancer Ther. 2018;17:2271-84.

538. Kang HG, Song SH, Han YB, et al. Proof-of-concept of a multimodal laparoscope for simultaneous NIR/gamma/visible imaging using wavelength division multiplexing. Opt Express. 2018;26:8325-39.

539. Park SY, Oh AY, Cho JH, et al. Therapeutic Effect of Quinacrine, an Antiprotozoan Drug, by Selective Suppression of p-CHK1/2 in p53-Negative Malignant Cancers. Mol Cancer Res. 2018;16:935-46.

540. Kang HM, Jeong SY, Jo AL, et al. Ultrasensitive NIR-SERRS Probes with Multiplexed Ratiometric Quantification for In Vivo Antibody Leads Validation. Adv Healthc Mater. 2018;7.

541. Lee MS, Han HJ, Han SY, et al. Loss of the E3 ubiquitin ligase MKRN1 represses diet-induced metabolic syndrome through AMPK activation. Nat Commun. 2018;9:3404.

542. Kim KM, Zamaleeva AI, Lee YW et al. Characterization of Brain Dysfunction Induced by Bacterial Lipopeptides That Alter Neuronal Activity and Network in Rodent Brains. J Neurosci. 2018;38:10672-91.

2019년

543. Kim SJW, Seo S, Kim HS, et al. Multi-atlas cardiac PET segmentation. Phys Med. 2019;58:32-39.

544. Koh Y, Lee JM, Woo GU, et al. FDG PET for Evaluation of Bone Marrow Status in T-Cell Lymphoma. Clin Nucl Med. 2019;44:4-10.

545. Jeong H, Kim S, Hong BJ, et al. Tumor-Associated Macrophages Enhance Tumor Hypoxia and Aerobic Glycolysis. Cancer Res. 2019;79:795-806.

546. Kim E, Wu HG, Keam B, et al. Significance of 18F-FDG PET Parameters According to Histologic Subtype in the Treatment Outcome of Stage III Non-small-cell Lung Cancer Undergoing Definitive Concurrent Chemoradiotherapy. Clin Lung Cancer. 2019;20:e9-e23.

547. Kim M, Kim TM, Keam B, et al. A Phase II Trial of Pazopanib in Patients with Metastatic Alveolar Soft Part Sarcoma. Oncologist. 2019;24:20-e29.

548. Han JH, Lee HJ, Kang H, et al. Brain Plasticity Can Predict the Cochlear Implant Outcome in Adult-Onset Deafness. Front Hum Neurosci. 2019;13:38.

549. Park JY, Song MG, Kim WH, et al. Versatile and Finely Tuned Albumin Nanoplatform based on Click Chemistry. Theranostics. 2019;9(12):3398-3409.

550. Kang SY, Bang JI, Kang KW, et al. FDG PET/CT for the early prediction of RAI therapy response in patients with metastatic differentiated thyroid carcinoma. PLoS One. 2019;14:e0218416.

551. Park JE, Park J, Jun Y, et al. Expanding therapeutic utility of carfilzomib for breast cancer therapy by novel albumin-coated nanocrystal formulation. J Control Release. 2019;302:148-59.

552. Shagera QA, Cheon GJ, Koh Y, et al. Prognostic value of metabolic tumour volume on baseline 18F-FDG PET/CT in addition to NCCN-IPI in patients with diffuse large B-cell lymphoma: further stratification of the group with a high-risk NCCN-IPI. Eur J Nucl Med Mol Imaging. 2019;46:1417-27.

553. Lodhi NA, Park JY, Kim K, et al. Development of 99mTc-Labeled Human Serum Albumin with Prolonged Circulation by Chelate-then-Click Approach: A Potential Blood Pool Imaging Agent. Mol Pharm. 2019;16:1586-95.

554. Lee CH, Kim MJ, Lee HH, et al. Adenine Nucleotide Translocase 2 as an Enzyme Related to [18F] FDG Accumulation in Various Cancers. Mol Imaging Biol. 2019;21:722-30.

555. Jeong CW, Suh J, Yuk HD, et al. Establishment of the Seoul National University Prospectively Enrolled Registry for Genitourinary Cancer (SUPER-GUC): A prospective, multidisciplinary, biobank linked cohort and research platform. Investig Clin Urol. 2019;60:235-43.

556. Lodhi NA, Park JY, Hong MK, et al. Development of 99mTc-labeled trivalent isonitrile radiotracer for folate receptor imaging. Bioorg Med Chem. 2019;27:1925-31.

557. Lee SH, Yoon SH, Nam JG, et al. Distinguishing between Thymic Epithelial Tumors and Benign Cysts via Computed Tomography. Korean J Radiol. 2019;20:671-82.

558. Berek JS, Matsuo K, Grubbs BH, et al. Multidisciplinary perspectives on newly revised 2018 FIGO staging of cancer of the cervix uteri. J Gynecol Oncol. 2019;30:e40.

559. Lee SH, Seo HG, Oh BM, et al. 18F-FDG positron emission tomography as a novel diagnostic tool for peripheral nerve injury. J Neurosci Methods. 2019;317:11–9.

560. Seo KS, Suh M, Hong S, et al. The New Possibility of Lymphoscintigraphy to Guide a Clinical Treatment for Lymphedema in Patient With Breast Cancer. Clin Nucl Med. 2019;44:179–85.

561. Kim HM, Sohn DW, Paeng JC. Prevalence of Positive 99 mTc-DPD Scintigraphy as an Indicator of the Prevalence of Wild-type Transthyretin Amyloidosis in the Elderly. Int Heart J. 2019;60:643–7.

562. Lee SP, Seo JK, Hwang IC, et al. Coronary computed tomography angiography vs. myocardial single photon emission computed tomography in patients with intermediate risk chest pain: a randomized clinical trial for cost-effectiveness comparison based on real-world cost. Eur Heart J Cardiovasc Imaging. 2019;20:417–25.

563. Choi H, Ha S, Kang H, et al. Alzheimer's Disease Neuroimaging Initiative. Deep learning only by normal brain PET identify unheralded brain anomalies. EBioMedicine. 2019;43:447–53.

564. Gupta A, Lee MS, Kim JH, et al. Preclinical voxel-based dosimetry through GATE Monte Carlo simulation using PET/CT imaging of mice. Phys Med Biol. 20196;64:095007.

565. Gupta A, Shin JH, Lee MS, et al. Voxel-Based Dosimetry of Iron Oxide Nanoparticle-Conjugated 177Lu-Labeled Folic Acid Using SPECT/CT Imaging of Mice. Mol Pharm. 2019;16:1498–1506.

566. Lee H, Kim E, Ha S, et al. Volume entropy for modeling information flow in a brain graph. Sci Rep. 2019;9:256.

567. Hwang DW, Choi Y, Kim D, et al. Graphene oxide-quenching-based fluorescence in situ hybridization (G-FISH) to detect RNA in tissue: Simple and fast tissue RNA diagnostics. Nanomedicine. 2019;16:162–72.

568. Oh HJ, Kim J, Park H, et al. Graphene-oxide quenching-based molecular beacon imaging of exosome-mediated transfer of neurogenic miR–193a on microfluidic platform. Biosens Bioelectron. 2019;126:647–56.

569. Lee DS, Trujillo PB, Frangos S. First steps in an uncharted territory by WFNMB. Eur J Nucl Med Mol Imaging. 2019;46:524–30.

570. Lee JY, Yoon EJ, Kim YK, et al. Nonmotor and Dopamine Transporter Change in REM Sleep Behavior Disorder by Olfactory Impairment. J Mov Disord. 2019;12:103–12.

571. Yoon EJ, Lee JY, Nam H, et al. A New Metabolic Network Correlated with Olfactory and Executive Dysfunctions in Idiopathic Rapid Eye Movement Sleep Behavior Disorder. J Clin Neurol. 2019;15:175–83.

572. Choi JS, Seo HG, Oh BM, et al. 18F-FDG uptake in denervated muscles of patients with peripheral nerve injury. Ann Clin Transl Neurol. 2019;6:2175–85.

573. Jeong CW, Suh J, Yuk HD, et al. Establishment of the Seoul National University Prospectively Enrolled Registry for Genitourinary Cancer (SUPER-GUC): A prospective, multidisciplinary, biobank linked cohort and research platform. Investig Clin Urol. 2019;60:235–43.

574. Kang YK, Choi JY, Paeng JC, et al. Composite criteria using clinical and FDG PET/CT factors for predicting recurrence of hepatocellular carcinoma after living donor liver transplantation. Eur Radiol. 2019;29:6009–17.

575. Lodhi NA, Park JY, Hong MK, et al. Development of 99mTc-labeled trivalent isonitrile radiotracer for folate receptor imaging. Bioorg Med Chem. 2019;27:1925-31.
576. Park CR, Jo JH, Song MG, et al. Secreted protein acidic and rich in cysteine mediates active targeting of human serum albumin in U87MG xenograft mouse models. Theranostics. 2019;9:7447-57.
577. Lee HS, Kang YK, Lee H, et al. Compartmental-modelling-based measurement of murine glomerular filtration rate using 18F-fluoride PET/CT. Sci Rep. 2019;9:11269.
578. Park HR, Kim IH, Kang H, et al. Electrophysiological and imaging evidence of sustained inhibition in limbic and frontal networks following deep brain stimulation for treatment refractory obsessive compulsive disorder. PLoS One. 2019;14:e0219578.
579. Park JY, Kim YJ, Lee JY, et al. Iging of the third gasotransmitter hydrogen sulfide using 99mTc-labeled alpha-hydroxy acids. Nucl Med Biol. 2019;76-77:28-35.
580. Kim HY, Lee JY, Lee YS, Jeong JM. Design and synthesis of enantiopure 18 F-labelled [18 F] trifluoromethyltryptophan from 2-halotryptophan derivatives via copper(I)-mediated [18 F]trifluoromethylation and evaluation of its in vitro characterization for the serotonergic system imaging. J Labelled Comp Radiopharm. 2019;62:566-79.
581. Kim S, Jang JY, Koh J, et al. Programmed cell death ligand-1-mediated enhancement of hexokinase 2 expression is inversely related to T-cell effector gene expression in non-small-cell lung cancer. J Exp Clin Cancer Res. 2019;38:462.
582. Kim H, Goo JM, Paeng JC, et al. Evaluation of maximum standardized uptake value at fluorine-18 fluorodeoxyglucose positron emission tomography as a complementary T factor in the eighth edition of lung cancer stage classification. Lung Cancer. 2019;134:151-7.
583. Kolossváry M, Park J, Bang JI, et al. Identification of invasive and radionuclide imaging markers of coronary plaque vulnerability using radiomic analysis of coronary computed tomography angiography. Eur Heart J Cardiovasc Imaging. 2019;20:1250-8.
584. Hwang D, Kang SK, Kim KY, et al. Generation of PET Attenuation Map for Whole-Body Time-of-Flight 18F-FDG PET/MRI Using a Deep Neural Network Trained with Simultaneously Reconstructed Activity and Attenuation Maps. J Nucl Med. 2019;60:1183-9.
585. Kim JW, Byun MS, Yi D, et al. KBASE Research Group. Coffee intake and decreased amyloid pathology in human brain. Transl Psychiatry. 2019;9:270.
586. Choe YM, Byun MS, Yi D, et al. KBASE Research Group. Sleep experiences during different lifetime periods and in vivo Alzheimer pathologies. Alzheimers Res Ther. 2019;11:79.
587. Byun MS, Kim HJ, Yi D, et al. KBASE Research Group. Region-specific association between basal blood insulin and cerebral glucose metabolism in older adults. Neuroimage Clin. 2019;22:101765.
588. Moon SW, Byun MS, Yi D, et al. KBASE Research Group. The Ankle-Brachial Index Is Associated with Cerebral β-Amyloid Deposition in Cognitively Normal Older Adults. J Gerontol A Biol Sci Med Sci. 2019;74:1141-8.
589. Jeon SY, Byun MS, Yi D, et al. KBASE Research Group. Influence of hypertension on brain amyloid deposition and Alzheimer's disease signature neurodegeneration. Neurobiol Aging. 2019;75:62-70.

590 Han SH, Park JC, Byun MS, et al. KBASE Research Group. Blood acetylcholinesterase level is a potential biomarker for the early detection of cerebral amyloid deposition in cognitively normal individuals. Neurobiol Aging. 2019;73:21−9.

591. Park J, Bae S, Seo S, et al. Measurement of Glomerular Filtration Rate using Quantitative SPECT/CT and Deep-learning-based Kidney Segmentation. Sci Rep. 2019;9:4223.

592. Ko GB, Lee JS. Time-based signal sampling using sawtooth-shaped threshold. Phys Med Biol. 2019;64:125020.

593. Lee JS, Kovalski G, Sharir T, et al. Advances in imaging instrumentation for nuclear cardiology. J Nucl Cardiol. 2019;26:543−56.

594. Han YB, Kang HG, Song SH, et al. SiPM-based dual-ended-readout DOI-TOF PET module based on mean-time method. J Inst. 2019;14:P02023.

595. Lee MS, Hwang D, Kim JH, et al. Deep-dose: a voxel dose estimation method using deep convolutional neural network for personalized internal dosimetry. Sci Rep. 2019;9:10308.

596. Park H, Kim HS, Hong YJ, et al. Therapeutic Effect of Fimasartan in a Rat Model of Myocardial Infarction Evaluated by Cardiac Positron Emission Tomography with [18F]FPTP. Chonnam Med J. 2019;55:109−115.

597. Kim S, Jung WH, Howes OD, et al. Frontostriatal functional connectivity and striatal dopamine synthesis capacity in schizophrenia in terms of antipsychotic responsiveness: an [18F]DOPA PET and fMRI study. Psychol Med. 2019;49:2533−42.

598. Suh HY, Choi H, Paeng JC, et al. Comprehensive gene expression analysis for exploring the association between glucose metabolism and differentiation of thyroid cancer. BMC Cancer. 2019;19:1260.

599. Park SH, Song YS, Moon BS, et al. Combination of In Vivo [123I]FP-CIT SPECT and Microdialysis Reveals an Antipsychotic Drug Haloperidol-induced Synaptic Dopamine Availability in the Rat Midbrain and Striatum. Exp Neurobiol. 2019;28:602−11.

600. Jeong Y, Kim GR, Jeong SH, et al. Cancer Selective Turn-On Fluorescence Imaging Using a Biopolymeric Nanocarrier. Biomacromolecules. 2019;20:1068−76

601. Gupta A, Lee MS, Kim JH, et al. Preclinical voxel-based dosimetry through GATE Monte Carlo simulation using PET/CT imaging of mice. Phys Med Biol. 2019;64:095007.

602. Kim KJ, Kim JM, Bae YJ, et al. Occurrence of Stridor During Sleep in a Patient With Spinocerebellar Ataxia Type 17. J Clin Sleep Med. 2019;15:153−5.

603. Park JY, Bae SW, Seo SH. Measurement of Glomerular Filtration Rate using Quantitative SPECT/CT and Deep-learning-based Kidney Segmentation. Sci Rep. 2019;9:4223

604. Bae SW, Kang YS, Song YS, et al. K-SPECT Group. Maximum standardized uptake value of foot SPECT/CT using Tc−99m HDP in patients with accessory navicular bone as a predictor of surgical treatment. Medicine. 2019;98:e14022.

605. Chang H, Lee SJ, Lim J, et al. Prognostic significance of metabolic parameters measured by 18F-FDG PET/CT in limited-stage small-cell lung carcinoma. J Cancer Res Clin Oncol. 2019;145:1361−7.

606. Lee JW, Song YS, Kim HY, et al. Alteration of Tremor Dominant and Postural Instability Gait Difficulty Subtypes During the Progression of Parkinson's Disease: Analysis of the PPMI Cohort. Front Neurol. 2019;10:471.

607. Lee HS, Kang YK, Lee HJ, et al. Compartmental-modelling-based measurement of murine glomerular filtration rate using 18F-fluoride PET/CT. Sci Rep. 2019;9:11269.
608. Das S, Ko NK, Lee ES, et al. Stereoselective three-component cascade synthesis of α-substituted 2,4−dienamides from gem-difluorochloro ethanes. Chem Commun. 2019;55:14355−8.
609. Jang KS, Lee SS, Oh YH, et al. Raffel Control of Reactivity and Selectivity of Guanidinyliodonium Salts Toward 18F-Labeling by Monitoring of Protecting Groups: Experiment and Theory. J Fluor Chem. 2019;227:109387.
610. Park HS, Moon BS, Lee HJ, et al. A simple decontamination procedure for unintended iodide impurity during [11C]methionineproduction. J Radioanal Nucl Chem. 2019;322:933 – 9
611. Lu Y, Choi JY, Kim SE, et al. HPLC-free in situ 18F-fluoromethylation of bioactive molecules by azidation and MTBD scavenging. Chem Commun. 2019;55:11798−801
612. Denora N, Lee C, Maria R, et al. TSPO-targeted NIR-fluorescent ultra-small iron oxide nanoparticles for glioblastoma imaging. Eur J Pharm Sci. 2019;139:105047.
613. Ahn SJ, Lee HY, Hong HK, et al. Preclinical SPECT Imaging of Choroidal Neovascularization in Mice Using Integrin-Binding [99mTc]IDA-D−[c(RGDfK)]2. Mol Imaging Biol. 2019;21:644−53.
614. Tran VH, Park HJ, Park JK, et al. Synthesis and Evaluation of Novel Potent TSPO PET Ligands with 2−Phenylpyrazolo[1,5−a]pyrimidin−3−yl Acetamide. Bioorg. Med. Chem. 2019;27:4069−80.
615. Lee SS, Jang KS, Lee BC, et al. Origin of Difference in Reactivity of Aliphatic and Aromatic Guanidine-Containing Pharmaceuticals toward [18F]fluorination: Coulombic Forcesand Hydrogen Bonding. Bull. Korean Chem. Soc. 2019;40:894−7